Wei Hu

Né le 30 Septembre 1972 à An Hui, CHINE

L'utilisation non conventionnelle de l'échographie endovasculaire

Composition du jury

Directeur de thèse :	SCHIELE François, Professeur	Université de Franche-Comté
Rapporteurs :	OHLMANN Patrick, Professeur	Université de Strasbourg
	METZ Damien, Professeur	Université de Reims
Examinateurs :	SCHIELE François, Professeur	Université de Franche-Comté
	BASSAND Jean-Pierre, Professeur	Université de Franche-Comté

UNIVERSITE DE FRANCHE-COMTE
FACULTE DE MEDECINE ET DE PHARMACIE

THESE

Pour l'obtention du diplôme de Doctorat de l'Université de Franche-Comté

Présentée et soutenue publiquement le
7 Janvier 2008, par

Wei Hu

Né le 30 Septembre 1972 à An Hui, CHINE

L'utilisation non conventionnelle de l'échographie endovasculaire

Composition du jury

Directeur de thèse :	SCHIELE François, Professeur	Université de Franche-Comté
Rapporteurs :	OHLMANN Patrick, Professeur	Université de Strasbourg
	METZ Damien, Professeur	Université de Reims
Examinateurs :	SCHIELE François, Professeur	Université de Franche-Comté
	BASSAND Jean-Pierre, Professeur	Université de Franche-Comté

Remerciements

D’abord, Je voudrais remercier profondément le Professeur Jean-pierre BASSAND qui m’a donné la chance d’étudier en France, ce joli pays, qui m’a enseigné un grande nombre de choses et de techniques dans le domaine de la cardiologie, et qui m’a offert beaucoup son aide.

Ensuite, Je voudrais remercier le Professeur François SCHIELE, qui est très intelligent et capable, et qui met beaucoup de ponctualité et de minutie pour exécuter les choses. Grâce à son enseignement, j’ai fait des progrès durant toutes ces années. Je vais prendre exemple sur sa manière de travailler toute ma vie.

Merci au Professeur Nicolas MENEVEAU le responsable de la salle de cathétérisme, avec qui j’ai été content de travailler.

Merci à la secrétaire Fiona CAULFIELD :
Je n’oublierai pas votre accueil chaleureux lors de mon arrivée. Vous avez fait une correction attentive de la langue dans mes manuscrits, ce qui m’a rendu service.

Merci aux Professeur REGNARD Jacques, OHLMANN Patrick et Damien METZ :
Je tiens à vous témoigner mes profondes reconnaissances pour avoir accepté de siéger dans le jury de cette thèse, et consacré votre temps à la lecture, l’analyse et la critique de ce travail.

Et aussi merci à tous mes camarades : Marie-France, Pierre, Katy, Catherine, Sylvie, Jérôme, Marie-Line, Florence, Géraldine, François, Denis, Guillaume, Guy etc. Vous m’avez accompagné durant toutes ces années, et m’avez soutenu dans mon travail. J’étais très heureux de travailler avec vous tous.

À la fin, merci à ma femme Chun Yan Xu, mon fils Julien Hu, ma famille et mes amis !

SOMMAIRE

Abréviations

1. Intravascular ultrasound	IVUS
2. Patients	Pts
3. Intravascular ultrasound virtual histology	IVUS-VH
4. Acute aortic syndrome	AAS
5. Percataneous coronary intervention	PCI
6. Cross-sectional area	CSA
7. Coronary angiography	CAG
8. Acute coronary syndrome	ACS
9. Intracoronary ultrasound	ICUS
10. Two dimensional	2D
11. Integrated backscatter IVUS	IB-IVUS
12. Intraaorta ultrasound	IAUS
13. Transoesophageal echocardiography	TEE
14. Electron beam computed tomography	EBCT
15. European Society Cardiology	ESC
16. Aortic dissection	AD
17. Classic aortic dissection	CAD
18. Electrocardiogram	ECG
19. Transthoracic echocardiography	TTE
20. Magnetic resonance imaging	MRI
21. Intramural hematoma	IMH
22. Penetrating atherosclerotic ulcer	PAU
23. Coronary heart disease	CHD
24. Aortic intramural hematoma	AIH
25. Hypertension	HTA
26. Hypercholesterolemia	HCT
27. Diabetes mellitus	DM
28. Family history	FH
29. Descending aorta	DA
30. Ascending aorta	AA
31. Matrix metalloproteinase	MMP
32. Temperature difference	ΔT
33. Composite graft	CG

34. Single graft	SG
35. Stable angina pectoris	SAP
36. Unstable angina pectoris	UAP
37. Myocardium infarction	MI
38. C-reactive protein	CRP
39. Directional coronary atherectomy	DCA
40. Stable plaque	SP
41. Vulnerable plaque	VP
42. Ultrafast computed tomography	UFCT
43. Drug eluting stent	DES
44. Balloon angioplasty	BA
45. Gray scale	GS
46. Cardiovascular disease	CVD
47. Radiofrequency	RF
48. IVUS-derived thin-cap fibroatheroma	IDTCFA
49. Optical coherence tomography	OCT
50. Near-infrared	NIR
51. External elastic membrane	EEM

Listes des materials

Intraaorta ultrasound imaging (Ultra ICE^{TM} intracardiac Echocatheter, Boston Scientific, USA).

Spiral CT scanning (4 multibarret, Simens, Germany).

Transoesophageal echocardiography (Hewlett Packard, USA).

Magnetic resonance imaging (3 Tesla, General Electricity, USA).

IVUS-VH (2.9 F Eagle Eye, Volcano Corp, Rancho Cordova, California, USA).

Title

The non-conventional use of intravascular ultrasound imaging

Titré

L´utilisation non conventionnelle d’échographie endovasculaire

Abstract

Background: The non-conventional use of intravascular ultrasound (IVUS) imaging has not been fully explored.

Objective: We aimed to study two different non-conventional uses of IVUS. In part I, we assessed the potential value of IVUS imaging in patients (pts) with acute aortic syndrome (AAS). In part II, we used IVUS virtual histology (IVUS-VH) to observe plaque composition changes after percantaneous coronary intervention (PCI).

Methods :In part I, we performed IVUS in 16 consecutive pts with suspected or established AAS using a 9-MHz probe. We compared IVUS results with aortography, transesophageal ultrasound, computed tomography and magnetic resonance imaging. In part II, we performed IVUS-VH in 20 consecutive pts with acute coronary syndrome before and after PCI. Quantitative and qualitative plaque changes were determined by comparison between pre- and post-PCI images.

Results: In part I, intra-aorta IVUS imaging was safe; it had almost 100% accuracy in diagnosis of AAS; in 12/15(80%) pts, it supplied additional useful information beyond other imaging techniques. In part II, PCI resulted in an 80% increase in lumen cross-sectional area (CSA); 35% due to an increase in total vessel CSA and 65% to a decrease in plaque CSA, and plaque reduction resulted from a longitudinal redistribution. Fibrous and fibro-fatty tissues were able to move longitudinally, whereas calcium remained at the same level. About 1/3 of necrotic tissue was lost after PCI, suggesting that embolization occurred.

Conclusion: We conclude that IVUS can supply additional useful information beyond other imaging techniques in pts with suspected or established AAS. After PCI, lumen enlargement was explained by 35% vessel stretching and 65% plaque decrease, which was the result of longitudinal redistribution of fibrous and fibro-fatty tissues, and the disappearance of one third of necrotic tissue present at baseline.

Key words: Intravascular ultrasound; Acute aortic syndrome; Percantaneous balloon angioplasty; Intravascular ultrasound virtual histology.

Résumé

Rationnel: L´utilisation non conventionnelle de l'échographie endovasculaire (IVUS) n'est pas suffisamment documentée dans la littérature médicale.

Objectif: Nous avons étudié deux utilisations non conventionnelles différentes de l´IVUS. Dans une première phase, nous avons évalué l'intérêt potentiel de l´IVUS chez les malades avec syndrome aortique aigu (SAA). Dans la 2° phase, nous avons utilisé l'histologie virtuelle (IVUS-VH) pour quantifier les changements de composition de la plaque après angioplastie au ballon (angioplastie).

Méthodes: Dans la phase 1, IVUS a été réalisé chez 16 patients consécutifs avec une suspicion ou un diagnostic confirmé de SAA, en utilisant une sonde 9 MHz. Les résultats ont été comparés à une imagerie par aortographie, échographie transoesophagienne, scanner et imagerie par résonance magnétique. Dans la phase 2, IVUS-VH a été réalisé chez 20 patients consécutifs avec syndrome coronarien aigu avant et après angioplastie. Les changements quantitatifs et qualitatifs des plaques ont été identifiés en comparant les images pré- et post-angioplastie.

Résultats: Dans la phase 1, la sécurité d'emploi de l´IVUS était appropriée. La sensibilité de l'IVUS pour déceler les SAA est de presque 100%. Dans 12/15 patients (80%), l'IVUS fournit des informations diagnostiques utiles supplémentaires au-delà des autres techniques d'imagerie. Dans la phase 2, l'angioplastie a permis une augmentation de 80% de la superficie à la coupe de section (L-CSA), expliquée pour 35% par une augmentation du vaisseau CSA, et pour 65% par une diminution de la surface de la plaque, à cause d'une redistribution longitudinale. Le tissu fibreux et fibrolipidique été capable de se déplacer longitudinalement, mais le tissu calcique reste au même niveau. Environ un tiers du tissu nécrotique a été perdu après angioplastie, suggérant la présence d'un processus d'embolisation.

Conclusion:

L´IVUS fournit des informations utiles supplémentaires au-delà des autres techniques d'imagerie chez les patients avec suspicion ou diagnostic de SAA. Après angioplastie, l´augmentation de la lumière peut être expliqué pour 35% par une augmentation du vaisseau CSA et pour 65% par une diminution de la plaque, qui est le résultat d'une redistribution longitudinale du tissu fibreux et fibrolipidique et la disparition d'un tiers du tissu nécrotique présent à l'inclusion.

Mots clés: Échographie endocoronaire; Syndrome aortique Aigu ; angioplastie; Histologie Virtuelle.

Introduction

Although coronary angiography (CAG) is still thought as the standard method of diagnosis of coronary heart disease, it has some limitations. The main limitation of CAG is that it only provides information about the vessel lumen without characterizing the vessel wall. The reliability of the degree of angiographic stenosis is affected by three followed factors: 1), Visual assessment of the degree of stenosis has significant intra-operator variability, however, this problem has been solved by using quantitative coronary analysis software; 2), It can only be diagnosed by comparing an area to an adjacent reference segment that is assumed to be disease free, whereas there is often no normal referent segment because atherosclerosis is usually diffuse; 3), Positive remodeling firstly described by Glagov S et al make a diseased vessel undetectable angiographically. Only at a very advanced (plaque occupies 40% vessel area) stage of the plaque is evident by angiography. Moreover, most importantly, we know that the degree of luminal stenosis does not correlate with the risk of lesions leading to acute coronary syndromes (ACSs) and that these events often occur from rupture of a modestly stenotic plaque not detectable by angiography.

Intracoronary ultrasound (ICUS) has been extensively studied since its development from early 1990's. The safety of ICUS is well documented. Studies report the complications of ICUS imaging varying from 1% to 3% and most of them are transient spasm, which responds rapidly to intracoronary nitroglycerin. Compared with CAG that depicts only a two-dimensional (2D) silhouette of the lumen, ICUS allows tomographic assessment of lumen area, plaque size, distribution and composition. So, ICUS has several advantages: 1), It commonly detects occult disease in angiographically "normal" sites; 2), It is an optimal method of detection of transplant vasoculopathy; 3), It permits us to assess vessels that are difficult to image by CAG, including diffusely diseased segments, ostial or bifurcation stenoses, eccentric plaques, and angiographically foreshortened vessels; 4), It helps us to understand the mechanisms of action of interventional devices; 5), It is often used to select the most suitable device; 6), ICUS-derived residual plaque burden is the most useful predictor of clinical outcome; 7), In restenosis after balloon angioplasty, negative remodeling is a major mechanism of late lumen loss; 8), It has proven useful in evaluating brachytherapy; 9), In the ear of drug-eluting stenting, it permits us to accurately judge if stents are properly developed (all stent struts completely

touch the vessel wall), a very important factor which has been demonstrated to decide in-stent thrombosis. Therefore, in current clinical practice, ICUS is generally thought as a valuable tool adjunct to CAG. However, ICUS also has some limitations, especially in distinguishing different plaque components. Although on the basis of plaque echogenicity, ICUS is able to distinguish some of the components of atherosclerotic plaque: 1), Highly echoreflective regions with acoustic shadows correspond to calcified tissue; 2), Hypoechoic regions correspond to lipid-rich tissue; 3), Hyperechoic regions represent fibrous tissue. However, because the interpretation is based on visual inspection, echogenicity and texture of different tissue may appear very similar, ICUS does not consistently provide actual histology.

From pathologic studies, we know that ACSs are often results from vulnerable plaques that have three characteristics: a rich lipid core, a thin fibrous cap and inflammated cells infiltration. In order to detect these vulnerable plaque, many new imaging modalities have been introduced into clinical practice in recent years, some of them were developed on basis of IVUS such as: wavelet-IVUS, integrated backscatter IVUS (IB-IVUS), IVUS elastography/palpography, virtual histologic IVUS (IVUS-VH). These improved IVUS techniques are often called as non-conventional use of IVUS imaging.

Moreover, IVUS imaging is not only used in coronary artery but also used in pulmonary artery, intracardiac, and intraaorta, when it is performed in the latter fields, it is often used a probe with lower frequency. So, in some sense, the non intracoronary use of IVUS imaging can be also called as non conventional one.

In our article, we evaluated two aspects of non-conventional use of IVUS imaging. In part I, we firstly reviewed the definition, diagnosis and management of aortic dissection, then we presented our finding when performed intraaorta ultrasound (IAUS) imaging with a 9MHz mechanic probe in patients with established or suspected aortic dissection. While in part II, we firstly reviewed the concept of vulnerable plaque and current used imaging techniques in detecting vulnerable plaques, then we presented our observations of changes in unstable coronary atherosclerotic plaque compositions after balloon angioplasty by using IVUS-VH.

Part I

The general conception of aortic dissection

I: Introduction

Cardiovascular diseases are the major cause of death in the majority of the developed countries and in many developing countries. New imaging modalities — transoesophageal echocardiography (TEE), magnetic resonance imaging (MRI), helical computed tomography (HCT), electron beam computed tomography (EBCT) — were introduced during the last decade. These new imaging techniques allow better and earlier diagnosis of aortic diseases even in emergency situations. These new imaging techniques have changed patient management during recent years, allowing more rapid diagnosis and decision- making [1-5]. Despite this rapid progress, overall agreement about the strategy for patient management has not yet been achieved. For this reason, in 2001, European Society Cardiology (ESC) published guidelines for the diagnosis and management of aortic dissection[6]. This review was briefly adapted from this guideline.

II: The etiology of aortic dissection

All mechanisms that weaken the aortic wall, the aortic lamina media in particular, lead to higher wall stress, which can induce aortic dilatation and aneurysm formation, eventually resulting in aortic dissection or rupture.

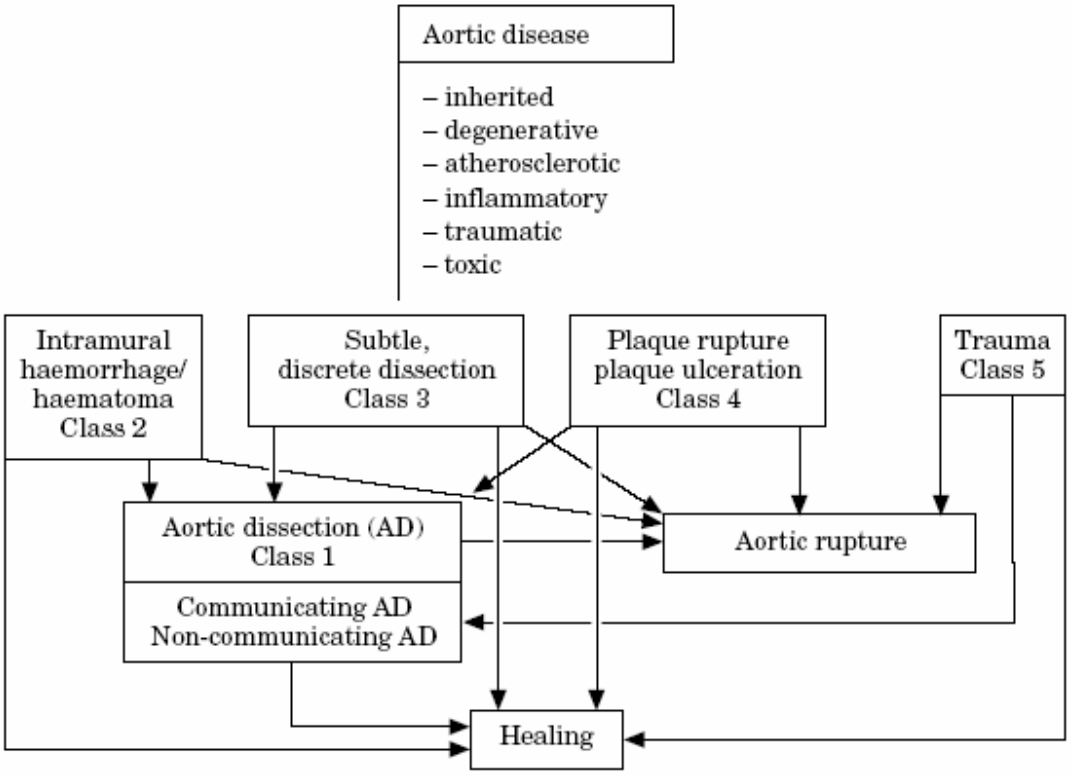

Figure 1 **Schematic illustration of different aortic disease aetiologies which can result in aortic dissection including progression or regression of the disease.**

II-1: Inherited disease

Three major inherited disorders are found in this group: Marfan's syndrome, Ehler-Danlos syndrome and other familial forms of thoracic aortic aneurysm and dissection.

II-2: Ageing of the aorta

The aortic expansion rate over 10 years is about 1-2 mm[7]. Factors that weaken the aortic wall can lead to aneurysm formation. According to the law of LaPlace ($\sigma = p \times r/2h$), wall stress (σ) in a thin wall model is directly proportional to pressure (p) and radius (r) and inversely proportional to vessel wall thickness (h). This makes hypertension as well as cystic media necrosis factors related to the development of aortic disease[8-10]. The expansion rate of aneurysm in the ascending aorta is about 1·3±1·2 mm.year-1 and in the abdominal aneurysm 3·1±3·2 mm.year-1[11]. Interestingly, aortic diameters in cases with and without dissection were found to be the identical (6 cm vs 6·4 cm)[12].

II-3: Atherosclerosis

Atherosclerosis is the main cause of aortic aneurysms. Atherosclerosis leads to gross thickening of the intima. The intima shows massive fibrosis and calcification, and increased amounts of extracellular fatty acids. The integrity of this layer can be compromised by the extracellular matrix being degraded by histiocytic cells. Additional degenerative changes can develop within the fibrous tissue. These changes are characterized by reduced cellularity and collagen fibre hyalinization. Both mechanisms may lead to intimal rupture, most often at the edges of plaques. Intimal thickening increases the distance between the endothelial layer and the media, compromising the nutrient and oxygen supply. Adventitial fibrosis may obstruct vessels feeding small intramural vasa vasorum. Reduced nutritional supply of the media results in medial thinning secondary to necrosis primarily due to necrosis of the smooth muscle cells. Another consequence is a fibrotic change in the elastic structures of the medial layer[13]. All these changes contribute to increased vessel stiffness and to higher vulnerability to shear stress, eventually leading to the formation of aneurysms and dissections, especially in the infrarenal aorta.

The main risk factor for aneurysm formation in atherosclerosis is hypertension, which is found in 85% of those with ruptured or 52% of those with non-ruptured aneurysms. The risk factors, e.g. smoking and hypercholesterolaemia, are also associated with an increased incidence of aortic aneurysms[14]. However, 60% of patients have a cholesterol level of less than 240 mg. dl-1 (6·2 mmol /L)[14].

II-4: Traumatic and iatrogenic dissection.

Blunt chest trauma usually causes dissection of the ascending aorta and/or the region of the ligamentum Botalli at the aortic isthmus. Iatrogenic dissection of the aorta rarely occurs during heart catheterization[15]. It is regularly seen following angioplasty of an aortic coarctation (in adults), but can also be observed after cross-clamping of the aorta and after intra-aortic balloon pumping[16-18]. Most catheter-induced dissections are retrograde dissections. They will usually decrease in size as the false lumen thromboses. Proximal progression of the coronary dissection into the aortic root may be observed.

II-5: Inflammatory disease.

Inflammatory diseases can destroy the medial layers of the aortic wall and lead to weakening of the aortic wall, hastening expansion and causing higher wall stress.

II-5-1: Suppurative bacterial or fungal aortitis.

Suppurative bacterial or fungal aortitis is rare. It can cause focal destruction of the vessel wall with subsequent aneurysm formation and/or rupture.

II-5-2: Autoimmune diseases.

Autoimmune diseases of the aorta can severely affect the vasa vasorum, and decrease the blood supply of the media[19].

II-5-3: Takayasu arteritis.

Takayasu arteritis may develop inside the aortic wall. Such inflammatory lesion consists of an inflammatory infiltrate, smooth muscle and fibroblast necrosis, and fibrosis of the vessel wall.

II-5-4: Luetic aortitis.

Luetic aortitis can lead to similar changes as Takayasu arteritis.

II-5-5: Aortitis.

Aortitis is the principal cardiovascular manifestation of syphilis, found mainly in the ascending aorta, but distal segments can be involved[20]**.**

II-5-6: Rheumatoid arthritis.

Rheumatoid arthritis can also lead to aortitis. Secondary typical aortic dissections are unusual. The diseased aorta may rupture.

II-6: Toxic aortic disease.

Toxic aortic disease is seen in animals after the administration of beta-aminopropionitrile fumarate which leads to changes in the media morphologically similar to mucoid degeneration of the aortic wall[21]**.** Other chemicals have been

shown to cause cellular necrosis in the media[22]**.** The administration of high doses of zinc can also lead to aortic dissections in animal models. In humans, different drugs such as cocaine and amphetamine are associated with aneurysm formation and aortic dissection[23, 24]**.**

III: The classification of aortic dissection.

It has to be noted that all classes of dissection defined by different methods can be seen in their acute and chronic stages; chronic dissections are considered to be present if >14 days have elapsed.

III-1: Stanford's classification[25, 26].

Type A: means the dissection includes the ascending aorta.

Type B: dissection does not involve the ascending aorta.

III-2: DeBakey's classification[26, 27].

Type I: dissection involves the entire aorta.

Type II: dissection involves the ascending aorta.

Type III: dissection involves the descending aorta.

III-3: ESC classification[6].

Class 1: classical aortic dissection (CAD) with an intimal flap between true and false lumen.

Class 2: medial disruption with formation of intramural haematoma/haemorrhage.

Class 3: discrete/subtle dissection without haematoma, eccentric bulge at tear site.

Class 4: plaque rupture leading to aortic ulceration, penetrating aortic atherosclerotic ulcer with surrounding haematoma, usually subadventitial.

Class 5: iatrogenic and traumatic dissection.

IV: Symptoms

IV-1: Pain alone (chest pain and/or back pain).

IV-2: Pain with syncope.

IV-3: Pain with signs of congestive heart failure.

IV-4: Pain with cerebrovascular accident (stroke).

IV-5: Congestive heart failure without pain.

IV-6: Cerebrovascular accident without pain.

IV-7: Abnormal chest roentgenogram without pain.

IV-8: Pulse loss without pain.

V: Diagnosis

V-1: Physical examination

Physical examination can provide important clues as to the presence and origin of the aortic dissection.

V-1-1: Pulse deficits.

Pulse deficits were found in 50% of patients with proximal aortic dissection in their 70s, a large current registry of patients with acute aortic dissection reported this finding in less than 20% of patients[28]. These pulse phenomena may be transient due to the intimal flap's changing position.

V-1-2: Neurological deficits.

Loss of consciousness and ischaemic paresis occur in up to 40% of patients with proximal aortic dissection[29].

V-1-3: Rare symptoms.

1,Vocal chord paralysis (caused by compression of the left recurrent laryngeal nerve);

2, Haemoptysis or haematemesis (due to haemorrhage into the tracheobronchial tree or perforation into the oesophagus)[30];

3, Superior vena cava syndrome (upper airway obstruction due to compression)[31];

4, Horner's syndrome (due to compression of the superior cervical sympathetic ganglion);

5, Pulmonary embolism (if there is extravasation of blood from the false channel into the common adventitia of the ascending aorta and pulmonary artery leads to severe compression of the pulmonary artery)[32];

6, Mesenteric or renal ischaemia (iliac bifurcation is completely obstructed)[28, 33, 34];

7, Leriche's syndrome (pulse loss in both legs).

V-1-4: Aortic regurgitation.

A diastolic murmur indicative of aortic regurgitation is present in about half of the patients with proximal aortic dissection[28, 34, 35]**.**

V-1-5: Pericardial involvement.

Signs of pericardial involvement such as the presence of a pericardial friction rub, jugular venous distension or a paradoxical pulse should alert the physician to call for rapid surgical intervention.

V-1-6: Pleural effusions.

Pleural effusions may be caused by rupture of the aorta into the pleural space, the left side is usually involved. Pleurocentesis reveals the presence of blood indicating the need for emergency surgery. However, an effusion may simply be the expression of an exudative inflammatory reaction from the dissected aorta and no further action is required.

V-1-7: Other confused diagnoses.

Up to 30% of patients later found to have aortic dissection are initially suspected to have other conditions, such as acute coronary syndromes, non-dissecting aneurysms, pulmonary embolism, or aortic stenosis[34, 36].

V-2: Diagnostic steps.

It has to be noted that speed is of utmost importance.

V-2-1: ECG.

ECG must be acquired in all patients. This test helps distinguish aute aortic dissection from acute myocardial infarction, however, a normal ECG is present in one third of patients with coronary involvement and most of these patients have non-specific ST-T segment changes[37].

V-2-2: Chest X-ray.

The role of the chest X-ray is currently unclear[38]. A routine chest X-ray will be abnormal in between 60%[28] to 90% [35] of cases with suspected aortic dissection and will thus make the diagnosis of aortic dissection more likely. However, in unstable patients, a chest X-ray will result in further delay before instituting treatment and should thus be omitted.

V-2-3: Laboratory findings.

The often large wound surface and haematoma may be reflected in laboratory findings such as elevated C-reactive protein, mild-to-moderate leukocytosis and slight elevations of bilirubin and lactic acid dehydrogenase[39]. More recently, the biochemical diagnosis of aortic dissection has become possible by identifying raised concentrations of smooth muscle myosin heavy chain[39].

V-2-4: Specific imaging techniques.

Specific imaging techniques include transthoracic echocardiography (TTE)/ transoesophageal echocardiography (TEE)/ computed tomography (CT)/ magnetic resonance imaging (MRI)/aortography. Not as a frequent used but as a studied tool, intravascular ultrasound (IVUS) imaging has been demonstrated to be useful in patients with aortic dissection. The decision for a specific technique depends on two

major factors: availability in emergency situations and experience of the emergency room and imaging status.

V-2-4-1: Transthoracic/transoesophageal echocardiography (TTE/TEE.)

The diagnosis of aortic dissection by standard transthoracic

M-mode and two-dimensional echocardiography is based on detecting intimal flaps in the aorta. Sensitivity and specificity of transthoracic echocardiography range from 77% to 80% and 93% to 96%, respectively, for the involvement of the ascending aorta[40-42]. The value of transthoracic echocardiography is limited in patients with abnormal chest wall configuration, narrow intercostal spaces, obesity, pulmonary emphysema, and in patients on mechanical ventilation.

A multiplane TEE reaches sensitivity 99%, specificity 89% and positive predictive accuracy and negative predictive accuracy 89% and 99%, respectively[43]. A problem exists in visualizing small circumscript dissected segments within the distal part of the ascending aorta and the anterior portion of the aortic arch, which is known as the 'blind spot'[2]. This problem is caused by interposition of the trachea and the left main stem bronchus between the oesophagus and the aorta. Artifacts due to reverberation within the lumen of the ascending aorta can be observed. These artifacts may present a problem to non-experienced observers[2]. By two-dimensional TEE, the intimal tear can be identified in 61% of patients. Doppler flow analysis has shown that not only unidirectional but also bi-directional flow occurs between the two lumina. Bi-directional flow is present in 75% of patients. TEE in addition to TTE can be used for decision making in the emergency room or even operating theatre in acute aortic dissection with high accuracy. Pitfalls have to be taken into account.

V-2-4-2: Computed tomography.

Since its introduction, helical CT has dramatically improved CT diagnostics because it minimizes motion artifacts and eliminates respiratory misregistration. With conventional CT, each cycle of the X-ray tube generates data, which are used to reconstruct transaxial images. With helical CT, patient translation and X-ray exposure are simultaneous. This technique provides a data set acquired during a single breathhold. These data can be used to reconstruct 2-D and 3-D images in any plane. In fact, CT is currently the most commonly used imaging modality in patients with suspected aortic dissection[44]. Sensitivities of 83%–94% and specificities of 87%–100% have been reported in the early 1990s in large prospective studies on the

evaluation of aortic dissections with conventional incremental CT[2, 45]. By comparison with conventional CT, helical CT needs shorter examination times and reduces the artifacts, its average sensitivity is better than 95%[45, 46]. In summary, CT has the sensitivity greater than 90% and specificity greater than 85%. The extent, localization and side branch involvement of aortic dissection can be assessed, signs of emergency detected. Limitations are related to diagnosis of aortic regurgitation, tear localization as well as detection of intimal tears and subtle /discrete aortic dissection (class 3).

V-2-4-3: Magnetic resonance imaging (MRI)

Although MRI is both highly sensitive and specific in diagnosing aortic dissection[45-47], the technique is often not available on an emergency basis and examination of haemodynamically unstable patients may be difficult. MRI clearly demonstrates the extent of the disease and depicts the distal ascending aorta and the aortic arch in more detail than even transoesophageal echocardiography[48]. The localization of entry and re-entry is nearly as accurate as with transoesophageal echocardiography, the sensitivity approaches 90%[48]. Accordingly, classification of the disease into proximal and distal aortic dissection, which is crucial for selecting the appropriate management, can be easily accomplished with MRI. Adverse signs such as the presence of pericardial effusion or aortic regurgitation can be assessed accurately[49, 50]. Flow in the false and true lumen can be quantified using phase contrast cine magnetic resonance imaging or by tagging techniques[51, 52]**.**

Despite the accuracy of MRI, certain pitfalls and artifacts on MRI images need to be recognized and experience in reading MRI images of aortic dissection is essential[53]. Some kind of artifacts may occur in up to 64% of patients but most of these artifacts are only seen in one section but not in the neighbouring ones.

MRI has the highest accuracy and sensitivity as well as specificity (nearly 100%) for detection of all forms of dissection (class 1, 2 and 4, 5) except subtle/discrete forms (class 3). Distribution and availability is limited particularly in emergency situations. Most often MRI is used in stable haemodynamic conditions and chronic aortic dissection for follow-up. MRI provides excellent visualization of tear localization, aortic regurgitation, side branch involvement and complications.

V-2-4-5: Aortography.

Retrograde aortography was the first accurate diagnostic tool to assess patients with suspected aortic dissection. The diagnosis of aortic dissection was first reported by

Robb and Steinberg in 1939 and it became routine in the 1960s[54, 55]. Thereafter, aortography was considered for several decades as the diagnostic standard for the evaluation of aortic dissection[56]. However, because other accurate methods for the antemortem diagnosis of aortic dissection were not yet available, the low sensitivity of angiography was accepted.

The angiographic diagnosis of aortic dissection is based upon ‘direct’ (diagnostic) angiographic signs, such as the visualization of the intimal flap (negative, often mobile, linear image) or the recognition of two separate lumens, or ‘indirect’ (suggestive) signs, including aortic lumen contour irregularities, rigidity or compression, branch vessels abnormalities, thickening of the aortic walls and aortic regurgitation[42]. Aortography is able to localize the site of origin of the dissection[57]. The true lumen is typically compressed and tends to adopt a spiral shape. Injections in the false lumen are characterized by the absence of branch vessels or the characteristic sinus of Valsalva configuration and late filling or staining with contrast[58]. Contrast aortography accurately identifies branch vessel involvement[58]. It is mandatory to rule out this complication in patients with neurological symptoms, acute renal failure, and hypertensive crisis or mesenteric/limb ischaemia. Peripheral pulse deficits can provide important diagnostic clues. In particular, angiography is an excellent technique to define renal or mesenteric compromise[59]. The occurrence of associated aortic regurgitation and its severity may be readily recognized during aortography. However, this technique has recently been replaced by other new imaging modalities with respect to its ability to evaluate the precise mechanism of aortic regurgitation. In some patients, however, angiography may reveal widening of the aortic root, displacement of a valve cusps or even prolapse of an intimal flap into the left ventricle as the underlying mechanism[60, 61]. Aortography may also demonstrate aortic wall rupture into the pericardial cavity, right atrium, left atrium, right ventricle and pulmonary artery[61].

The specificity of aortography for diagnosing aortic dissection is better than 95% but its sensitivity may be lower than that of other techniques, especially in atypical forms of aortic dissection[60]. In the European cooperative study, the sensitivity and specificity of aortography for the diagnosis of aortic dissection was 88%[2]. False-negative aortograms are mainly the result of the inability of the technique to differentiate the two classic lumens within the aorta[2, 5, 62-64].

Some limitations of this technique should be recognized. It is invasive and therefore has an inherent risk. The advancement of catheters should be performed with care and only by experienced angiographers. Forceful pushing of the catheter or the guidewire should be strongly discouraged to avoid injury, particularly if the catheter is located within the false lumen. In addition, this technique requires the administration of potentially nephrotoxic radiopaque contrast media and ionizing radiation. Furthermore, the intimal flap as well as the distal end of the dissection are not clearly defined when slow flow is present. It is important to emphasize that aortic wall thickness cannot be accurately visualized.

Aortography is highly valuable to diagnose classical aortic dissection, but limitations are obvious in dissection subtypes such as non-communicating aortic dissection and intramural haematoma and haemorrhage formation (class 2) as well as plaque rupture (class 4). Aortography is the standard technique for guiding interventions in aortic dissection.

V-2-4-6:Intravascular ultrasound.

The use of intravascular ultrasound (IVUS) has been advocated to complement angiographic information in the diagnosis of patients with aortic dissection[33, 65]. During a cardiac catheterization procedure, this technique can overcome most of the potential limitations and pitfalls of conventional angiography. IVUS directly visualizes the vessel wall architecture from inside the aortic lumen. It therefore allows the accurate recognition of aortic wall characteristics and pathology, and completes the indirect information of ‘the lumen shadowgram’ depicted by contrast angiographic techniques.

In patients with classic forms of aortic dissection this catheter-based imaging tool provides crisp visualization of the intimal-medial flap, its movement (pulsatility), its circumferential and longitudinal extent and the degree of luminal compromise. This technique appears particularly well suited to delineate the most distal extent of abdominal aortic dissections[33, 65]. Sensitivities and specificities of close to 100% have been reported [33]. The shape of the true and false lumen is readily displayed, whereas false lumen thrombosis is detected with a higher sensitivity and specificity than with TEE[33]. IVUS may also help to distinguish the true from the false lumen when it is difficult to make this distinction. It has been suggested that the three-layered appearance of the intact normal aortic wall may be differentiated from the single-layered appearance of the outer wall of the false lumen. In addition, cobwebs

may be identified in the false lumen in some patients. Branch involvement appears to be better defined with IVUS than with TEE (blind spot in the ascending aorta and the anterior portion of the arch, abdominal vessels) or with CT[33]. In addition, the precise mechanism of vessel compromise (dissection intersecting and narrowing the vessel origin versus ostium spared by the dissection but covered by a prolapsing flap) may be clarified by IVUS[33, 65, 66]. (Precise delineation of the entry tears is difficult, however, this may be seen more frequently in the abdominal aorta than in the thoracic aorta[65]**.** The lack of Doppler capabilities is still a drawback of the technique. Thrombus formation within the false lumen may be predicted by of the appearance of spontaneous echo-contrast. Changes in the aortic wall due to haemorrhage into the media are visible by IVUS because of the accompanying increase in wall thickness[65, 66]. IVUS is very accurate in displaying the circumferential and longitudinal extent of the haematoma. Aortic haematomas appear as crescent-shaped or circumferential thickening of the aortic wall[33]. In some segments, an echo-free space is visualized, yielding atypical image of a layered aortic wall[33, 65, 66]. In other areas, speckled granular reflections are recognized within the aortic wall. The shape of this intramural haemorrhage may be concentric and affect the complete aortic circumference, but it is typically limited to a segment of the aorta. IVUS appears particularly useful to rule out the presence of pulsatile intimal flaps and deeply penetrating atherosclerotic ulcers, when others techniques give inadequate results. In addition, it appears particularly attractive for patients with suspected aortic dissection and a normal aortography[33].

Table 1: Comparing the diagnostic value of imaging techniques in aortic dissection.

	TTE/TEE	CT	MRI	Aortography	IVUS
Sensitivity	++	++	+++	++	+++
Specificity	+++	++	+++	++	+++
Classification	+++	++	++	+	++
Tear localization	+++	-	++	+	+
Aortic regurgitation	+++	-	++	++	-
Pericardial effusion	+++	++	++	-	-
Mediastinal haematoma	++	+++	+++	-	+
Side branch involvement	+	++	++	+++	+++
Coronary artery involvement	++	-	+	+++	++
Follow-up studies	++	++	+++	-	-
Intra-operative availability	+++	-	-	+	+

TTE/TEE=transthoracic/transoesophageal echocardiography.

CT=computed tomography.

MRI=magnetic resonance imaging.

IVUS=intravascular ultrasound.

VI: Therapy.

VI-1: Medical therapy.

1, An intensive care unit for appropriate monitoring.

2, A separate intravenous line.

3, Blood pressure monitoring.

4, Control pain (morphine sulphate).

5, Reduce systolic blood pressure to values between 100 and 120 mmHg (beta-blockers, calcium antagonists, sodium nitroprusside).

VI-2: Surgical and interventional therapy.

CAD, IMH and PAU of type A need surgical intervention.

CAD, IMH and PAU of type B should be treated medically; unless with involvement of a branch, untractable pain, rapid progress, unstable hemostasis et al.

References:

1. Godwin JD. Conventional CT of the aorta. J Thorac Imaging 1990; 5: p 18-31.
2. Erbel R, Engberding R, Daniel W et al. Echocardiography in diagnosis of aortic dissection. Lancet 1989; 1: p 457-61.
3. Posniak HV, Olson MC, Demos TC et al. CT of thoracic aortic aneurysms. Radiographics 1990; 10: p 839-55.
4. Nienaber CA, Spielmann RP, von Kodolitsch Y et al. Diagnosis of thoracic aortic dissection.Magnetic resonance imaging versus transesophageal echocardiography. Circulation 1992; 85: p 434-47.
5. Erbel R, Oelert H, Meyer J et al. Influence of medical and surgical therapy on aortic dissection evaluated by transesophageal echocardiography. Circulation 1993; 87: p 1604-15.
6. Erbel R, Alfonso F, Boileau C, et al. Diagnosis and management of aortic dissection. Recommendations of the Task Force on Aortic Dissection, European Society of Cardiology. Eur Heart J 2001; 22: p 1642-1681.
7. Mohr-Kahaly S, Erbel R. Advantages of biplane and multiplane transesophageal echocardiography for the morphology of the aorta. Am J Card Imaging 1995;9: p 115-20.
8. Roberts WC. Aortic dissection:anatomy,consequences and causes. Am Heart J 1981; 101: p 195-214.
9. Nevitt MP, Ballard DJ, Hallet JW . Prognosis of abdominal aortic aneurysms.A population-based study. N Engl J Med 1989; 321: p 1009-14.
10. McNamara JJ, Pressler V. Natural history of atherosclerotic thoracic aortic aneurysms. Ann Thorac Surg 1978; 26: p 468-73.
11. Masuda Y, Takanashi K, Takasu J et al. Expansion rate of thoracic aortic aneurysms and influencing factors. Chest 1992; 102: p 461-6.
12. Sutsch G, Jenni R., von Segesser L et al. Predictability of aortic dissection as a function of aortic diameter. Eur Heart J 1991; 12: p 1247-56.
13. Stefanadis CI, Karayannacos PE, Boudoulas HK et al. Medial necrosis and acute alterations in aortic distensibility following removal of the vasa vasorum of canine ascendind aorta. Cardiovasc Res 1993; 27: p 951-6.
14. Reed D, Reed C, Stemmermann G et al. Are aortic aneurysms caused by atherosclerosis? Circulation 1992; 85: p 205-11.

15. Moles VP, Chappuis F, Simonet F et al. Aortic dissection as complication of percutaneous transluminal coranary angioplasty. Cathet Cardiovasc Diagn 1992; 26: p 8-11.
16. Ammons MA, Moore EE, Moore FA et al. Intra-aortic balloon pump for combined myocardial cotusion and thoracic aortic rupture. J Thauma 1990; 30: p1606-8.
17. Dorsa FB, Tunick PA, Culliford A et al. Pseudo-aneurysm of the thoracic aorta due to cardiopulmonary resuscitation:diagnosis by transesophageal echocardiography. Am Heart J 1992; 123: p1398-400.
18. Fredman C, Serota H, Deligonul U et al. Ascending aortic aneurysm masquerading as fever,altered mental status and mediastinal mass. Am Heart J 1990; 119: p 408-10.
19. Leu HJ. Classification of vasculitides.A survey. Vasa 1995; 24: p 319-24.
20. Webster B, Rich C, Densen PM et al. Studies on cardiovascular syphilis. Am Heart J 1953; 46: p 117-45.
21. Boussou H, Julian M, Pieraggi MT. Aortic lathyrism and atheroma in the rat by prolonged hyperlipidic diet. Gerontology 1978; 24: p 250-65.
22. Boor PJ, Gotlieb AI, Joseph EC et al. Chemical-induced vasculature injury. Toxicol Appl Pharmacol 1995; 132: p 177-95.
23. Grannis FW Jr, Bryant C, CaffarattiJD et al. Acute aortic dissection associated with cocaine abuse. Clin Cardiol 1988; 11: p 572-4.
24. Rashid J, Eisenberg MJ, Topol EJ. Cocaine-induced aortic dissection. Am Heart J 1996; 132: p 1301-4.
25. Crawford ES, Svensson LG, Coselli JS et al. Surgical treatment of aneurysm and/or dissection of the ascending aorta,transverse aortic arch,and ascending aorta and transverse aortic arch.Factors influencing survival in 717 patients. J Thorac Cardiovasc Surg 1989; 98: p 659-74.
26. De Bakey ME, McCollum CH, Crawford ES et al. Dissection and dissecting aneurysms of the aorta:twenty-year follow-up of five hundred and twenty-seven patients treated surgically. Surgery 1982; 92: p 1118-34.
27. Reul GJ, Cooley DA, Hallman GL et al. Dissecting aneurysm of the descending aorta. Arch Surg 1975; 110: p 632-40.

28. Hagan PG, Nienaber CA, Isselbacher EM et al. The international registry of acute aortic dissection (IRAD): new insights into an old disease. JAMA 2000; 283: p 897-903.
29. Fann JI, Sarris GE, Mitchell RS et al. Treatment of patients with aortic dissection presenting with peripheral vascular complications. Ann Surg 1990; 212: p 705-13.
30. Roth JA, Parekh MA. Dissecting aneurysms perforating the esophagus. N Engl J Med 1978; 299: p 776.
31. Spitzer S, Blanco G, Adam A et al. Superior vena cava obstruction and dissecting aortic aneurysm. JAMA 1975; 233: p 164-5.
32. Buja LM, Ali N, Fletcher RD et al. Stenosis of the right pulmonary artery: a complication of acute dissecting aneurysm of the ascending aorta. Am Heart J 1972; 83: p 89-92.
33. Yamada E, Matsumura M, Kyo S et al. Usefulness of a prototype intravascular ultrasound imaging in evaluation of aortic dissection and comparison with angiographic study, transesophageal echocardiography,computed tomography,and magnetic resonance imaging. Am J Cardiol 1995; 75: p 161-5.
34. Spittell PC, Spittell JA, Joyce JW et al. Clinical features and differential diagnosis of aortic dissection:experirence with 236 cases(1980 through 1990). Mayo Clin Proc 1993; 68: p 642-51.
35. Slater EE, DeSanctis RW. The clinical recognition of dissecting aortic aneurysm. Am J Med 1976; 60: p 625-33.
36. Alfonso F, Almeria C, Fernandez-Ortiz A et al. Aortic dissection occurring during coronary angioplasty:angiographic and transesophageal echocardiographic findings. Cathet Cardiovasc Diagn 1997; 42: p 412-5.
37. Kamp TJ, Goldschmidt-Clermont PJ, Brinker JA et al. Myocardial infarction,aortic dissection,and thrombolytic therapy. Am Heart J 1994; 128: p 1234-7.
38. Hartnell GG, Wakeley CJ, Tottlr A et al. Limitations of chest radiography in discriminating between aortic dissection and myocardial infarction: implications for thrombolysis. J Thorac Imaging 1993; 8: p 152-5.
39. Suzuki T, Katoh H, Watanabe M et al. Novel biochemical diagnostic method for aortic dissection. Results of a prospective study using an immunoassay of smooth muscle myosin heavy chain. Circulation 1996; 93: p 1244-9.

40. Mintz GS, Kotler MN, Segal BL et al. Two-dimensional echocardiographic recognition of the desending thoracic aorta. Am J Cardiol 1979; 44: p 232-8.
41. Khandheria BK, Tajik AJ, Taylor CL et al. Aortic dissection: review of value and limitation of two-dimensional echocardiography in a six-year experience. J Am Soc Echocardiogr 1989; 2: p 17-24.
42. Iliceto S, Ettore G, Francisco G et al. Diagnosis of aneurysm of the thoracic aorta. Comparison between two non invasive techniques: two-dimensional echocardiography and computed tomography. Eur Heart J 1984; 5: p 545-55.
43. Gueret P, Senechal C, Roudaut R. Comparison of transesophageal and transthoracic echocardiography in acute aortic dissection. A multicenter prospective study. J Am Coll Cardiol 1991; 17: p 264.
44. Eagle KA. Current management of aortic dissection-data from the International Registry for Aortic Dissection (IRAD). Eur Soc Cardiol 1999; p 3278.
45. Sommer T, Fehske W, Holzknecht N et al. Aortic dissection: a comparative study of diagnosis with spiral CT,multiplanar transesophageal echocardiography, and MR imaging. Radiology 1996; 199: p 347-52.
46. Nienaber CA, von Kodolitsch Y. Diagnostic imaging of aortic diseases. Radiology 1997; 37: p 402-9.
47. Kersting-Sommerhoff BA, Higgins CB, White RD et al. Aortic dissection:Sensitivity and specificity of MR imaging. Radiology 1988; 166: p 651-5.
48. Deutsch HJ, Sechtem U, Meyer H et al. Chronic aortic dissection: comparison of MR imaging and transesophageal echocardiography. Radiology 1994; 192: p 645-50.
49. Nienaber CA, von Kodolitsch Y, Nicolas V et al. The diagnosis of thoracic aortic dissection by noninvasive imaging procedures. N Engl J Med 1993; 328: p 1-9.
50. Wagner S, Auffermann W, Buser P et al. Diagnostic accuracy and estimation of the severity of valvular regurgitation from the signal void on cine magnetic resonance imagings. Am Heart J 1989; 118: p 760-7.
51. Pelc NJ, Herfkens RJ, Shimakawa A et al. Phase contrast cine magnetic resonance imaging. Magn Reson Q 1991; 7: p 229-54.
52. Honda T, Hamada M, Matsumoto Y et al. Diagnosis of Thrombus and Blood Flow in Aortic Aneurysm using Tagging Cine Magnetic Resonance Imaging. Int J Angiol 1999; 8: p 57-61.

53. Solomon SL, Brown JJ, Glazer HS et al. Thoracic aortic dissection:pitfalls and artifacts in MR imaging. Radiology 1990; 177: p 223-8.
54. Robb GP, Steinberg I. Visualization of chambers of heart, pulmonary circulation and great blood vessels in man: a practical method. AM J Roentgenol 1939; 41: p 1-17.
55. Dinsmore RE, Rourke JA, Desanctis RW et al. Angiographic findings in dissecting aortic aneurysm. N Engl J Med 1966; 275: p 1152-7.
56. Shuford WH, Sybers RG, Weens HS. Problems in the aortographic diagnosis of dissecting aneurysms of the aorta. N Engl J Med 1969; 280: p 225-31.
57. Sanders C. Current role of conventional and digital aortography in the diagnosis of aortic disease. J Thorac Imaging 1990; 5: p 48-59.
58. Williams DM, Lee DY, Hamilton BH et al. The dissected aorta: part III. Anatomy and radiologic diagnosis of branch vessel compromise. Radiology 1997; 203: p 37-44.
59. Rackson ME, Lossef SV, Sos TA. Renal artery stenosis in patients with aortic dissections;increasing prevalence. Radiology 1990; 177: p 555-8.
60. Khandheria BK. Aortic dissection: the last frontier. Circulation 1993; 87: p 1765-8.
61. Cigarroa JE, Isselbacher FM, De Sanctis RW et al. Diagnostic imaging in the evaluation of suspected aortic dissection. Old standards and new directions. N Engl J Med 1993; 328: p 35-43.
62. Keren A, Kim CB, Hu BS et al. Accuracy of biplane and multiplane transesophageal echocardiography in diagnosis of typical acute aortic dissection and intramural hematoma. J Am Coll Cardiol 1996; 28: p 627-36.
63. Chirillo F, Cavallini C, Longhini C et al. Comparative diagnostic value of transesophageal echocardiography and retragrade aortography in the evaluation of thoracic aortic dissection. Am J Cardiol 1994; 74: p 590-5.
64. Eagle KA, Quertermous T, Kritzer GA et al. Spectrum of conditions initially suggesting acute aortic dissection but with negative aortograms. Am J Cardiol 1986; 57: p 322-6.
65. Weintraub AR, Erbel R, Gorge G et al. Intravascular ultrasound imaging in acute aortic dissection. J Am Coll Cardiol 1994; 24: p 495-503.
66. Alfonse F, Goicolea J, Aragoncillo P et al. Diagnosis of aortic intramural hematoma by intravascular ultrasound imaging. Am J Cardiol 1995; 76: p 735-8.

Intra-aorta ultrasound imaging in patients with acute aortic syndrome

This article had been submitted to Chinese Medical Journal and its abstract had been orally presented at 2005 ESC meeting.

Hu Wei[1], MD, Francois Schiele[1], MD, PhD, Nicolas Meneveau[1], MD, Marie-France Seronde[1], MD, Pierre Legalery[1], MD, Jean-Francois Bonneville[2], MD, Sidney Chocron[3], MD, Jean-Pierre Bassand[1], MD

[1]Department of Cardiology, University Hospital Jean Minjoz, Besançon, France
[2]Department of Radiology, University Hospital Jean Minjoz, Besançon, France
[3]Department of Cardiac Surgery, University Hospital Jean Minjoz, Besançon, France

Abstract

Background: Computer tomography (CT), transesophageal echography (TEE), magnetic resonance imaging (MRI) and aortography have been demonstrated to be useful in patients with acute aortic syndrome (AAS).

Objectives: To explore potential values of intra-aorta ultrasound (IAUS) imaging in patients with AAS.

Methods: Patients with established or suspected AAS who underwent CT alone or combination with TEE, MRI or aortography were enrolled. IAUS imaging was performed by use of a 9-MHZ probe. Compared with other imaging techniques, we assess that if IAUS can provide additional useful information.

Results: From August 2002 to October 2004, 13 consecutive patients were included. IAUS had no complications in all patients. In one patient with aortic aneurysm: both CT and IAUS excluded possible dissection or rupture of the aneurysm. In one patient with acute chest pain: IAUS detected a subtle aortic dissection omitted by CT and TEE. In four patients with intrumural hematoma (IMH): IAUS not only detected longitudinal and circumferential extent, relationship with side branches, pleural effusion, it also detected an accompanied penetrating atherosclerotic ulcer (PAU) in 3 of them (one was suspected by CT, one was overlooked by CT and one escaped other four imaging techniques). In seven patients with classic aortic dissection: IAUS delineated intimal flap, true and false lumen, longitudinal and circumferential extent, relationship with side branches, thrombus, pleural effusion, replaced graft and its pathologic changes, accompanied aneurysm, IMH and PAU. Among these aspects: 3 entry sites, 10 re-entry sites, 2 thrombus, 1 involved branch, 2 pathologic changes of the graft, 1 complex dissection morphology and 1 multiple PAUs that detected by IAUS were overlooked by other imaging techniques. In all, IAUS could provide additional useful information in 11 (85%) patients.

Conclusion: IAUS imaging is safe and may be useful in patients with established or suspected AAS.

Key word: Acute aortic dissection; intramural haematoma; acute aortic syndrome; intravascular ultrasound.

1.Introduction:

Classic aortic dissection (CAD), intramural hematoma (IMH) and penetrating atherosclerotic ulcer (PAU) are three anatomic presentations of acute aortic syndrome (AAS) [1]. Although AAS is an uncommon disease, it has high mortality and modality. A prompt diagnosis is often imperative in patients with type A AAS because the mortality rate increases with time[2]. Aortography had been considered as a standard modality for the diagnosis of AAS. During the past two decades' years, non-invasive imaging techniques such as computer tomography (CT), transesophageal echography (TEE) and magnetic resonance imaging (MRI) have been demonstrated to have high sensitivity and specificity [1, 2]. However, under non-urgent circumstances, complete information of the entire aorta is often necessary for the diagnosis and the management of the patients with established or suspected AAS. Four current used modalities, namely as aortography, CT, TEE and MRI, all have limitations in doing so[1-3].

IVUS has been demonstrated as a useful tool in patients with coronary heart disease (CHD). Because it can directly visualise vascular wall from interior and supply us a good real-time cross-sectional image, so it potentially plays an important role in patients with AAS. Some authors have performed intra-aorta ultrasound (IAUS) imaging for the diagnosis of AAS and the performance of endovasular repair [4-8]. However, its role has far more established. Moreover, most of these studies used a 20-MHZ IVUS probe, which has limitation in a dilated aorta. Recently, a new IVUS probe with 9-MHZ was commercially available, which may theoretically overcome this problem.

Therefore, in this study, we aimed to explore potential values of IAUS imaging with a 9-MHZ probe in patients with established or suspected AAS.

2.Methods:

Patients: This is a single centre, perspective and observational study. We included patients with established or suspected AAS who underwent CT alone or combination with TEE, MRI or aortography, and excluded patients who wouldn't give their informed content or under unstable conditions. CAD was defined as an aortic intimal flap separating the true and the false lumen. IMH was defined as a variant of aortic dissection (AD) characterized by absence of flow in the false lumen. PAU was defined as an ulceration of an atherosclerotic lesion that penetrates from the internal elastic lamina into the media. The Stanford's classification was adopted for AAS

(type A means AAS involves the ascending aorta, whereas type B means AAS doesn't involve the ascending aorta). AAS was defined as the occurrence within 14 days.

IAUS imaging: A 9 F 9-MHZ mechanic IVUS probe (Ultra ICE^{TM} intracardiac Echo catheter, Boston Scientific) was introduced to the root of aorta with the help of a 0.035-inch guide wire and a 110 cm sheath under fluoroscopy via right femoral artery. After obtaining an optimal cross-sectional aortic image, it was manually pulled back and IVUS imaging was simultaneously recorded on the videotape for subsequent analysis. A single bolus of 5000 U classic heparin was administrated intravenously before procedure. The accessing site was closed by 8F Angioseal after procedure.

IAUS image analysis: Two cardiologists (HW&FS) who were blinded to the results of other imaging techniques performed IAUS image analysis respectively and gave the final report after discussion. The intimal flap was defined as a moving structure that separated different lumens. The true and the false lumen were distinguished by following criteria: First, the true lumen is usually smaller. Second, the false lumen is often partly thrombosed. Third, the IAUS probe locates in the true lumen. Forth, most branches take off from the true lumen. Fifth, the flow pattern is often whirling in the false lumen. The entry site and the re-entry site were defined as uncontinuous site of intimal flap, which permitted blood goes from one lumen into another lumen, the most proximal one was defined as the entry site and the rests were defined as the re-entry sites. A protractor that was put on the centre of the true lumen measured the circumferential extent. The longitudinal extent was measured by using side branches and two-dimensional image reconstruction. Thrombus was defined as a hyperechogenecity or hypoechogenecity intraluminal mass with a layered or lobulated appearance that located in the false lumen. Side branches and their relationship with true and false lumen and intimal flap were also recorded. The replaced tube graft appeared as a single density hyperechogeneric circular structure, its pathologic changes were also recorded. Aortic dissection was deemed present when an intimal flap separating the aorta into a true and false lumen (see figure 1) [6]. The appearance of IMH consisted of an aortic wall thickening that either included an echo-free space intramural or structures of different echogenecity within the aortic wall (see figure 2)[4-6]. PAU was defined as a ruptured plaque in connecting with an intramural echo-free space (see figure 3)[9].

Other imaging techniques and analysis: Spiral CT (Simens, 4 multibarret, with and without injection of contrast media), TEE (with mono-, bi- and multi- planar 5 MHZ probe, Hewlett Packard), MRI (General electricity, 3 Telsa , with and without contrast) and aortography(at least two orthogonal projections) were performed by using current available instruments and standard methods. Other experts interpreted these images by adopting standard definitions.

3.Results:

Patient demographics (see Table 1):

From August 2002 to October 2004, a cohort of 13 consecutive patients (12 men and 1 woman; mean age 65±12 years old) was included. 10(77%) patients with hypertension (HTA), 7(54%) with hypercholesterolemia (HCT), 2(15%) with diabetes mellitus (DM), 7(54%) with cigarette smoking (CS), 2(15%) with family history (FH). 5(38%) patients had coronary heart disease (CHD) and 4(31%) patients had chronic insufficient renal function (CIRF). For all 13 enrolled patients: 1 with ascending aortic aneurysm(AAA), 1 with subtle AD, 4 with acute type B IMH and 7 with CAD (2 chronic type A, 3 acute and 2 chronic type B; 4 of them had undergone a Bentall's procedure with replacement of ascending aorta by a tube graft).

IAUS findings and compared with other imaging techniques (see table 2):

CT, TEE, MRI and aortography were performed in 13(100%), 5(38%), 2(15%) and 5(38%) patients respectively. In all patients, IAUS was performed without complications. The mean procedure time was 15±8 minutes. IAUS supplied us a good cross-sectional image of entire aorta (from aortic root to bifurcation of iliac artery) even of a very dilated one (the biggest aortic diameter was 79mm) and most of its branches. The detecting rate of three arch branches (innominate artery, left common carotid artery and left subclavian artery), celiac trunk artery, superior and inferior mesenteric artery, and two renal arteries were 100%.

The patient with AAA occurred acute chest pain, both CT and IAUS excluded possible dissection or rupture of his aneurysm. In the patient with SAD:IAUS documented no rupture evidence of an atherosclerotic plaque locating at ascending aorta doubted by CT and TEE, and it detected a SAD at descending aorta omitted by CT and TEE. In 4 patients with IMH: IAUS could detect longitudinal and circumferential extent, relationship with side branches, pleural effusion, it also detected three PAUs in 3 of them (one per case), one was suspected by CT, one was overlooked by CT and one escaped CT, TEE, MRI and aortography. In 7

patients with CAD: IAUS could delineate intimal flap, true and false lumen, longitudinal and circumferential extent, relationship with side branches, thrombus, pleural effusion, graft and its pathologic changes, the accompanied aneurysm, IMH and PAU, among these aspects, 3 entry sites (particularly in one patient with acute type B CAD, of whom the entry site was omitted by CT and TEE, he received endovascular stent repair because of rapid progression and the procedure was guided by IAUS), 10 re-entry sites, 2 thrombus, involvement of a left carotid artery, 2 pathologic changes of the graft (two suture dehiscences, one with IMH and one with leakage, 1 complex dissection morphology (one true and two false lumens) and 1 multiple PAUs (3 PAUs in one patient) detected by IVUS were overlooked by other imaging techniques. In summary, IAUS could provide additional information in 11 (85%) patients, which was considered as helpful for the diagnosis and management.

Treatment and follow up:

All patients were followed by telephone interview or clinic visit. The mean follow up time was 14±8 months (from 1 month to 26 months). 3 were operated on because of aneurismal dilatation, 1 was treated by endovascular stent-graft repair and the rests received medical therapy. All kept well except three, one patient who received a stent occurred cerebral haemorrhage 18 months later, two patients with IMH accompanied by a PAU developed into a big aneurysm several months later.

Discussion:

CAD, IMH and PAU are three anatomic presentations of acute aortic syndrome[1]. Although AAS is an uncommon disease, it has high mortality and modality. A prompt diagnosis is often imperative in patients with type A AAS because the mortality rate increases with time[2]. Aortography had long time been considered as a standard modality for the diagnosis of AAS. During the past two decades' years, non-invasive imaging techniques such as CT, TEE and MRI have been demonstrated high sensitivity and specificity [1, 2] However, under non-urgent circumstances, complete information of the entire aorta is often necessary for the diagnosis and the management. 4 current used modalities, namely as aortography, CT, TEE and MRI, all have some limitations in doing so[1, 2, 10, 11].

Intravascular ultrasound (IVUS) permits a direct visualising of vascular wall, it supplies us a good real-time cross-sectional image, and it has been demonstrated as a useful tool in patients with CHD. A few studies have evaluated its role in patients with AAS. In 1990, Weintraub et al first performed IVUS in a patient with acute AD[12].

In 1994, the same authors performed IVUS in 23 patients with AD, and demonstrated that IVUS could detect the true and the false lumen, the longitudinal and circumferential extent of AD, the content of the false lumen, involvement of branch vessels and the presence of IMH in the aortic wall. They thought that IVUS could be used as an alternative or adjunct diagnostic modality in patients with AD[6]. In 1995, Yamada et al performed IVUS in 15 patients with chronic AD, and concluded that IVUS was very useful in providing complete information on the abdominal aorta[5]. Alfonso et al performed IVUS in 8 patients with IMH. The correct diagnosis was not evident by TEE in 2 of these patients. Their findings indicated the value of IVUS in patients with IMH in ruling out classic aortic dissection[4]. However, up to now, the role of IVUS in the setting of AAS has far more established. Moreover, these previous studies often used a 20-MHZ IVUS probe, which had limitations in a dilated aorta. Recently, a 9-MHZ mechanic IVUS probe was commercially available, which may theoretically overcome this problem.

In our study, we performed IAUS imaging with a 9-MHZ probe in 13 patients with or with suspected AAS. According to IRAD study, CT is the most often used modality in patients with suspected AD because it is easily available and less cost. TEE is the second often used modality. In our study, CT, TEE, MRI and aortography were performed in 13(100%), 5(38%), 2(15%) and 5(38%) patients respectively, so our choice of imaging techniques could reflect current clinic practice. However, we didn't perform TEE routinely as the second choice because most of ADs and IMHs in our patients extended into abdominal aorta. Moreover, we excluded unstable patients because of whom an urgent intervention is often needed.

Our study showed that IAUS imaging was very safe and it supplied us a good cross-sectional image of entire aorta even of a very dilated one and most of its branches. The biggest aortic diameter was 79 mm in our patients, while IAUS with a 20-MHZ probe had difficulty in interrogating an aorta bigger than 45 mm. The detecting rate of three arch branches, celiac trunk artery, superior and inferior mesenteric artery, and renal branch were 100%. However, as stated by other authors, IAUS imaging with a 20-MHZ probe had difficulty in detecting three arch branches.

In 7 patients with AD, IAUS could delineate the intimal flap, the true and false lumen, the longitudinal and circumferential extent, the relationship with a side branch, the thrombus, the pleural effusion, the graft and its pathologic changes, the accompanied aneurysm, IMH and PAU. Among these aspects, 3 entry sites, 10 re-entry sites, 2

thrombus, 1 involvement of a branch, 2 pathologic changes of the graft, 1 complex dissection morphology and 1 multiple PAUs that detected by IAUS were overlooked by other imaging techniques. Therefore, we think that IAUS imaging could provide more details of these aspects, and it is worth to note IAUS imaging had a dramatic advantage over other modalities in detecting the entry and the re-entry site. Furthermore, some authors showed that IAUS was helpful for directing endovascular stent-graft repair and fenestrating of an intimal flap[7, 8] in patients with AD, in one of our patients, IAUS was used to guide endovascular stent-graft repair.

Many studies have demonstrated that IMH with a PAU often has a worse outcome than IMH without a PAU[13, 14] and proposed an aggressive treatment. So, it is very important to make sure if IMH is caused by a PAU. However, sometimes because of its small size, the detection of a PAU is challenged by other imaging techniques. Our study included 4 patients with IMH. IAUS could detect the longitudinal and circumferential extent, the relationship with a side branch, the pleural effusion. Moreover, IAUS detected three PAUs in 3 of them (one per case) , one was suspected by CT, one was overlooked by CT and one escaped CT, aortography, TEE and MRI. Therefore, compared with other imaging techniques, IAUS was more sensitive to detect a PAU in patients with IMH. Considering together with the patient with multiple PAUs that were omitted by CT, MRI and aortography, we think that IVUS imaging may be an optimal modality of detecting a PAU. Till now, the occurrence rate and the natural history of PAU are not known and there is no standard treatment strategy. In our study, the PAUs in the patient with CAD were treated surgically because of aneurismal dilatation, the PAUs in other three patients with IMH were treated conservatively and two of them developed into a big aneurysm. Thus, we agree with others, IMH with a PAU should be treated aggressively and the endovascular stent-graft repair seems to be a good choice.

In summary, compared with CT alone or combination with TEE, MRI and aortography, IAUS could provide additional information in 11 (85%) patients that was helpful for the diagnosis or for the management. However, we had to admit that our outcome was possibly overestimated: First, IAUS imaging was performed in some selected patients when there are some doubts or difficulties for the diagnosis and the management by other imaging techniques. Second, we didn’t include other important information such as aortic valve, pericardium effusion and coronary arteries, however,

we think that these situations usually attribute to urgent ones and may be provided by simple transthroacic echocardiography.

Study Limitations: First, our patient group was very small and highly selected one, a randomised study needs to be performed. Second, although there was no complication in our study, IAUS imaging is an invasive examination that has potential damages. Third, the IAUS system we used couldn’t supply us a circular cross-sectional image at the beginning of descending aorta. But it didn’t affect the analysis of this segment. Forth, although the time interval between IAUS imaging and other imaging techniques was within one week and there was no evidence of clinic progression, we couldn't exclude possible changes of AAS during that period of time.

Conclusion: Our study showed that IAUS imaging was very safe. Even in a very dilated aorta, it could supply us a good cross-sectional image of entire aorta and most of its branches. By comparison with CT alone or combination with TEE, MRI or aortography, IAUS can supply us more detailed data those are very useful in the diagnosis and management of patients with established or suspected AAS.

References:

1. Erbel R. Alfonso F, Boileau C, Dirsch O, Eber B, et al., *Diagnosis and management of aortic dissection.* Eur Heart J, 2001. **22**(18): p. 1642-81.
2. Hagan PG, Nienaber CA, Isselbacher EM, Bruckman D, Karavite DJ, et al., *The International Registry of Acute Aortic Dissection (IRAD): new insights into an old disease.* Jama, 2000. **283**(7): p. 897-903.
3. Khan IA, Nair CK. *Clinical, diagnostic, and management perspectives of aortic dissection.* Chest, 2002. **122**(1): p. 311-28.
4. Alfonso F, Goicolea J, Aragoncillo P, Hernandez R, Macaya C. *Diagnosis of aortic intramural hematoma by intravascular ultrasound imaging.* Am J Cardiol, 1995. **76**(10): p. 735-8.
5. Yamada E, Matsumura M, Kyo S, Omoto R. *Usefulness of a prototype intravascular ultrasound imaging in evaluation of aortic dissection and comparison with angiographic study, transesophageal echocardiography, computed tomography, and magnetic resonance imaging.* Am J Cardiol, 1995. **75**(2): p. 161-5.
6. Weintraub AR, Erbel R, Gorge G, Schwartz SL, Ge J, et al., *Intravascular ultrasound imaging in acute aortic dissection.* J Am Coll Cardiol, 1994. **24**(2): p. 495-503.
7. Dake MD, Miller DC, Semba CP, Mitchell RS, Walker PJ, et al. *Transluminal placement of endovascular stent-grafts for the treatment of descending thoracic aortic aneurysms.* N Engl J Med, 1994. **331**(26): p. 1729-34.
8. Chavan A, Hausmann D, Dresler C, Rosenthal H, Jaeger K, et al. *Intravascular ultrasound-guided percutaneous fenestration of the intimal flap in the dissected aorta.* Circulation, 1997. **96**(7): p. 2124-7.
9. Vilacosta I, San Roman JA, Aragoncillo P, Perreiros J, Mendez R, et al. *Penetrating atherosclerotic aortic ulcer: documentation by transesophageal echocardiography.* J Am Coll Cardiol, 1998. **32**(1): p. 83-9.
10. Svensson LG, Labib SB, Eisenhauer AC, Butlerly JR. *Intimal tear without hematoma: an important variant of aortic dissection that can elude current imaging techniques.* Circulation, 1999. **99**(10): p. 1331-6.
11. Batra P, Bigoni B, Manning J, Aberle DR, Brown K, et al. *Pitfalls in the diagnosis of thoracic aortic dissection at CT angiography.* Radiographics, 2000. **20**(2): p. 309-20.

12. Weintraub AR, Schwartz SL, Pandian NG, Katz SE, Kwon OJ, et al. *Evaluation of acute aortic dissection by intravascular ultrasonography.* N Engl J Med, 1990. **323**(22): p. 1566-7.
13. Ganaha F, Miller DC, Sugimoto K, Do YS, Minamiguchi H, et al. *Prognosis of aortic intramural hematoma with and without penetrating atherosclerotic ulcer: a clinical and radiological analysis.* Circulation, 2002. **106**(3): p. 342-8.
14. Coady MA, Rizzo JA, Hammond GL, Poerce JG, Kopf GS, et al. *Penetrating ulcer of the thoracic aorta: what is it? How do we recognize it? How do we manage it?* J Vasc Surg, 1998. **27**(6): p. 1006-15; discussion 1015-6.

Table 1: patient demographics.

Case	Gendre	Age	HTA	HCT	DM	Smoke	FH	CIRF	CHD	AS	Symptom
1	M	53	+	-	-	-	-	-	-	+	-
2	M	68	-	+	-	+	-	-	+	+	-
3	M	74	+	+	+	-	-	-	-	+	-
4	M	66	+	+	-	+	+	-	-	+	+
5	M	63	+	-	-	-	-	+	-	-	+
6	F	73	+	+	-	-	+	-	+	+	+
7	M	70	+	+	-	-	-	+	-	+	+
8	M	54	+	-	-	+	-	-	-	-	+
9	M	75	+	-	-	-	-	+	+	-	+
10	M	73	-	-	-	+	-	-	+	-	+
11	M	74	+	-	-	+	-	+	-	+	+
12	M	61	+	+	+	+	-	-	-	-	+
13	M	66	-	+	-	+	-	-	+	-	+

M=male, F=female, CIRF=chronic insufficient renal function, AS=aortic syndrome, Symptom represented acute chest, back and abdominal pain.

Table2: IAUS findings and compared with other imaging techniques.

Diagnosis	Total	Other imaging techniques				IAUS	Additional information
		CT	TEE	MRI	Aortography		
CAD	7	7	2	2	2	7	7
Entry site	7	4	1	1	1	7	
Re-entry site	13	2	1	1	0	13	
Thrombus	4	2	1	1	0	4	
With IMH	2	1	1	1	0	2	
Involved a branch	2	1	0	1	0	2	
With PAU	3	0	0	0	0	3	
Graft changes	3	1	1	1	0	3	
IMH	4	4	1	1	1	4	3
With PAU	3	1	0	0	0	3	
Non-AAS	**2**	**2**	**1**	**0**	**1**	**2**	1
Aneurysm	1	1	0	0	0	1	
Subtle AD	1	0	0	0	0	1	

Figure 1:

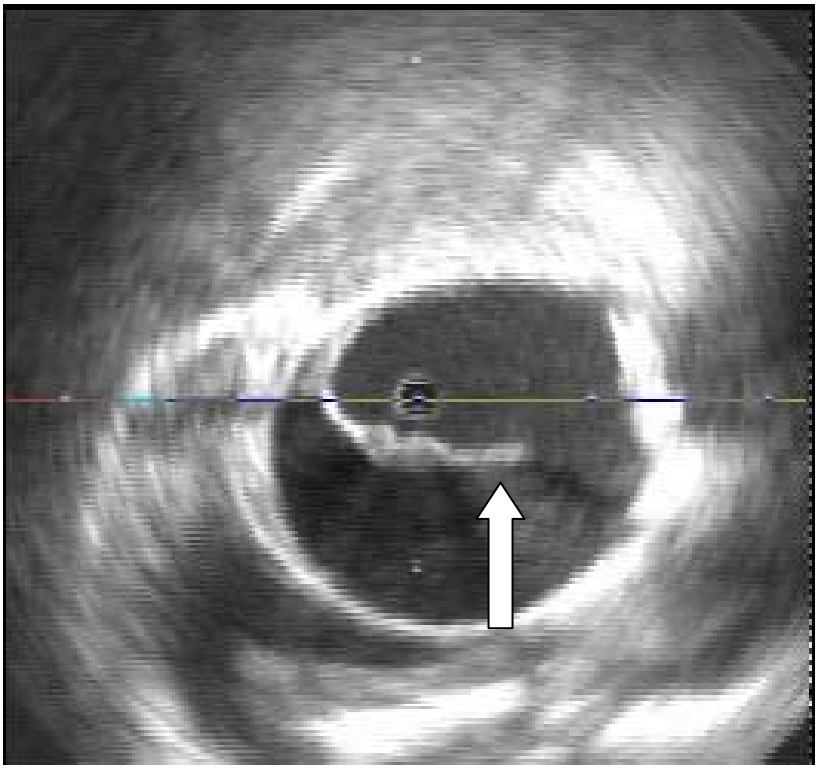

An example of classic aortic dissection (IVUS image).

Figure 2:

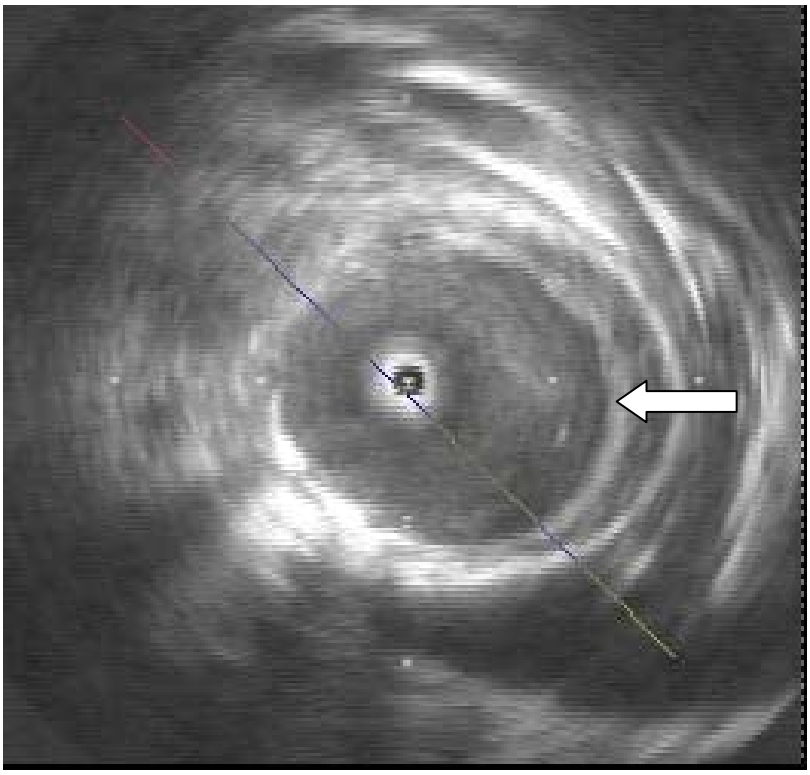

An example of intramural hematoma (IVUS image).

Figure 3:

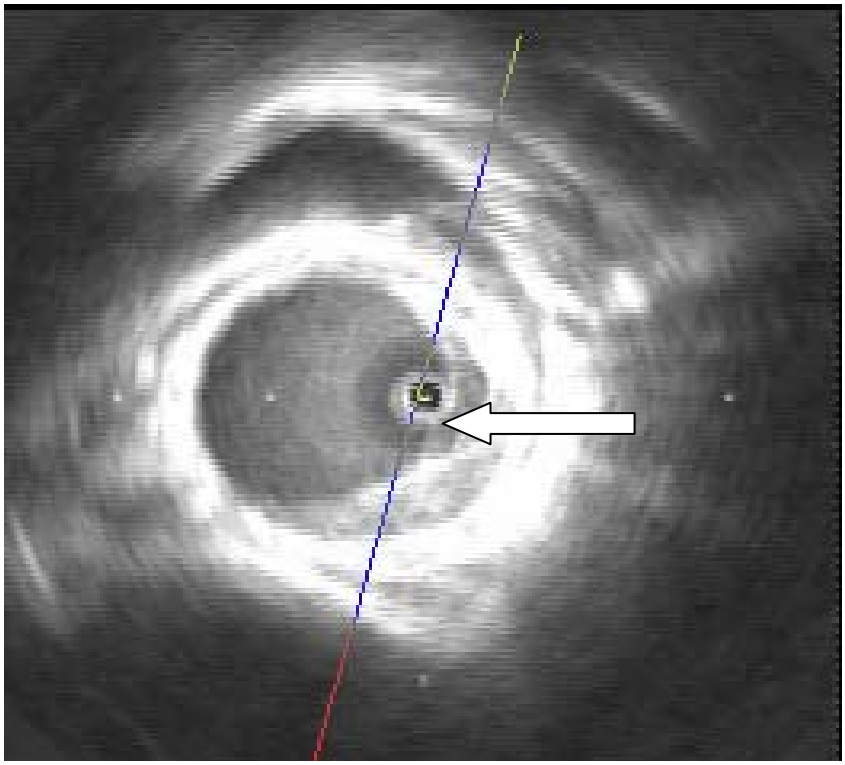

An example of penetrating atherosclerotic ulcer (IVUS image).

The value of intravascular ultrasound imaging in diagnosis of aortic intramural hematoma

This article had been submitted to Chinese Medical Journal (Under consideration)

Hu Wei[1], MD, Francois Schiele[1], MD, PhD, Nicolas Meneveau[1], MD, Marie-France Seronde[1], MD, Pierre Legalery[1], MD, Jean-Francois Bonneville[2], MD, Sidney Chocron[3], MD, Jean-Pierre Bassand[1], MD

[1]Department of Cardiology, University Hospital Jean Minjoz, Besançon, France
[2]Department of Radiology, University Hospital Jean Minjoz, Besançon, France
[3]Department of Cardiac Surgery, University Hospital Jean Minjoz, Besançon, France

Abstract:

Backgrounds: The value of intravascular ultrasound (IVUS) imaging is undefined in diagnosis of aortic intramural hematoma (AIH).

Objectives: To evaluate the value of IVUS imaging in diagnosis of AIH.

Methods: From September 2002 to May 2005, a consecutive series of 15 patients with suspected aortic dissection (AD) underwent both IVUS imaging and spiral computed tomography (CT). Six patients diagnosed as type B AIH by CT or IVUS composed the present study group.

Results: There were no complications related to IVUS imaging in all the patients. The study group consisted of five males and one female with mean age of 66 years old. Four of them had hypertension and symptom. In one patient, CT omitted a localized AIH and an associated penetrating atherosclerotic ulcer (PAU) those were detected by IVUS. In another patient, CT mistook a partly thrombosed false lumen as an AIH, whereas IVUS detected a subtle intimal tear and slow moving blood in the false lumen. In the four rest patients, Both CT and IVUS made the diagnosis of AIH, however, IVUS detected 3 PAUs in 3 of them, only 1 of them was also detected by CT, and 2 of them escaped initial CT and were confirmed by follow up CT or magnetic resonance imaging (MRI).

Conclusions: IVUS imaging is a safe examination and has high accuracy in diagnosis of AIH, and it is specially helpful for diagnosing localized AIH, distinguishing AIH with thrombosed classic AD and detecting accompanied small PAU.

Key words: Intravascular Ultrasound, Aortic Intramural Hematoma.

1. Introductions:

AIH, first described in 1920 by Krukenberg[1], is characterized by the absence of intimal tear and direct flow communicating between the true and the false lumen. With advent of non-invasive imaging techniques such as: CT, MRI and transesophageous echography (TEE), AIH has been frequently recognized. Although these non-invasive modalities have been reported to have accuracy in diagnosis of AIH [2-5], they also have some limitations [3, 6-8].

Only a few studies have evaluated the value IVUS imaging in patients with acute aortic syndrome (AAS), moreover, all of them used a 20 MHZ IVUS probe that has limitations in a dilated aorta [6, 9-12]. Recently, a 9 MHZ IVUS probe is commercially available, however, the experiences about it are very scant.

2. Methods:

2.1 Patients: This was a single centre, prospective and observational study. We included patients with suspected AD after obtaining an informed content and excluded patients who need an urgent intervention. All patients underwent both IVUS imaging and spiral CT. CT was performed within 24 hours from onset of symptom, and the interval time between CT and IVUS imaging was less than 1 week. In the present study, we will focus on the patients who were diagnosed as AIH by CT or IVUS.

2.2 IVUS imaging: A 9 F 9-MHZ mechanic IVUS probe (Ultra ICE^{TM} intracardiac Echo catheter, Boston Scientific) was introduced to aortic root with the help of a 0.035-inch guide wire and a 110 cm long sheath under fluoroscopy via right femoral artery. After obtaining an optimal cross-sectional aortic image, it was manually pulled back and IVUS images were simultaneously recorded on the videotape for subsequent analysis.

2.3 IVUS imaging analysis: Two cardiologists (HW&FS) who were blinded to the results of other imaging techniques performed IVUS imaging analysis. We adopted Alfonso's definition for AIH by IVUS and made some modifications, AIH was defined as a crescentic, focal or diffuse thickening aortic wall with layered structures separated by echolucent spaces. PAU was defined as a crescentic, localized and outpouching thickening aortic wall with heterogenerous echoic density that communicated with the lumen via an uncontinuous intimal. The circumferential and

longitudinal extent of an AIH, as well as its relationship with aortic side branches and peri-aortic effusion were also recorded.

2. Spiral CT and analysis: We performed spiral CT (Simens, 4 multibarret, with and without injection of contrast media) by using standard methods. Expertise radiologists interpreted CT by adopting standard definitions. Briefly, without contrast, an AIH is defined as crescentic or circular, focal or diffuse thickening aortic wall with a higher density than blood, with contrast, it has the same features, while with a lower density than blood. PAU is defined as a narrow neck, outpouching, contrast filled ulceration [2, 4, 5].

3. Results:

3.1 Patient demographics (see table 1): From September 2002 to May 2005, a consecutive series of 15 patients underwent both IVUS imaging and spiral CT. Six of them diagnosed as AIH by these two modalities composed the current study, which included five males and one female with mean age was 66 years old. Four of them had hypertension and symptom. Except CT and IVUS, four of them were also performed TEE or MRI or aortography,

3.2 IVUS findings and compared with CT (see table 2): There were no complications related to IVUS imaging in all the patients and the mean procedure time was 15 minutes. Even in a very dilated aorta, IVUS could provide a good cross-sectional aortic image of entire aorta and most of side branches. The biggest aortic diameter was 89 mm. The detecting rate of three arch branches, celiac trunk artery, superior and inferior mesenteric arteries, and renal arteries were 100%.

In case 1 (see figure 1), CT omitted a localized AIH and an associated PAU those were detected by IVUS. In case 2 (see figure 2), CT mistook a partly thrombosed false lumen as an AIH, whereas IVUS detected a subtle intimal tear and slow moving blood in the false lumen. In case 3, 4, 5 and 6, both CT and IVUS made the diagnosis of type B AIH. However, IVUS detected three accompanied PAUs, only one of them was also detected by CT (see figure 5), two others were overlooked by CT and confirmed by follow up CT or MRI (see figure 3 and 4).

3.3 Treatment and follow up information (see table 2): All patients received medical therapy except case 1, who was treated surgically because of aneurismal dilatation of the false lumen. All of them were followed by clinic visits or telephone interviews and received regular CT examinations. The mean follow up time was 17.7±12.2 months (ranged from 4 to 33). No deaths occurred. In case 3, 4 and 5, the

AIH developed into aneurysm at site of the PAU. The AIH almost resolved completely in case 6. The subtle intimal tear kept unchanged in case 2.

Discussion

AIH was first described in 1920 by Krukenberg [1], characterized by the absence of intimal tear and direct flow communicating between true and false lumen. Because aortogrphy had been long time as a standard imaging technique in patients with aortic disease and it is insensitive in diagnosis of AIH, AIH was less recognized before. With advent of non-invasive imaging techniques such as CT, TEE and MRI, AIH has been frequently reported. By using these non-invasive modalities, the prevalence of AIH among patients with suspected AAS is ranged from 5% to 20%, correlated well with autopsy studies that ranged from 4% to 13% [4, 13-15]. Although these non-invasive modalities have been demonstrated to have high accuracy in diagnosis of AIH, they also have some limitations [2-8].

In 1990, Weintraub et al first performed IVUS imaging in a patient with acute CAD[9] .After that, several studies have evaluated the value of IVUS imaging in patients with CAD, but up to now, only one study performed IVUS imaging in a series of 8 patients with AIH [6, 9-12]. Therefore, the role of IVUS imaging is far more established in patients with AIH. Moreover, all these studies used a 20-MHZ IVUS probe, which had limitations in a very dilated aorta. Recently, a 9 MHZ IVUS probe is commercially available, which can theoretically overcome this kind of limitation. However, the experiences about it are very scant. To our knowledge, our study is the first one that used this new system in a series of patients with suspected AD. Not surprisingly, our study showed that it could supply us a good cross-sectional aortic image of entire aorta even in a very dilated aorta and most of its side branches.

According to international registration of aortic dissection (IRAD) study, CT is presently the most often used imaging technique, and it often needs two or more imaging techniques to establish the diagnosis of AIH [4, 5]. In our study, all six patients underwent spiral CT and 4 of them were also performed TEE or MRI or aortography, which may reflect the actual clinical practice. It is generally accepted that spiral CT has similar accuracy as TEE and MRI in diagnosis of AIH. Therefore, IVUS findings were mainly compared with those of spiral CT in our study.

We adopted Alfonso's definition for AIH by IVUS and made some modifications [6]. By using this definition, IVUS imaging made the diagnosis of AIH in five patients, CT

confirmed four, but one localized AIH was overlooked by CT. In addition, CT made a false diagnosis of AIH in one case, because it overlooked a subtle intimal tear and slow moving blood in the false lumen those were detected by IVUS. Thus, we believe that IVUS has high accuracy in diagnosis of AIH. However, we can't draw any definite conclusions on the sensitivity and specificity of IVUS in diagnosis of AIH because of our small sample size and non-randomised characteristics.

In 1995, Alfonso et al reported that two localized AIHs detected by IVUS were overlooked by TEE [6]. In our study, as stated above, one localized AIH detected by IVUS was overlooked by CT. Therefore, we think that IVUS may be more sensitive than non-invasive imaging techniques to detect a localized AIH.

Although current used imaging techniques have high sensitivity and specificity in diagnosis of CAD, it is still a big problem for them to differentiate an AIH from a CAD with a subtle intimal tear and a fully or partly thrombosed false lumen[2]. One case example in our study showed that IVUS could be helpful in this aspect.

Despite it still exists debates [16-19], more and more authors agree that the prognosis of AIH with a PAU is worse than that without a PAU. Recently, Ganaha et al reported the occurrence of 52% PAU in their patients with AIH by using CT, and they demonstrated that AIH with PAU had poorer outcome than AIH without PAU [17]. However, small PAU will escape current used imaging techniques [18, 19]. In our study, four of five AIH were found by IVUS to be accompanied by a PAU, one of them was also detected by CT, and two of three rests were confirmed by follow up CT or MRI. So we believe that IVUS is more sensitive than CT to detect a small PAU. The frequency of PAU in patients with AIH reported by us was strikingly higher than that reported by others, which should be interpreted cautiously because we included exclusively type B AIH and used a different modality.

Study limitations: 1) Although there were no complications in our study, IVUS imaging is an invasive examination that has potential damages. 2), Although the time interval between IVUS imaging and CT was short and there was no evidence of clinic progression, we couldn't exclude possible changes during that period of time. 3) Not all PAUs had confirmations, so we can't exclude the false positive one.

Conclusion: IVUS imaging is a safe examination and has high accuracy in diagnosis of AIH, and it is specially helpful for diagnosing localized AIH, distinguishing AIH with thrombosed classic AD and detecting accompanied small PAU.

References:

1. Krukenberg, E. *beitrage zur Frage des Aneurysma dissecans.* Beitr Pathol Anat Allg Pathol, 1920. **67**: p. 329-351.

2. Erbel R, Alfonso F, Boileau C, Dirsch O, Eber B, et al. *Diagnosis and management of aortic dissection.* Eur Heart J, 2001. **22(18)**: p. 1642-1681.

3. Harris JA, Braverman AC, Guierrez FR, Barzilai B, Davila-Roman VG. *Transesophageal echographic and clinical features of aortic intramural hematoma.* J Thorac Cardiovasc Surg, 1997. **114**: p. 619-626.

4. Evangelista A, Mukherjee D, Mehta RH, O'Gara PT, Fattori R, et al. *Acute intramural hematoma of aorta: a mystery in evolution.* Circulation, 2005. **111**: p. 1063-1070.

5. Hagan PG, Nienaber CA, Isselbacher EM, Bruckman D, Karavite DJ, et al. *The international Registry of Acute Aortic Dissection (IRAD): New insights into an old disease.* JAMA, 2000. **283(7)**: p. 897-903.

6. Alfonso F, Goicolea J, Aragoncillo P, Hernandez R, Macaya C. *Diagnosis of aortic intramural hematoma by intravascular ultrasound imaging.* Am J Cardiol, 1995. **76(10)**: p. 735-738.

7. Berdat PA, Carrel T. *Aortic dissection limited to the ascending aorta mimicking intramural hematoma.* Eur J Cardiothorac Surg, 1999. **15**: p. 108-109.

8. Svensson LG, Labib SB, Eisenhauer AC, Butterly JR. I*ntimal tear without hematoma : an important variant of aortic dissection that can elude current imaging techniques.* Circulation, 1999. **99**: p. 1331-1336.

9. Weintraub AR, Schwartz SL, Pandian NG, Katz SE, Kwon DJ, et al. *Evaluation of acute aortic dissection by intravascular ultrasonography (letter).* N Engl J Med, 1990. **323(22)**: p. 1566-1567.

10. Weintraub AR, Erbel R, Gorge G, Schwartz SL, Ge J, et al. *Intravascular ultrasound imaging in acute aortic dissection.* J Am Coll Cardiol, 1994. **24(2)**: p. 495-503.

11. Yamada E, Matsumura M, Kyo S, Omoto R. *Usefulness of a prototype intravascular ultrasound imaging in evaluation of aortic dissection and comparison*

with angiographic study, transesophageal echocardiography, computed tomography, and magnetic resonance imaging. Am J Cardiol, 1995. **75(2)**: p. 161-165.

12. Chavan A, Hausmann D, Dresler C, Rosenthal H, Jaeger K, et al. *Intravascular ultrasound-guided percutaneous fenestration of the intimal flap in the dissected aorta.* Circulation, 1997. **96(7)**: p. 2124-2127.

13. Maraj R, Rerkpattanapipat P, Jocobs LE, Makornwattana P, Kotler MN. *Meta-analysis of 143 reported cases of aortic intramural hematoma.* Am J Cardiol, 2000. **86**: p. 664-668.

14. Hirst A, JohnsVJ,Kime,SW. *Dissecting aneurysm of the aorta:a review of 505 subjects.* Medicines, 1958. **37**: p. 217-279.

15. Wilson S, Hutchins GM. *Aortic dissecting aneurysms: causative factors in 204 subjects.* Arch Pathol Lab Med, 1982. **106**: p. 175-180.

16. Stanson AW, Kazmier AC, Hollier LH, Edwards WD, Pairolero PC, et al. *Penetrating atherosclerotic ulcers of the thoracic aorta : natural history and clinicopathologic correlations.* Ann Vasc Surg, 1986. **1**: p. 15-23.

17. Ganaha F, Miller C, Sugimoto K, Do YS, Minamiguchi H, et al. *Prognosis of aortic intramural hematoma with and without penetrating atherosclerotic ulcer.* Circulation, 2002. **106**: p. 342-348.

18. Harris JA, Bis KG, Glover JL, Bendick PJ, Shetty A, et al. *Penetrating atherosclerotic ulcers of the aorta.* J Vasc Surg, 1994. **19**: p. 90-99.

19. Quint LE, Williams DM, Francis IR, Monaghan HM, Sonnad SS, et al. *Ulcerlike lesions of the aorta : imaging features and natural history.* Radiology, 2001. **218**: p. 719-723.

Table 1: Patient demographics.

Case	Sex	Age	HTA	HCT	DM	Smoke	FH	Symptom
1	M	53	+	-	-	-	-	-
2	F	64	-	-	-	-	-	+
3	M	74	+	-	-	+	-	+
4	M	54	+	-	-	+	-	+
5	M	73	-	-	-	+	-	-
6	M	75	+	-	-	-	-	+

M=male,F=female,HTA=hypertension,HCT=hypercholesterolemia, DM=diabetes mellitus, FH=family history, Symptom represented acute chest or back pain.

Table 2: IVUS imaging compared with CT.

Case	CT	IVUS	Interval time(days)	Confirmations	Treatment	Outcome
1	CAD	CAD+AIH+PAU	5	no	surgical	stable
2	CAD+AIH	CAD	0	reviewing	medical	stable
3	AIH	AIH+PAU	0	Follow up MRI	medical	aneurysm
4	AIH	AIH+PAU	1	Follow up CT	medical	aneurysm
5	AIH+PAU	AIH+PAU	7	no	medical	aneurysm
6	AIH	AIH	2	no	medical	regressed
CAD=classic aortic dissection, AIH=aortic intramural hematoma, PAU=penetrating atherosclerotic ulcer.						

Figure 1 (from case 1):

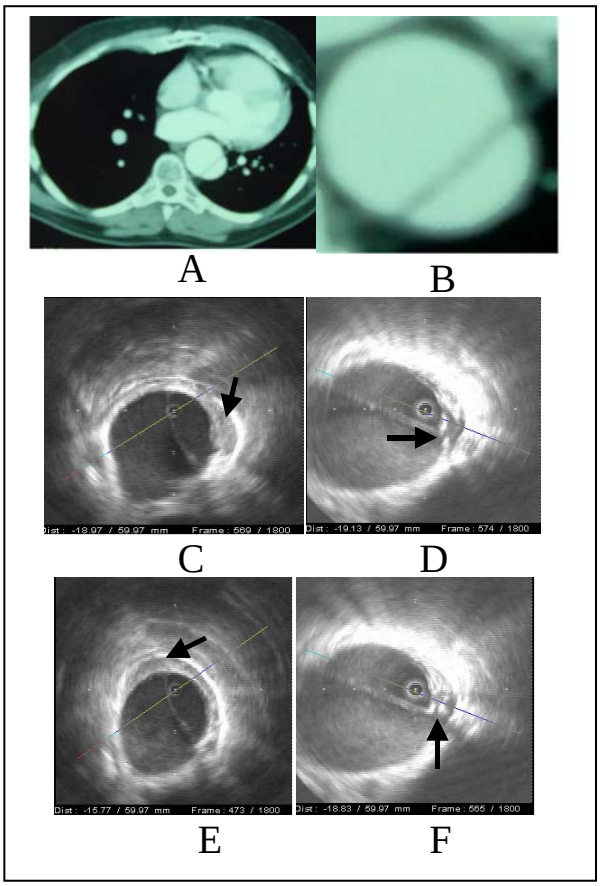

1. No evidence of AIH or PAU in image A and B (CT with contrast, 2002/10/18).
2. A localized AIH in image C and E (indicated by a black arrow, IVUS, 2002/10/23).
3. This AIH was accompanied by a small PAU (indicated by a black arrow in image D and F, redo IVUS imaging after adjusting zoom, 2002/10/23).

Figure 2 (from case 2):

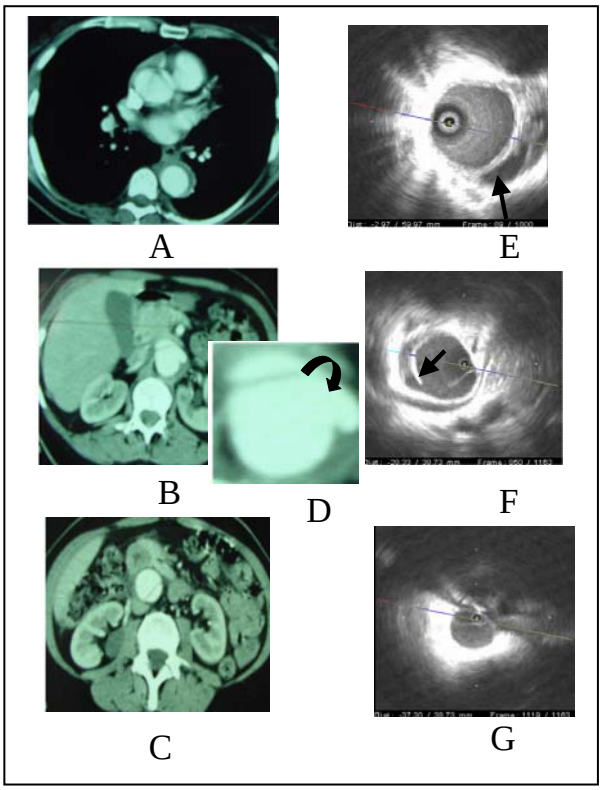

1. Descending AIH and abdominal CAD were documented in image A-D (CT with contrast, 2005/02/25). Image E-G were correspondent IVUS images (2002/02/25). The black arrow in image E indicated slow moving blood. The black arrow in image F indicated a subtle intimal tear.
2. After carefully reviewing CT images, we found this intimal tear (indicated by a black arrow in image D).

Figure 3 (from case 3):

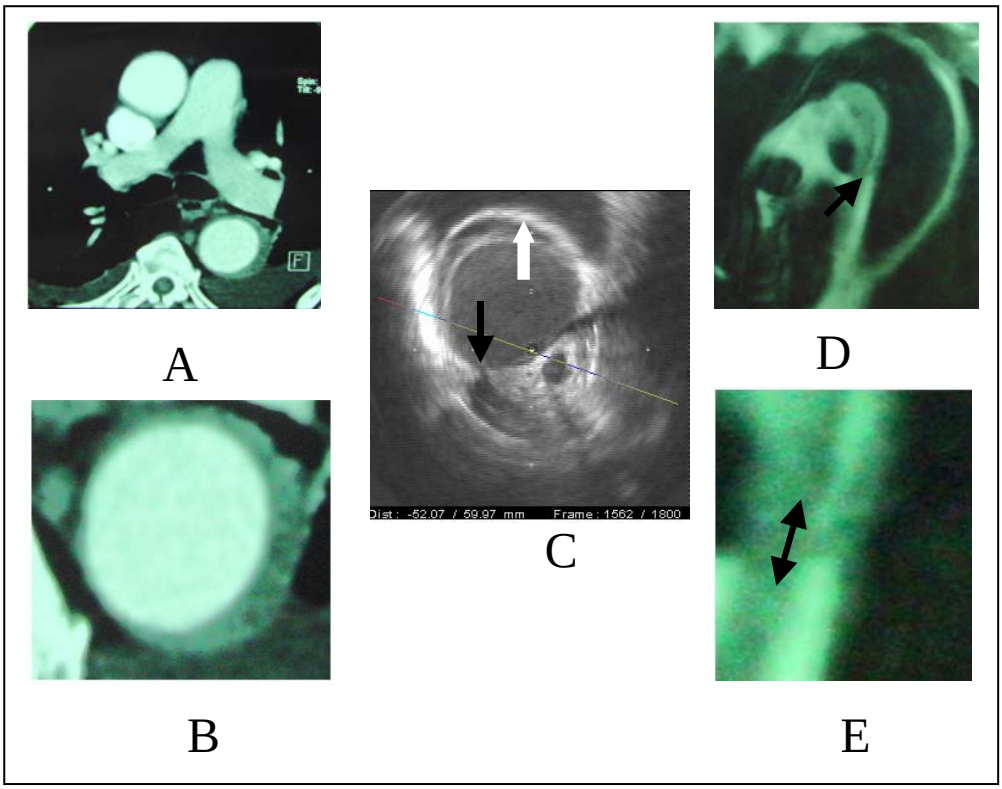

1. A descending AIH was showed in image A and B, but with no evidences of PAU (CT with contrast, 2002/09/18. Image B was a zoomed copy of image A).
2. Image C was a correspondent IVUS image (2002/09/18). The white arrow indicated AIH and the black arrow indicated a PAU.
3. This PAU was confirmed by MRI (2002/09/25, indicated by a black arrow in image D and E, Image E was a zoomed copy of image D).

Figure 4 (from case 4):

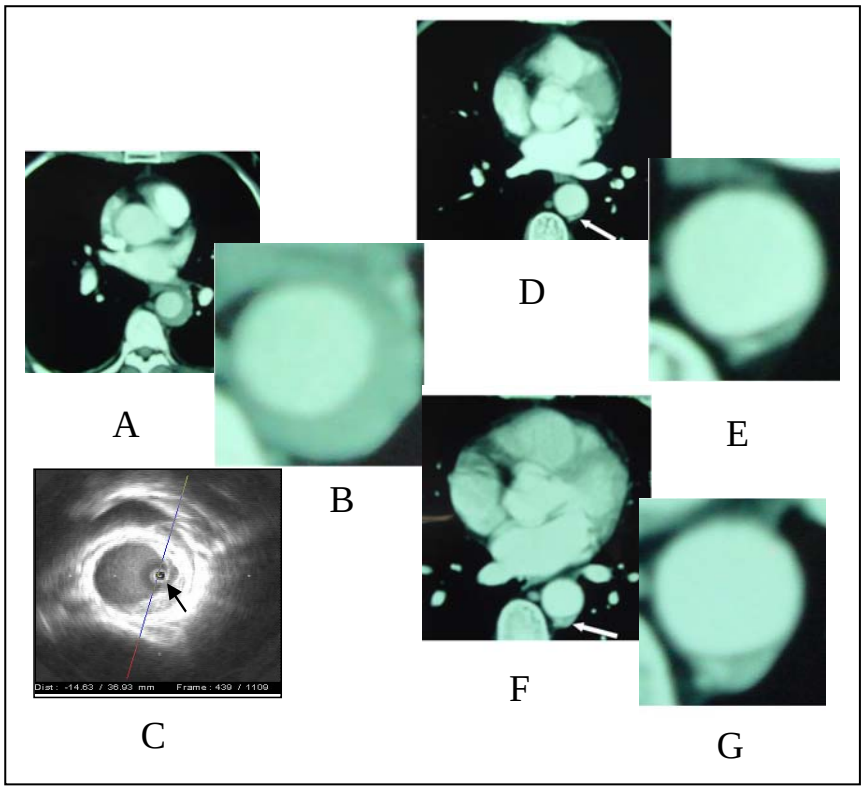

1. AIH was showed in image A and B (CT with contrast, 2004/03/17), there were no evidence of a PAU.
2. A small PAU was detected by IVUS imaging (2004/03/19), which was indicated by a black arrow in image C.
3. The disappearance of AIH and the appearance of a small PAU were showed in image D and E (indicated by a white arrow in image D. CT with contrast, 2004/04/14).
4. The enlargement of the PAU was showed in image F and G (indicated by a white arrow in image F. CT with contrast, 2004/08/03).

Figure 5 (from case 5):

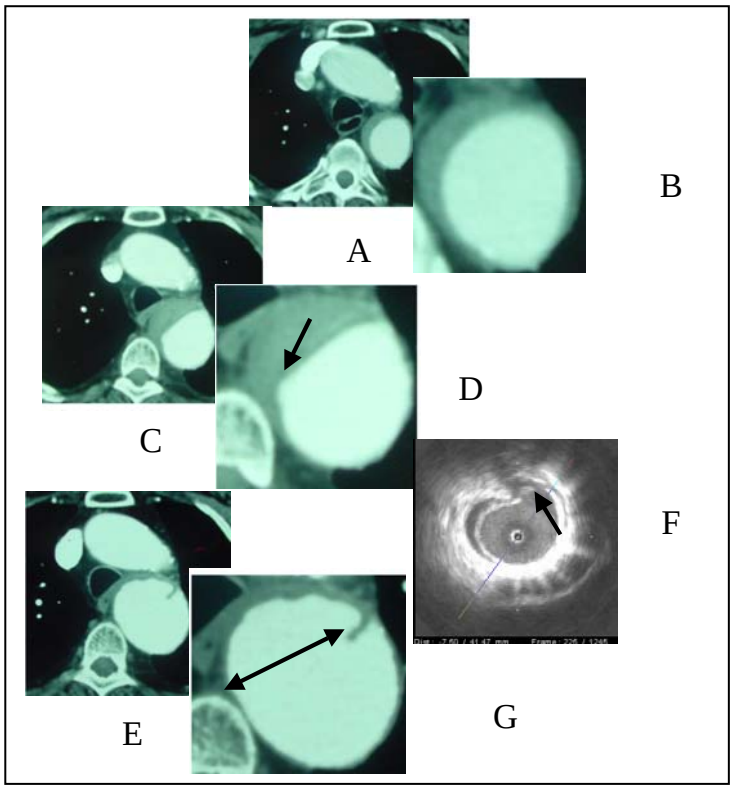

1. There was no ulcer-like projection in imaging A and B (CT with contrast, 2004/04/17).
2. A new onset of ulcer-like projection suspected as a PAU in image C and D (indicated by a black arrow in image D, CT with contrast, 2004/06/08)..
3. This new onset of ulcer-like projection was demonstrated as a PAU by IVUS in image F (indicated by a black arrow in image F, 2004/06/15).
4. This PAU was also confirmed by follow up CT in image E and G (indicated by a double –head arrow in image G, CT with contrast, 2004/08/03).

The value of intravascular ultrasound imaging in diagnosis of aortic penetrating atherosclerotic ulcer

This article was published in the journal of Eurointervention. 2006 ;Vol(4) :P432-437.

Hu Wei[1], MD, Francois Schiele[1], MD, PhD, Nicolas Meneveau[1], MD, Marie-France Seronde[1], MD, Pierre Legalery[1], MD, Fiona Caulfield[1], MSc, Jean-François Bonneville[2], MD, Sidney Chocron[3], MD, Jean-Pierre Bassand[1], MD

[1]Department of Cardiology, University Hospital Jean Minjoz, Besançon, France
[2]Department of Radiology, University Hospital Jean Minjoz, Besançon, France
[3]Department of Cardiac Surgery, University Hospital Jean Minjoz, Besançon, France

Address for Correspondence:
Dr Hu Wei
Department of Cardiology, EA3920
University Hospital Jean Minjoz
25000 Besançon
France
Tel: 33.381.668.187
Fax: 33.381.668.582

Abstract

Background: Aortic penetrating atherosclerotic ulcer (PAU) is one of the causes of acute aortic syndrome. Few studies have evaluated the value of intravascular ultrasound (IVUS) imaging in the diagnosis of PAU.

Objectives: We aimed to evaluate the value of IVUS imaging in diagnosis of PAU. Methods: From September 2002 to May 2005, a consecutive series of 15 patients with suspected aortic dissection underwent both IVUS imaging and spiral Computed Tomography (CT).

Results: CT documented 4 PAUs in three patients. There were no complications related to IVUS imaging. The common IVUS features of these four PAUs appeared as a crescentic, localized, outpouching thickened aortic wall with heterogeneous echoic density that communicated with the lumen via a discontinuous intima. By using these features, IVUS detected five other PAUs in four patients, which were overlooked by CT. The width of PAU detected by CT was significantly wider than that of PAU not detected by CT (1.33±0.67cm vs 0.43±0.27cm, P=0.027). Two of five PAUs omitted by initial CT were confirmed by follow-up CT or magnetic resonance imaging (MRI). During follow up, three PAUs, including two of those overlooked by CT, developed into aneurysms.

Conclusion: IVUS imaging is a safe examination, and more sensitive than spiral CT to diagnose PAU.

Key words: Intravascular ultrasound, spiral computed tomography, penetrating atherosclerotic ulcer.

Introduction

Classic aortic dissection (CAD), intramural hematoma (IMH) and penetrating atherosclerotic ulcer (PAU) are three anatomical presentations of acute aortic syndrome (AAS)[1]. PAU is defined as an ulceration of an atherosclerotic lesion that penetrates from the internal elastic lamina into the media[2,3]. With advanced imaging techniques such as CT, MRI and transesophageal echography (TEE), PAUs are diagnosed more frequently than before. However, sometimes because of their small size, the detection of PAU is challenging by these non-invasive modalities[4-6].

Intravascular ultrasound (IVUS) is an imaging technique that can supply real time, cross-sectional vascular images. Several studies have shown an adjunctive role for IVUS imaging in patients with CAD and IMH[7-10]. However, few authors have evaluated the value of IVUS imaging in patients with PAU.

Methods

Patient population :

This was a single centre, prospective, observational study. From September 2002 to May 2004, 92 patients suspected as AAS were admitted for our hospital, and the diagnosis of AAS was established in 63 of them. Among these 63 patients, 5 died shortly after admission and 20 received urgent intervention. In the remaining 38 patients, IVUS imaging was performed in 15 in order to clarify an obscure diagnosis, to supply complete information for an established diagnosis, to explain a persistent symptom or to find a clue of a rapid progression of the pleural effusion. Among these 15 patients, by CT, the initial working diagnosis was CAD in 8, IMH in 5, PAU in 1, and ascending aortic aneurysm in 1. In the present study, we will focus on the patients who were diagnosed as PAU by CT or IVUS imaging.

IVUS imaging:

IVUS imaging was performed after CT scan but within one week. Before the procedure, as a routine strategy, a single-dose of 70 UI/kg, non-fractionated heparin was administrated intravenously, as we do for fractional flow reserve assessment. Then we performed the procedure using the following steps: Firstly, the right femoral artery was punctured and a regular, 0.035- inch, “J” type guide wire was inserted into the aortic root. Secondly, a 101.5 cm long, 12F, "J" type delivery sheath kit

(Convey™, Boston Scientific, EP TECHNOLOGIES™, USA) straightened by a 106.9 cm long, 9.5F dilator was advanced to the aortic root through the guide wire. Thirdly, the dilator and the guide wire were removed, and the sheath kit was left in the aortic root, via which, a 9F, 9 MHZ mechanic IVUS probe (Ultra ICE™ intra-cardiac Echo catheter, Boston Scientific, USA) was introduced to the aortic root. Lastly, after obtaining an optimal cross-sectional aortic image, the sheath kit was kept in the aortic root and IVUS catheter was manually pulled back and IVUS images were simultaneously recorded on the videotape for subsequent analysis. All steps were performed very prudently and under fluoroscopy. After procedure, the assessing site was closed by a vascular closing system.

IVUS imaging analysis:

Two cardiologists (FS and HW) who were not blind to the findings of CT interpreted IVUS images. We adopted Alfonso's definition for IMH by IVUS but made some slight modifications[11]. IMH was defined as a crescentic, focal or diffuse thickened aortic wall with layered structures separated by echolucent spaces. Because there is no available definition for PAU by IVUS, the common IVUS features of PAUs diagnosed by CT were used to define PAU. Then we used this definition to analyse all IVUS images to detect PAU. We also measured the width and the depth of a PAU by adopting the method described by Cho et al and by using Echoplaque software (INDEC systems)[12]. The reliability of IVUS measurements in this context has previously been published[12,13].

Spiral CT and analysis:

CT scan was performed before IVUS imaging and within 24 hours from onset of symptoms. A 4-slice spiral CT scanner (Somatom Plus 4 Volumezoom, Siemens, Forchheim, Germany) was used. The examination started with conventional unenhanced CT scan, then we administrated 140 ml of non-ionic contrast agent with at least 350 mg iodine per millilitre through an 18-G intravenous antecubital catheter at a flow rate of 3.5ml/s (Ultravist, Schering, Berlin, Germany). The delay of enhanced CT scan was calculated using Test Bolus Technique with a region of interest placed in the ascending aorta (30 ml contrast agent at a flow rate of 3.5ml/s). Scan parameters such as tube current 300mA, tube voltage 120 kV, and rotation time 500 ms were the same for non-enhanced and enhanced CT scan, but we used collimation 4x2.5 mm and table feed per rotation 3.8 mm for non-enhanced scan and

collimation 4x1 mm and table feed per rotation 1.5 mm for enhanced scan. Scan coverage began from 2 cm above the aortic arch and continued to the iliac arteries, and scan data were acquired with the electrocardiogram (ECG) signal recorded simultaneously. Imaging reconstruction was performed using retrospective ECG gating. The acquired scan data were selected for image reconstruction with respect to a pre-defined cardiac phase. A certain R-wave delay time defined the start point of data, and reconstruction parameters were 220 mm field of view, kernel B35, 1.25 mm effective slice thickness, 0.6 mm increment. Multiple reformation in sagittal, coronal, oblique sagittal, and curved projections were generated on an independent workstation (Insight, Neo Imagery, Technologies, city of Industry, Calif, 3D-virtuoso, Siemens). Maximum-intensity projection and shade-surface display reconstruction images of target areas were also produced.

Two experienced radiologists (JFB and NB) who were not blind to the findings of IVUS imaging performed CT analysis using standard definitions. Briefly, without contrast, IMH is defined as crescentic or circular, focal or diffuse thickening aortic wall with a higher density than blood; with contrast medium, it has the same features, but with a lower density than blood. PAU is defined as a narrow neck, outpouching, contrast filled ulceration.

Statistical analysis:

We performed the statistical analyses using Spss 11.5 software. Quantitative data were expressed as mean±SD and qualitative data as frequency. Data were compared by using Fisher's exact probabilities or likelihood ratio x^2 test for qualitative data and Student's t or Analysis of variance (ANOVA) for quantitative data. $P<0.05$ was considered significant.

Results

Patient characteristics (table 1):

From September 2002 to May 2005, 15 consecutive patients underwent IVUS imaging and spiral CT. Six patients diagnosed as PAU by CT or IVUS were included in the present study. All of them were males and the mean age was 65±9.3 years old (range 53 to 74). Four of them had hypertension and were symptomatic. In addition to CT and IVUS, three of them also underwent TEE, MRI or aortography.

IVUS findings as compared with spiral CT (table 2):

In this experience, there was no complications occurred, related to IVUS imaging. The assessing site was closed by a vascular closing system after removing the sheath kit, and there was no need of manual compression and no hematoma occurred. Even in a very dilated aorta, IVUS could supply us a good cross-sectional image of entire aorta and most side branches. In our study, the biggest aorta diameter was 89 mm, and the detecting rate of three arch branches, celiac trunk artery, superior and inferior mesenteric arteries, and renal arteries was 100%.

CT documented 4 PAUs in three patients. The common IVUS features of these four PAUs appeared as a crescentic, localized, outpouching thickening aortic wall with heterogeneous echoic density that communicated with the lumen via an discontinuous intima (see figure 1). By using these features, IVUS detected five other PAUs in four patients, which were overlooked by CT. The width of PAU detected by CT was significantly wider than that of PAU not detected by CT (1.33±0.67cm vs 0.43±0.27cm, P=0.027). The depth of PAU detected by CT was greater than that of PAU not detected by CT, but the difference was not statistically significant (1.59±0.50 cm vs 0.99±0.51cm, P=0.121).

In all, IVUS detected 9 PAUs in six patients (one patient had 3 PAUs, one patient had 2 PAUs, and the 4 others had 1 PAU each), and the PAUs were located in the ascending aorta for 1, in the arch for 1, and in the descending aorta in the remaining 7 cases.

Treatment and follow up information (see table 2):

All patients initially received conservative therapy except one, who underwent surgical operation because of aneurismal dilatation of the false lumen. All of them were followed up by means of clinical visits or telephone interviews, and received regular CT examinations. The mean follow up time was 21.7±11.2 months (range 8-33). No deaths occurred. Two of the five PAUs that were overlooked by the initial CT scan were subsequently confirmed by follow-up CT or MRI (see figure 2). Three PAUs, including two overlooked by CT, developed into aneurysms. However, there was no significant difference in width or depth between PAUs with and without progression.

Discussions

PAU was first described as a distinct clinical and pathologic entity by Stanson et al in 1986 [2]. This condition is characterized by an ulceration that penetrates through the elastic lamina and into the media and is associated with a variable amount of hematoma within the aortic wall. Since it is not possible to differentiate PAU from IMH, CAD and other diseases by relying on clinic presentations alone, we need an imaging technique with high resolution in order to diagnose PAU. Although non-invasive imaging techniques such as: CT, TEE and MRI and invasive aortography have been reported to successfully diagnose PAU, they also have some limitations.

Several studies have shown an adjunctive role for IVUS imaging in patients with CAD and IMH[7-10], however, few authors have evaluated its value in the diagnosis of PAU. Moreover, previous studies used a 20 MHZ IVUS probe, which had limitations in a dilated aorta. Theoretically, a low frequency IVUS probe can overcome this limitation. Recently, a 9MHZ IVUS probe has been made commercially available, but as yet, reports of experiences with this probe are scant. We used this new system in 15 patients over a period of three years, and our study showed that it could provide a good cross-sectional image of entire aorta (even a very dilated one) and most of its side branches.

CT scan is presently the most frequently used imaging technique in patients with suspected AAS. By comparison with CT, IVUS imaging is invasive and requires a large femoral access (12F), but has the advantage of avoiding the use of contrast media. Up to now, only one case report has showed multiple PAUs detected by IVUS imaging [14], and our study is the first to evaluate the value of IVUS imaging in a series of patients with PAU. Because there is no available definition of PAU by IVUS, among those PAUs detected by CT, the common IVUS features were used to conclude the definition, and it was defined as a crescentic, localized, outpouching thickening aortic wall with heterogeneous echoic density that communicated with the lumen via a discontinuous intima. By using this definition, IVUS detected 9 PAUs in 6 of our patients, and 6 of them were confirmed by initial or follow up CT or MRI. Therefore, our study showed that IVUS is capable of diagnosing PAU.

Our study also demonstrated that IVUS was more sensitive than CT to detect small PAUs. The mean width and depth of PAU were 0.83 cm and 1.25 cm respectively in our study, relatively smaller than the dimensions reported by others [12,15,16]. In addition, the width of PAU detected by CT was significantly wider than that of PAU not detected by CT. The reason why some PAUs escaped CT may due to their small size and the limited spatial resolution of CT. According to their theoretical spatial resolutions, TEE, MRI and aortography can not do better than CT in detecting small PAUs, which was confirmed by our study. Thus, we believe that to date, IVUS imaging is the most sensitive modality in vivo for detecting small PAUs.

PAU is considered by most authors to have a poorer prognosis than CAD. Coady et al reported that the risk of aortic rupture was considerably higher among patients with PAU (40% of cases) than among patients with type A or type B aortic dissection (7.0% and 3.6% respectively) [6]. Ganaha et al reported that AIH with PAU had poorer outcome than AIH without PAU [15]. But some controversy still exists because the natural history of PAU is unknown, and so far there is no standard treatment strategy. In our study, all patients received medical therapy except one, who was operated on because of aneurismal dilatation of the false lumen. During follow up, three of the remaining 8 PAUs developed into aneurysms, which included 2 that had been overlooked by CT. Therefore, it is important to emphasize that small PAUs that escape CT could be also dangerous.

Clinical implications:

In our clinical practice, non-invasive CT scan (4-slice spiral CT) is the first choice of imaging technique in patients with suspected AAS. MRI, TEE and aortography play as additional tools. However, sometimes even after performing all these 4 examinations, some unsolved problems still exists such as: obscure diagnoses, persistent symptoms, rapid progression of pleural effusion etc. Under these circumstances, our experience showed that IVUS imaging with a 9 MHZ probe was very helpful. This study demonstrated that IVUS imaging was very sensitive to detect PAU, particularly for the small ones, which may due to its high spatial resolution. However, to date, the potential values of IVUS imaging for the treatment strategy for PAU remains unclear, and we do not think that IVUS imaging can replace a non-invasive imaging technique like CT scan as the first line examination in the setting of AAS, specially with the introduction of new generation of non-invasive imaging

techniques (for example, a 64-slice CT scanner), which have higher spatial resolutions.

Study limitations:

1) Not all PAUs that escaped CT were subsequently confirmed, thus, we couldn't exclude false positive results. 2) Although the time interval between IVUS imaging and CT was short and there was no evidence of clinical progression, we cannot exclude possible changes during that period of time. 3) Although there were no complications in our study, IVUS imaging is an invasive examination that has potential side effects.

Conclusions:

IVUS imaging is a safe examination that is able to diagnose PAU. It is very helpful in detecting small PAUs that can be overlooked by CT scan, and which may be dangerous.

References

1. Vilacosta I, San Roman JA. Acute aortic syndrome. *Heart*. 2001;85:P365-368.

2. Stanson AW, Kazmier FJ, Hollier LH, Edwards WD, Pairolero PC, Sheedy PF, Joyce JW, Johnson MC. Penetrating atherosclerotic ulcers of the thoracic aorta: natural history and clinicopathologic correlations. *Ann Vasc Surg*. 1986;1: P15-23.

3. Shennan T. Dissection aneurysm: special report no 193. *Med Res Council (Great Britain)*. 1935;86: P1933-1934.

4. Yucel EK, Steinberg FL, Egglin TK, Geller SC, Waltman AC, Athanasoulis CA. Penetrating aortic ulcers: diagnosis with MR imaging. *Radiology*. 1990;177: P779-81.

5. Hayashi H, Matsuoka Y, Sakamoto I, Sueyoshi E, Okimoto T, Hayashi K, Matsunaga N. Penetrating atherosclerotic ulcer of the aorta: imaging features and disease concept. *Radiographics*. 2000;20: P995-1005.

6. Coady MA, Rizzo JA, Hammond GL, Pierce JG, Kopf GS, Elefteriades JA. Penetrating ulcer of the thoracic aorta: what is it? How do we recognize it? How do we manage it? *J Vasc Surg*. 1998;27: P1006-15; discussion P1015-6.

7. Weintraub AR, Schwartz SL, Pandian NG, Katz SE, Kwon OJ, Millan V, Bojar R. Evaluation of acute aortic dissection by intravascular ultrasound [letter]. *N Engl J Med*. 1990;323:P1566-1567.

8. Weintraub AR, Elber R, Gorge G, Schwartz SL, Ge J, Gerber T, Meyer J, Hsu TL, Bojar R, Iliceto S. Intravascular Ultrasound Imaging in Acute Aortic Dissection. *J Am Coll Cardiol*. 1994;24: P495-503.

9. Alfonso F Goicolea J, Aragoncillo P, Hernandez R, Macaya C. Diagnosis of Aortic Intramural Hematoma by Intravascular Ultrasound Imaging. *Am J Cardiol*. 1995;76(10):P735-738.

10. Yamada E, Matsumura M, Kyo S, Omoto R. Usefulness of a Prototype Intravascular Ultrasound Imaging in Evaluation of Aortic dissection and Comprison Angiographic Study, Transesophageal Echocardiography, Computed Tomography, and Magnetic Resonance Imaging. *Am J Cardiol*. 1995;75:P161-165.

11. Cho KR, Stanson AW, Potter DD, Cherry KJ, Schaff HV, Sundt TM 3rd. Penetrating atherosclerotic ulcer of the descending thoracic aorta and arch. *J Thorac Cardiovasc Surg*. 2004;127:P1393-1399; discussion P1399-1401.

12. Schiele F, Meneveau N, Vuillemenot A, Zhang DD, Gupta S, Mercier M, Danchin N, Bertrand B, Bassand JP. Impact of intravascular ultrasound guidance in stent deployment on 6-month restenosis rate:a multicentre, randomized study comparing two strategies: with and without intravascular ultrasound guidance: RISIST Study Group: REStenosis after Ivus guided STenting. *J Am Coll Cardiol*. 1998;32:P320-328.

13. Multiple penetrating atherosclerotic ulcers of the abdominal aorta:treatment by endovascular stetn graft placement. *Heart*. 2001;85:526.

14. Ganaha F, Miller DC, Sugimoto K, Do YS, Mina miguchi H, Saito H, Mitchell RS, Dake MD. Prognosis of aortic intramural hematoma with and without penetrating atherosclerotic ulcer: a clinical and radiological analysis. *Circulation*. 2002;106:P342-8.

Table 1: Patient demographics.

Case	gender	age	HTA	HCT	DM	FH	Smoke	CHD	Symptom
1	M	53	+	-	-	-	-	-	-
2	M	70	+	+	-	-	-	-	+
3	M	66	-	+	-	-	+	+	+
4	M	54	+	-	-	-	+	-	+
5	M	73	-	-	-	-	+	+	-
6	M	74	+	-	-	-	+	-	+

M=male, F=female, HTA=hypertension, HCT=hypercholesterolemia, DM=diabetes mellitus, FH=family history, CHD=coronary heart disease, Symptom represented acute chest or back pain.

Table 2 : IVUS finding compared with CT.

Case	PAU	site	Width(cm)	Depth(cm)	IVUS	CT	treatment	outcome
1	I	DA	0.34	1.02	+	-	surgical	stable
	II	DA	0.89	1.39	+	-	medical	stable
	III	DA	2.0	2.2	+	+	medical	stable
2	IV	DA	0.43	0.35	+	-	medical	stable
3	V	AA	1.03	1.03	+	+	medical	stable
	VI	Arch	0.54	1.37	+	+	medical	stable
4	VII	DA	0.27	0.6	+	-	medical	aneurysm
5	VIII	DA	1.76	1.76	+	+	medical	aneurysm
6	IX	DA	0.21	1.57	+	-	medical	aneurysm
DA=descending aorta, AA=ascending aorta, PAU VII and IX were confirmed by follow up MRI or CT.								

Figure 1 (from case 5):

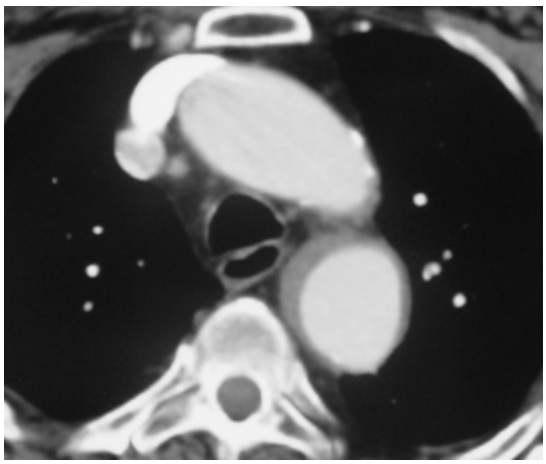

Figure 1a

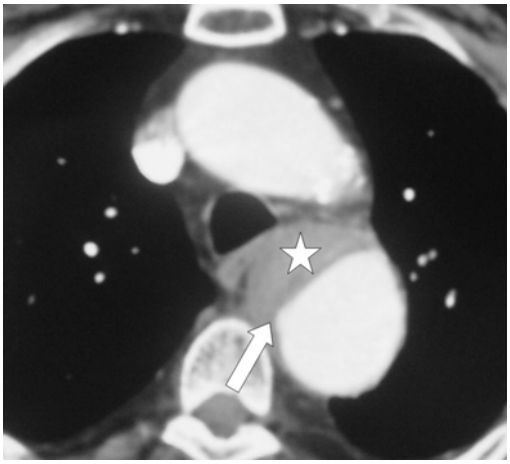

Figure 1b

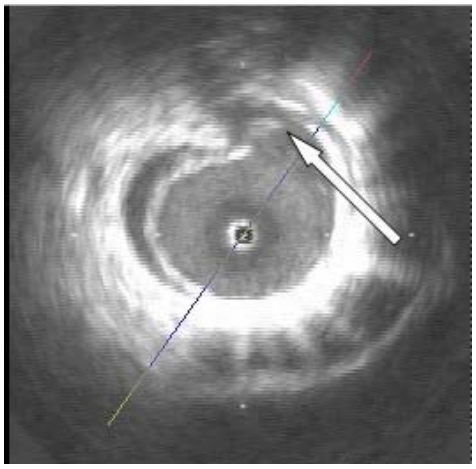

Figure 1c

Figure 1d

Figure 1a: IMH without evidence of PAU (CT with contrast, 2004/04/17)

Figure 1b: Enlargement of the IMH with a new onset PAU (CT with contrast, 2004/06/08, the white star represented IMH and the white arrow represented PAU).

Figure 1c: The corresponding IVUS image (2004/06/15) showed clearly this PAU (indicated by a white arrow).

Figure 1d: This PAU developed into a big aneurysm (indicated by a double head arrow, CT with contrast, 2004/08/03).

Potential interests of intra-aorta ultrasound imaging for the diagnosis of aortic penetrating atherosclerotic ulcer

This article was published in Int J Cardiovasc Imaging. 2006; Vol22:P653-656.

Hu Wei[1], MD, Francois Schiele[1], MD, PhD, Nicolas Meneveau[1], MD, Marie-France Seronde[1], MD, Pierre Legalery[1], MD, Fiona Caulfield[1], MSc, Jean-François Bonneville[2], MD, Sidney Chocron[3], MD, Jean-Pierre Bassand[1], MD

[1]Department of Cardiology, University Hospital Jean Minjoz, Besançon, France

[2]Department of Radiology, University Hospital Jean Minjoz, Besançon, France

[3]Department of Cardiac Surgery, University Hospital Jean Minjoz, Besançon, France

Address for Correspondence:

Dr Hu Wei

Department of Cardiology, EA3920

University Hospital Jean Minjoz

25000 Besançon

France

Tel: 33.381.668.187

Fax: 33.381.668.582

Abstract:

A 72-year-old man was admitted to our hospital for acute back pain. Transesophageal echocardiography (TEE), computed tomography (CT) and magnetic resonance imaging (MRI) all showed the presence of intramural hematoma locating in the descending aorta, with bilateral pleural effusions. The patient was initially referred for medical therapy with watchful waiting. But he continued to have back pain, so we decided to perform invasive aortography examination and intra-aorta ultrasound imaging. No PAU was found on multiple angiographic views, but intra-aorta ultrasound imaging clearly showed a 3x1mm^2 PAU in connecting with the intramural hematoma. Even after retrospective analysis of CT images, we failed to reveal this PAU. Therefore, we think that IVUS may be a useful tool in the diagnosis of PAU.

Introduction:

Classic aortic dissection, intramural hematoma (IMH) and penetrating atherosclerotic ulcer (PAU) are three anatomical presentations of acute aortic syndrome. PAU is defined as the ulceration of an atherosclerotic lesion that penetrates from the internal elastic lamina into the media[1]. Because of its small size, the diagnostic of PAU is challenged by non-invasive imaging techniques [2,3]. Here, we present a case report of a patient diagnosed as type B IMH by transesophageal echocardiography (TEE), computed tomography (CT) and magnetic resonance imaging (MRI), but in whom an accompanying PAU was overlooked by all these three non-invasive techniques as well as by invasive aortography examination, and which was eventually detected by intra-aorta ultrasound (IAU) imaging.

Case report

A 72-year-old man was admitted to our hospital for acute back pain. He was a previous smoker with controlled hypertension. On examination, the patient, 165 cm tall and 72 Kg, had a pulse at 84 beats per minute, and blood pressure at 130/80 mmHg bilaterally. There was no pulse deficit, no cardiac murmur and no neurological deficit. The electrocardiogram showed sinus rhythm with no evidence of ischemic changes. The chest X-ray was normal. Laboratory tests were within normal limits.

Firstly, the patient was submitted to non-invasive imaging (see figure 1 and 2): (1) 4-slice spiral CT scan, with and without enhancement of contrast media (with spatial

resolution 0.6x0.6x1 mm^3, Somatom Plus 4, Volumezoom, Siemens, Forchheim, Germany). (2) TEE with a 5 MHZ multi-plane probe (with in-plane resolution 0.5x2.0 mm^2, Toshiba PEF-510MB 270A and 140A imaging systems, Japan). (3) MRI with 1.5 Tesla (with spatial resolution 1.5x1.5x5.52 mm^3, Siemens MAGNETOM Sonata 1.5T High Field MRI, Germany). All these three non-invasive imaging techniques detected IMH in the descending aorta with bilateral pleural effusions. The patient was initially referred for medical therapy with watchful waiting. But he continued to have back pain, so we decided to perform invasive imaging (see figure 3 and 4): aortography and IAU imaging with a 9 MHz probe (with in-plane resolution 0.25x0.6 mm^2, Ultra ICE^{TM} intra-cardiac Echo catheter, Boston Scientific, USA). A mechanical 9 MHZ IAU probe was introduced to the aortic root with the help of a guide wire and a 110cm long sheath via right femoral artery. With manually pull-back, high quality cross-sectional images of the entire aorta were obtained. IAU imaging showed a clear aspect of a PAU (3x1 mm^2) in connecting with the IMH, which could not be detected by multiple angiographic views. Even after retrospective analysis of CT images, we failed to reveal this PAU.

Discussion

PAU was first described as a distinct clinical and pathologic entity by Stanson et al in 1986[1]. This condition is characterized by an ulceration that penetrates from the elastic lamina and into the media and is associated with a variable amount of hematoma within the aortic wall. Since the introduction of modern diagnostic techniques that provide high resolution images of the thoracic aorta, IMH and PAU have been increasingly recognized as causes of acute aortic pathology, in addition to classic aortic dissection. Because of their common clinical manifestations, these three disorders have been collectively called the acute aortic syndrome.

PAU is predominantly located in the descending aorta where atherosclerosis tends to be more severe. Patients with this disorder are typically older and have more cardiovascular risk factors and evidences of diffuse atherosclerosis than patients with aortic dissection or IMH. PAU has been considered by most authors to have a poorer prognosis than classic aorta dissection [1,4,5]. Coady et al reported that the risk of aortic rupture was considerably higher among patients with PAU (40% of cases) than

among patients with type A or type B aortic dissection (7.0% and 3.6% respectively) [5]. However, controversy still exists because little is known about the natural history of PAU[6].

Aortography has been considered as the reference for the diagnosis of aortic dissection. However, Beginning in the early 1980s, advances in non-invasive technology, specifically the development of TEE, CT and MRI, have challenged this concept. For the diagnosis of acute aorta dissection, all 4 diagnostic tests have been shown to have a high sensitivity and specificity[7]. By aortography, CT and MRI, PAU was defined as a localized, contrast-filled outpouching of the aortic wall[8,9]. On TEE, PAU was defined as a craterlike outpouching in the aortic wall with jagged edges, generally associated with extensive aortic atheroma [2,5].

Invasive intravascular ultrasound (IVUS) imaging has been proved to be safe and useful in coronary artery systems. Several authors have also demonstrated that IAU imaging had apparently 100% accuracy for the diagnosis of aortic dissection and IMH[10,11]. However, up to now, no study has evaluated the role of IAU imaging in the diagnosis of PAU. In our case report, 4 current frequent used image techniques, namely CT, TEE, MRI and aortography, failed to detect a PAU accompanying with an IMH. However, this PAU was clearly visible with IAU imaging. The reason why CT, TEE, MRI and aortography failed to detect this PAU may be explained by the small size of this PAU (3x1mm$^{2)}$, the different spatial resolutions of different imaging techniques (compared with them, IAU imaging has higher spatial resolutions). It has to be admitted that this small PAU can probably be detected non-invasively using more recent multi-slice CT scan (for example with a 64-slice scanner), which has a higher spatial resolution than a 4-slice scanner. However, when it is not available, IAU imaging may be considered.

Therefore, we think that small PAUs can be overlooked by all four current frequent imaging techniques, invasive aortography and non-invasive CT, TEE and MRI imaging, and IAU imaging may be helpful in this setting.

Figure 1:

CT scan showed clearly the IMH (indicated by an arrow) and the pleural effusion (represented by a star), but not the PAU

Figure 2:

This PAU was also overlooked by angio-MRI (The IMH was indicated by an arrow).

Figure 3:

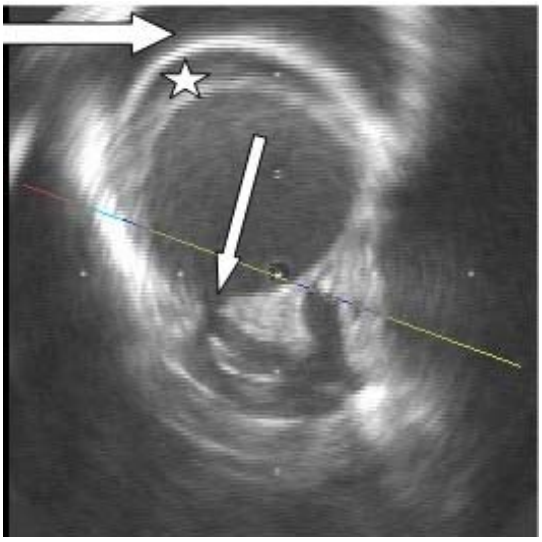

IVUS detected the IMH (represented by a star), the accompanying PAU (indicated by a small arrow) and the pleural effusion (indicated by a big arrow).

Figure 4:

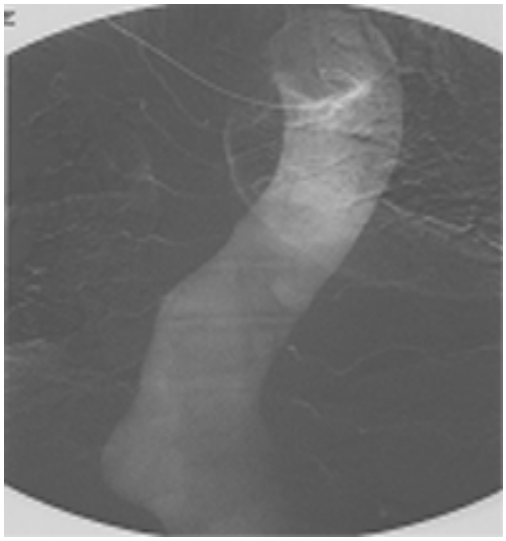

Neither the IMH nor the PAU was detected by aortography.

References

1. Stanson AW, Kazmier FJ, Hollier LH, et al. Penetrating atherosclerotic ulcers of the thoracic aorta: natural history and clinicopathologic correlations. *Ann Vasc Surg*. 1986; 1: p15-23.

2. Vilacosta I, San Roman JA, Aragoncillo P, et al. Penetrating atherosclerotic aortic ulcer: documentation by transesophageal echocardiography. *J Am Coll Cardiol*. 1998; 32: p83-89.

3. Sueyoshi E, Matsuoka Y, Imada T, et al. New development of an ulcerlike projection in aortic intramural hematoma: CT evaluation. *Radiology*. 2002; 224: p536-541.

4. Ganaha F, Miller DC, Sugimoto K, et al. Prognosis of aortic intramural hematoma with and without penetrating atherosclerotic ulcer: a clinical and radiological analysis. *Circulation*. 2002; 106: p342-348.

5. Coady MA, Rizzo JA, Hammond GL, et al. Penetrating ulcer of the thoracic aorta: what is it? How do we recognize it? How do we manage it? *J Vasc Surg*. 1998; 27: p1006-1015; discussion p1015-1016.

6. Cho KR, Stanson AW, Potter DD, et al. Penetrating atherosclerotic ulcer of the descending thoracic aorta and arch. *J Thorac Cardiovasc Surg*. 2004; 127: p1393-1399; discussion p1399-1401.

7. Hagan PG, Nienaber CA, Isselbacher EM, et al. The International Registry of Acute Aortic Dissection (IRAD): new insights into an old disease. *Jama*. 2000; 283: p897-903.

8. Hayashi H, Matsuoka Y, Sakamoto I, et al. Penetrating atherosclerotic ulcer of the aorta: imaging features and disease concept. *Radiographics*. 2000; 20: p995-1005.

9. Yucel EK, Steinberg FL, Egglin TK, et al. Penetrating aortic ulcers: diagnosis with MR imaging. *Radiology*. 1990; 177: p779-81.

10. Yamada E, Matsumura M, Kyo S, et al. Usefulness of a prototype intravascular ultrasound imaging in evaluation of aortic dissection and comparison with angiographic study, transesophageal echocardiography, computed tomography, and magnetic resonance imaging. *Am J Cardiol*. 1995; 75: p161-5.

11. Alfonso F, Goicolea J, Aragoncillo P, et al. Diagnosis of aortic intramural hematoma by intravascularultrasound imaging. *Am J Cardiol*. 1995; 76: p735-738.

The value of intravascular ultrasound imaging in following up patients with replacement of the ascending aorta for acute type A aortic dissection

This article had been submitted to Chinese Medical Journal (under revision)

Hu Wei[1], MD, Francois Schiele[1], MD, PhD, Nicolas Meneveau[1], MD, Marie-France Seronde[1], MD, Pierre Legalery[1], MD, Fiona Caulfield[1], MSc, Jean-François Bonneville[2], MD, Sidney Chocron[3], MD, Jean-Pierre Bassand[1], MD

[1]Department of Cardiology, University Hospital Jean Minjoz, Besançon, France

[2]Department of Radiology, University Hospital Jean Minjoz, Besançon, France

[3]Department of Cardiac Surgery, University Hospital Jean Minjoz, Besançon, France

Corresponding Author

Dr. Hu Wei

Department of Cardiology, EA3920

University Hospital Jean Minjoz

25000 Besançon

France

Tel: 33.381.668.187

Fax: 33.381.668.582

Email: huwei0516@hotmail.com

Abstract:

Purpose: The value of intravascular ultrasound (IVUS) imaging in patients with replacement of the ascending aorta for acute type A aortic dissection (AD) is unknown. The purpose of this study is to assess the potential use of IVUS imaging in this setting.

Methods: From September 2002 to July 2005, IVUS imaging with a 9 MHz probe was performed in a consecutive series of 16 patients with suspected or established aortic dissection (AD), and this study will focus on 5 of them with replacement of the ascending aorta for acute type A AD. Among these 5 patients, other imaging modalities including aortography, spiral computed tomography (CT), magnetic resonance imaging (MRI), and transesophageal echocardiography (TEE) were performed in 5, 3, 3, 1 of them, respectively.

Results: There were no complications related to IVUS imaging. For the replaced graft, as other imaging modalities, IVUS could identify all 5 grafts, the proximal and the distal anastomoses, and the ostia of the reimplanted coronary arteries. In 2 cases, IVUS detected 2 peri-graft pseudo-aneurysm (1 per case) those were also detected by MRI but omitted by aortography. For the residual dissection, IVUS had similar findings as other imaging modalities in detecting: the patency (5/5), the longitudinal and the circumferential extent, the thrombus (4/5), the recurrent dissection (1/5), and the aneurysm distal to the graft (5 in 4 patients). However, it detected more intimal tears and side branch involvements than other imaging modalities (15 vs 10 and 3 vs 1, respectively).

Conclusions: In following up patients with replacement of the ascending aorta for acute type A AD, IVUS imaging can provide complete information of the replaced graft and the residual dissection. So, IVUS imaging may be considered when 4 currently frequent used imaging modalities can't supply sufficient information or there are some discrepancies between them.

Key words: Intravascular ultrasound; type A aortic dissection; replaced graft.

1.**Introduction:**

Acute type A aortic dissection (AD) has high mortality and requires urgent operative treatment.[1, 2] Depending on the condition of the aortic root and aortic valve, the ascending aorta is replaced either by a single or a composite graft.[3] Recently, early diagnosis, advances of surgical techniques, and intensive postoperative surveillance have substantially improved the survival rate, however, the late complications caused by the replaced graft or the residual dissection are not uncommon, and two most frequent ones are the aneurysm distal to the graft and the peri-graft pseudo-aneurysm. [3-6]Now it is generally accepted that such patients warrant a long-term regular imaging follow-up, and currently, non-invasive examinations including computed tomography (CT) and magnetic resonance imaging (MRI) are two most frequent used imaging modalities. While semi-invasive transesophageal echocardiography (TEE) and invasive aortography often play as additional tools. However, all of them have their own limitations. [7-12]

IVUS have been demonstrated to supply additional information to arterial angiography in patients with coronary heart disease.[13]However, till now, only a few authors have evaluated the value of IVUS imaging in patients with AD, and most of them used a 20 MHZ probe that has limitation in a dilated aorta.[14-17] Compared with 4 currently frequent used imaging modalities, IVUS imaging has a higher spatial resolution, which permits us to detect small graft leakages and residual intimal tears those result in two frequent occurred post-operative complications. However, no previous studies have assessed the potential use of IVUS imaging in patients with replacement of the ascending aorta for acute type A AD. For a conventionally used 20 MHz probe, the maximal ultrasonic penetrating depth is about 70mm, in fact, according to the published data, it could not provide a good aortic image if the vessel>45mm; whereas for a currently available 9 MHz probe, the maximal ultrasonic penetrating depth is approximately 100mm, but the experiences about its use in the aorta are very scant.[14-16] From September 2002 to July 2005, we performed this new system in a consecutive series of 16 patients with suspected or established AD, and this study will focus on 5 of them with replacement of the ascending aorta for acute type A AD.

2.Methods:

Patients: This is a single-center, prospective and observational study that obeyed the Declaration of Helsinki and was approved by the local ethics. A written consent

form from all participants was obtained before the procedure. From September 2002 to July 2005, 102 patients suspected as acute AD were screened and IVUS imaging was performed in 16 of them (8 with classic AD, 6 with intramural hematoma, 1 with penetrating atherosclerotic ulcer, and 1 with ascending aortic aneurysm). This study will focus on 5 patients with replacement of the ascending aorta for acute type A AD. The 5 replaced grafts consisted of 3 single supracoronary Dacron tube grafts, and 2 composite grafts (one adopted classic Bentall technique and another adopted Cabrol modified Bentall technique. All procedures used an included technique, Teflon reinforcement and Gelatin-resorcin-formol glue. The indications of IVUS imaging have been published elsewhere.[18] It has to be noted that not all IVUS imaging procedures were performed after aortography, which plays as an additional tool for non-invasive imaging modalities.

IVUS imaging: IVUS imaging was performed using a Hewlett-Packard sonos intravascular imaging system (Hewlett-Packard, Andover, MA, USA) with a 9 MHz catheter-based ultrasound probe (Ultra ICE^{TM} intracardiac Echo catheter, Boston Scientific). This kind of probe has an in-plane resolution of 0.25x0.6mm^2 and a penetrating depth of 100m, whereas a frequent used 20MHz probe has an in-plane resolution of 0.2X0.3mm^2 and a penetrating depth of 70mm. This 9 MHz probe is contained within a 9F (110cm long) polyethylene catheter, and rotated by an external motor at 600 rpm. The ultrasound beam is emitted from a 10° forward-angling tip of the single-crystal focused element. The probe produces circular images with the catheter in the center at the frame rate up to 30/s. The technical details of IVUS imaging have been published elsewhere.[18] Briefly say, the IVUS probe was introduced to the aortic root with the help of a 0.035-inch guide wire and a 110 cm sheath under fluoroscopy via right femoral artery. After obtaining an optimal cross-sectional aortic image, it was manually pulled back and IVUS images were simultaneously recorded on the videotape for subsequent analysis. The scan order of IVUS imaging was aortic root, ascending aorta, aortic arch, descending aorta, thoracic aorta, abdominal aorta, and the right iliac artery. The fluoroscopy and fluorography were used to localise the position of the IVUS probe.

IVUS images analyses: Two cardiologists (HW&FS) who were blinded to the findings of other imaging modalities performed IVUS images analyses using the same definitions, and a third observer (N.M) was invited to settle the discrepancies. Echoplaque software (INDEC systems) was used to reconstruct a 2-dimensional

IVUS image and to perform quantitative analyses if necessary. Two criteria were used to distinguish the replaced graft and the normal aorta: 1) the replaced graft often had a higher echo reflection than the normal aorta; 2) the replaced graft appeared as a thin single-layer structure for the whole circumference, whereas the normal aorta often has three layers. The proximal and the distal anastomoses were judged by the suture lines (appeared as saw-shaped structures). The peri-graft pseudo-aneurysm was deemed to be presented if blood flow was detected in peri-graft space. The reimplanted ostia of coronary arteries were also recorded. We adopted Weintraub's method to interpret the residual or recurrent dissection (defined as the reopening of a thrombosed false lumen).[14] Briefly say, Intimal flap was defined as a moving curvilinear structure that separating the aorta into a true and a false lumen; aortic dissection was diagnosed if an intimal flap presented; intimal tear was defined as an uncontinuous site of an intimal flap; thrombus was defined as a piece of fixed substance with a soft granular echo signal that often located in the false lumen; the distal aneurysm was diagnosed when the diameter of a non-replaced aorta was more than 1.5 times than that of a normal aorta. The relations between the aortic side branches and the true or the false lumen or the intimal flap were also recorded.

Other imaging techniques and analysis: Spiral CT (with 4 detectors, Somatom Plus 4, Volumezoom, Siemens, Forchheim, Germany), TEE (with a 5 MHz multi-plane probe, Toshiba PEF-510MB 270A and 140A imaging systems, Japan), MRI (with 1.5 Tesla, Siemens MAGNETOM Sonata 1.5T High Field MRI, Germany were performed by using standard methods. The protocol of CT scan has been published elsewhere. [18]Other experts interpreted these images by adopting standard definitions.

3.Results:

Patients demographic (see table 1):

All five patients were males, and the mean age was 67±8.6 years old (ranged from 53 to 74). All except one were asymptomatic. Aortography, spiral CT, MRI, and TEE were performed in 5, 3, 3 and 1 patient, respectively. The mean interval time between the initial operation and IVUS imaging was 98.6±108.7 months (ranged from 20 to 252). All interval time between IVUS imaging and other imaging techniques was less than 7 days.

IVUS findings and compared with those of other imaging modalities:

There were no complications related to IVUS imaging. IVUS could supply us a good cross-sectional aortic image from the aortic root to the bifurcation of the iliac artery even in a very dilated aorta (the biggest aortic diameter was 90mm) and most of its side branches. The detecting rate of three arch branches, the celiac trunk artery, the superior and the inferior mesenteric arteries, and the renal arteries were 100%.

IVUS could easily identify all 5 replaced grafts (see figure 1b), the proximal and the distal anastomoses (see figure 1c), and the ostia of the reimplanted coronary arteries (see figure 1d). However, for two composite grafts, although IVUS detected the replaced aortic valve prostheses, it failed to judge their functional state. In case 1, 4 and 5, both IVUS and other imaging modalities demonstrated that there were no pathologic changes of the replaced graft. In case 2 (see figure 2) and in case 3 (see figure 3), IVUS detected a peri-graft pseudo-aneurysm caused by suture line dehiscence, which was found by MRI but omitted by aortography.

For the residual dissection, IVUS had similar findings as other imaging modalities in detecting: the patency (5/5), the longitudinal and circumferential extent, the thrombus (4/5), the recurrent dissection (1/5), and the aneurysm (5 in 4 cases). However, it detected more intimal tears and side branch involvements than other imaging modalities (15 vs 10 and 3 vs 1, respectively).

Treatment and follow-up:

All therapeutic decisions were made independent of IVUS imaging findings. Case 1 and 5 were operated on for their descending aortic aneurysms and kept well till now. Case 4 received medical therapy and had no adverse events. Case 2 refused the proposed operation and died of aortic rupture. Case 3 underwent a new operation but died of low cardiac output.

4. Discussion:

IVUS imaging in coronary arteries has been proved to be a safe examination.[13] According to the previous studies, there were no complications reported related to IVUS imaging in the aorta, with combination with ours, we believe that intra-aorta IVUS imaging is a safe procedure.[14-16, 18] In addition, our study showed that IVUS imaging with a 9 MHZ probe could overcome the limitations of a 20 MHZ probe in a very dilated aorta, which was often used in previous studies.[14-16] In our series, the biggest aortic diameter was 90 mm and the detecting rate of three arch branches:

the celiac trunk artery, the superior and inferior mesenteric arteries, and the renal arteries were 100%.

To our knowledge, this study is the first one that evaluates the value of IVUS imaging in patients with replacement of the ascending aorta for acute type A AD. We found that IVUS imaging could easily identify the replaced graft, the proximal and distal anastomoses, the ostia of the reimplanted coronary arteries. We also found that IVUS imaging was able to detect pathologic changes of the replaced graft, in this study, two peri-graft false aneurysms were detected by IVUS imaging and confirmed by other imaging techniques. Moreover, this study also showed that IVUS imaging could easily localize these pathologic changes and ascertain their causes, which will be very helpful for the treatment strategy. However, considering that all our five patients had been operated by adopting an included technique and using a Dacron tube graft, we can not draw any conclusion on IVUS imaging in patients with replacement of the ascending aorta by adopting an interposed technique and using other types of grafts.

Since the most frequent late complications were due to the aneurysmal dilatation of the false lumen in patients with replacement of the ascending aorta for acute type A AD, so it is very important to acquire residual dissection information for an imaging technique.[3, 4] In fact, several authors have already demonstrated that IVUS imaging could provide complete information of AD.[14, 15] Our study showed that: by comparison with other imaging techniques, IVUS imaging provided similar information such as: the patency of the false lumen, the thrombus in the false lumen, the longitudinal and circumferential extent of the residual dissection, the recurrent dissection, and the aneurysm distal to the graft, but it was more sensitive to detect the intimal tear and the involvement of a side branch vessel.

Compared with current used imaging techniques such as: Aortography, CT, TEE and MRI, IVUS imaging may have several advantages in identifying the replaced graft and its pathologic changes: 1) It has a unique interior view that may avoid the reflection of the replaced graft. 2) It has no potential blind zones. 3) It can directly identify the replaced graft. 4) It does not need contrast. However, IVUS imaging has also some limitations: 1) It is an invasive procedure and has potential damage. 2) It is unable to judge the functional state of the aortic valve prosthesis, but it is not a big

problem, because this information may be supplemented by a transthoracic echocardiography examination.

Therefore, we believe that as an invasive imaging technique, IVUS cannot be used as a regular examination in following up patients with replacement of ascending aorta for acute type A AD, and we agree with other authors that non-invasive MRI seems to the best choice.[7-10] However, IVUS imaging may be considered when 4 currently frequent used imaging modalities can't supply sufficient information or there are discrepancies between them.

Conclusion: In following up patients with replacement of the ascending aorta for acute type A AD, IVUS imaging can provide complete information of the replaced graft and the residual dissection. So, IVUS imaging may be considered when 4 currently frequent used imaging modalities can't supply sufficient information or there are some discrepancies between them.

References:

1. Hagan PG, Nienaber CA, Isselbacher EM, Bruckman D, Karavite DJ, et al.The International Registry of Acute Aortic Dissection (IRAD): New insights into an old disease. JAMA, 2000. 283(7): p 897-903.
2. Erbel R, Alfonso F, Boileau C, Dirsch O, Eber B, et al. Diagnosis and management of aortic dissection. Eur Heart J, 2001. 22(18): p 1642-1681.
3. Sioris T, David TE, Ivanov J, Armstrong S, Feindel CM, et al. Clinical outcomes after separate and composite replacement of the aortic valve and ascending aorta. J Thorac Cardiovasc Surg, 2004. 128(2): p 260-265.
4. Bachet JE, Termignon JL, Dreyfus G, Goudot B, Martinelli L, et al.Aortic dissection, Prevalence, cause, and results of late reoperations. J Thorac Cardiovasc Surg, 1994. 108(2): p 199-205.
5. Cabrol C, Pavie A, Mesnildrey P, Gandjbakhch I, Laughlin L, et al. Long-term results with total replacement of the ascending aorta and reimplantation of the coronary arteries. J Thorac Cardiovasc Surg, 1986. 91(1): p 17-25.
6. Kouchoukos NT, Wareing TH, Murphy SF, Perrillo JB. Sixteen -year experience with aortic root replacement. Results of 172 operations. Ann Surg, 1991. 214(3): p 308-318.
7. Rofsky NM, Weinreb JC, Grossi EA, Galloway AC, Libes RB, et al. Aortic aneurysm and dissection: normal MR imaging and CT findings after surgical repair with the continuous-suture graft-inclusion technique. Radiology, 1993. 186(1): p 195-201.
8. Lepore V, Lamm C, Bugge M, Larsson S. Magnetic resonance imaging in the follow-up of patients after aortic root reconstruction. Thorac Cardiovasc Surg, 1996. 44(4): p 188-192.
9. Fattori R, Descovich B, Bertaccini P, Celletti F, Caldarera I, et al. Composite graft replacement of the ascending aorta: leakage detection with Gadolinium-enhanced MR imaging. Radiology, 1999. 212(2):p 573-577.
10. Mesana TG, Caus T, Gaubert J, Collart F, Ayari R, et al. Late complications after prosthetic replacement of the ascending aorta: what did we learn from routine magnetic resonance imaging following up? Eur J Cardiothorac Surg, 2000. 18: p 313-320.

11. Riley P, Rooney S, Bonser R, Guest P. Imaging the post-operative thoracic aorta:normal anatomy and pitfalls. Br J Radiol, 2001. 74(888): p 1150-1158.
12. Quint LE, Francis I, Williams DM, Monaghan HM, Deeb GM. Synthetic interposition grafts of the thoracic aorta: postoperative appearance on serial CT studies. Radiology, 1999. 211(2): p 317-324.
13. Nissen SE. Application of intravascular ultrasound to characterize coronary artery disease and assess the progression or regression of atherosclerosis. Am J Cardiol, 2002. 89(4A): p 24B-31B.
14. Weintraub AR, Erbel R, Gorge G, Schwartz SL, Ge J, et al.Intravascular ultrasound imaging in acute aortic dissection. J Am Coll Cardiol, 1994. 24(2): p 495-503.
15. Yamada E, Matsumura M, Kyo S, Omoto. Usefulness of a prototype intravascular ultrasound imaging in evaluation of aortic dissection and comparison with angiographic study, transesophageal echocardiography, computed tomography, and magnetic resonance imaging. Am J Cardiol, 1995. 75(2): p 161-165.
16. Alfonso F, Goicolea J, Aragoncillo P, Hernandez R, Macaya C.Diagnosis of aortic intramural hematoma by intravascular ultrasound imaging. Am J Cardiol, 1995. 76(10): p 735-738.
17. Chavan A, Hausmann D, Dresler C, Rosenthal H, Jaeger K, et al. Intravascular ultrasound-guided percutaneous fenestration of the intimal flap in the dissected aorta. Circulation, 1997. 96(7): p 2124-2127.
18. Wei H, Schiele F, Meneveau N, Seronde MF, Legalery P, et al.The value of intravascular ultrasound imaging in diagnosis of aortic penetrating atherosclerotic ulcer. EuroIntervention, 2006. 1: p 432-437.

Table 1: patient demographics.

Case	Age	Gender	HTA	HCT	DM	Smoke	FH	Symptom	Graft
1	53	M	+	-	-	-	-	-	CG
2	74	M	+	+	+	+	+	-	SG
3	74	M	+	-	-	-	-	-	CG
4	66	M	+	+	-	+	+	+	SG
5	68	M	-	+	-	+	-	-	CG

M=male, HTA=hypertension, HCT=hypercholesterolemia, DM=diabetes mellitus, FH=family history, CG=composite graft, SG=single graft.

Table 2: Compared IVUS imaging finding with those of other imaging modalities.

	Total	IVUS (n=5)	Aortogaphy (n=5)	CT (n=3)	MRI (n=3)	TEE (n=1)
Replaced grafts	5	5	5	3	3	1
Proximal anastomose	3	3	3	3	3	0
Distal anastomose	5	5	5	3	3	1
Reimplanted coronary artery	3	3	3	2	1	0
Replaced aortic valve	2	2	2	1	0	0
Peri-graft false aneurysm	2	2	0	0	2	0
Residual dissection	5	5	5	3	3	1
Patency	5	5	5	3	3	1
Intimal tear	15	15	9	7	8	2
Thrombus	4	4	3	3	3	1
Longitudinal extent	5	5	5	2	3	1
Circumferential extent	5	5	5	3	3	1
Recurrent dissection	1	1	1	1	0	1
Branch involvement	3	3	1	1	0	0
Aneurysm distal to graft	5	5	5	3	4	0

Figure 1a:

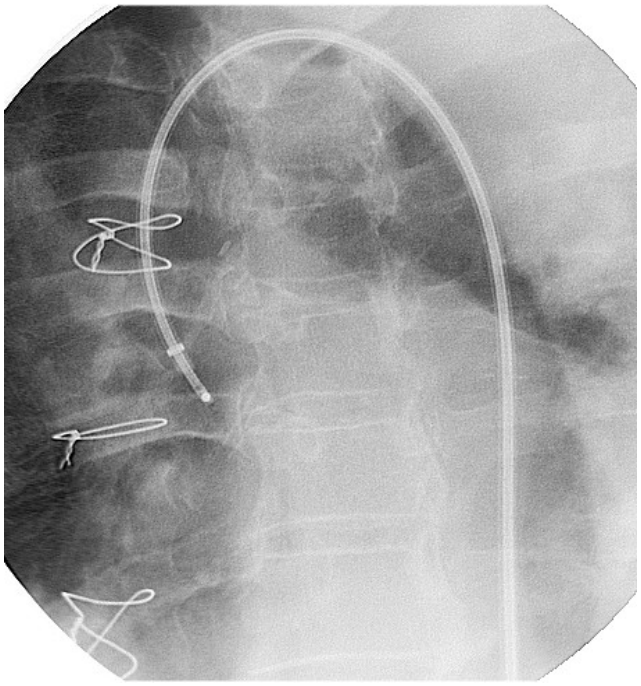

1a: IVUS catheter in the aorta (angiogram).

Figure 1b:

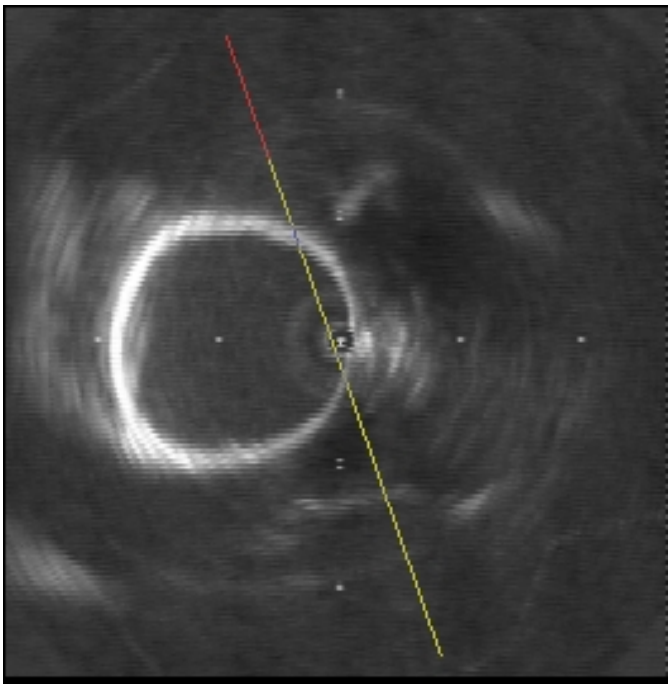

1b: Normal graft (transverse sonogram).

Figure 1c:

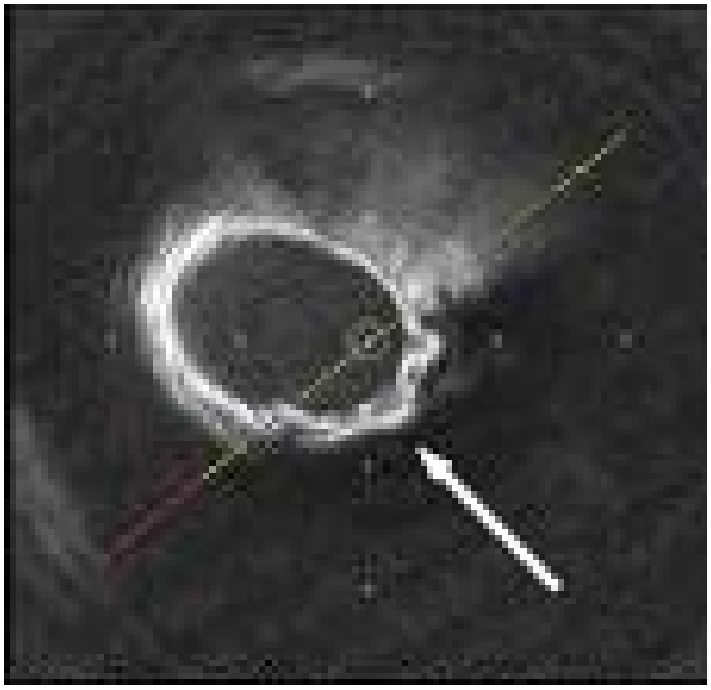

1c: Normal distal anastomosis (transverse sonogram).

Figure 1d:

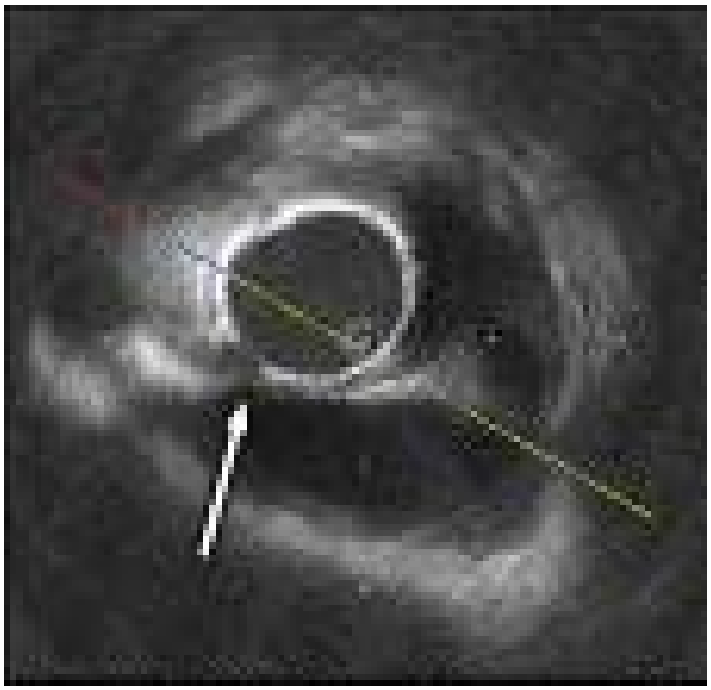

1d: Normal ostium of the reimplanted right coronary artery (transverse sonogram).

Figure 2:

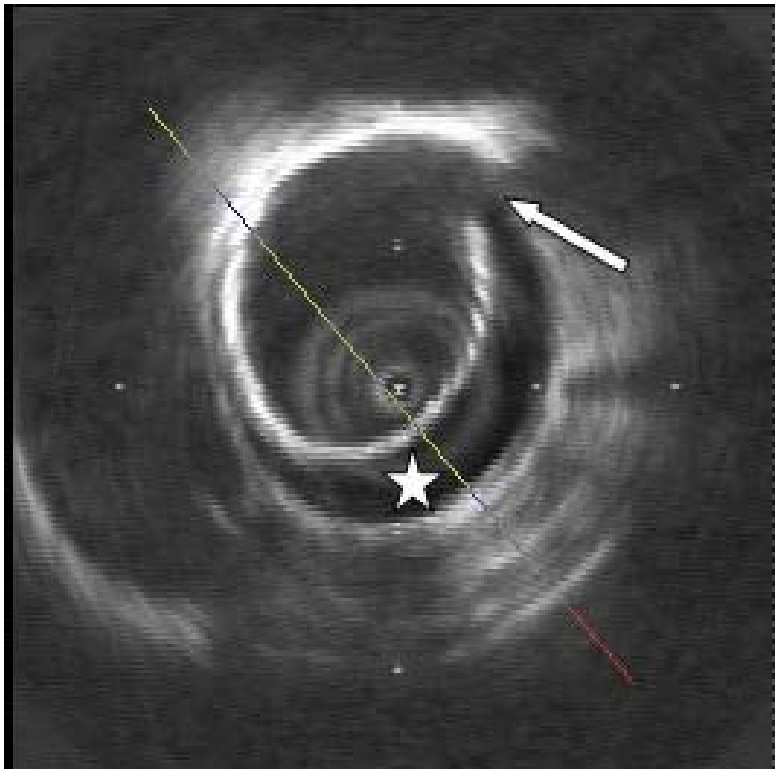

2: The star represented a small false aneurysm that was caused by suture line dehiscence (indicated by an arrow; transverse sonogram).

Figure 3a:

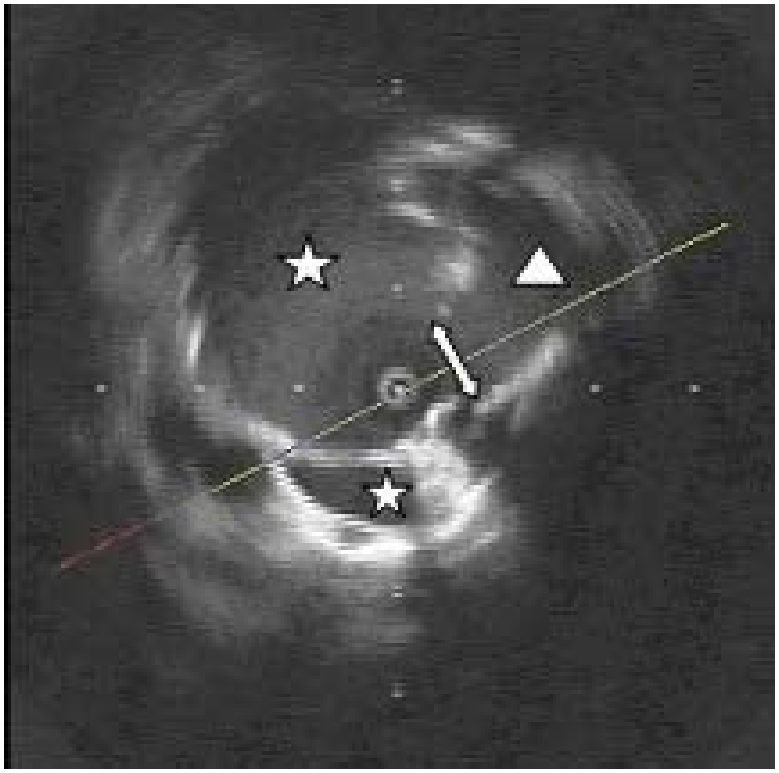

3a: IVUS detected a big peri-graft false aneurysm (represented by two stars) and their mouth (indicated by a double head arrow) at the distal anastomosis. The triangle represented the real lumen (transverse sonogram).

Figure 3b:

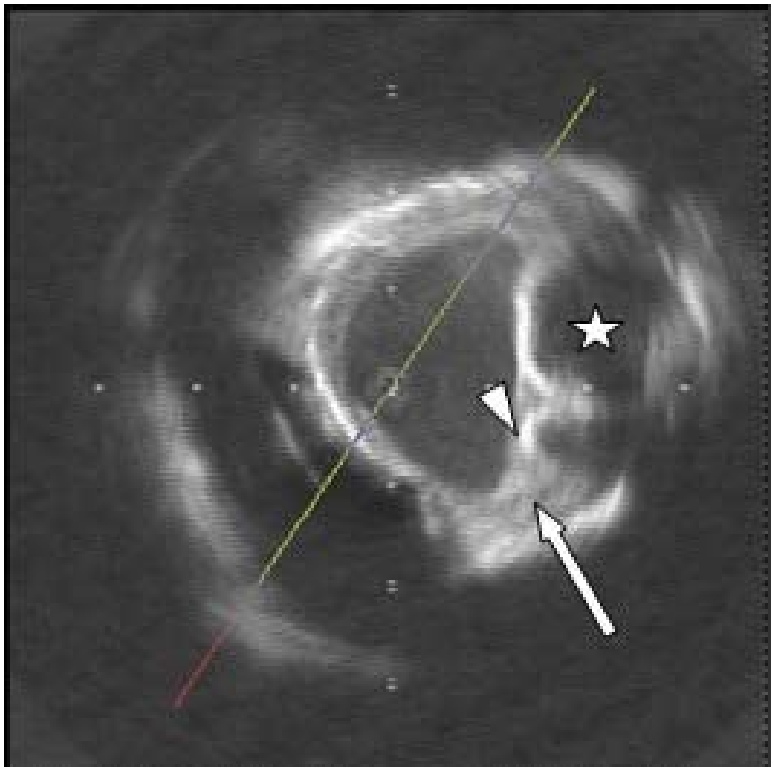

3b: IVUS probe was in the false aneurysm at the proximal anastomosis. The real lumen was represented by a star. The reimplanted ostia of the coronary arteries (indicated by a triangle) was surrounded by thrombus (indicated by an arrow; transverse sonogram).

Figure 3c:

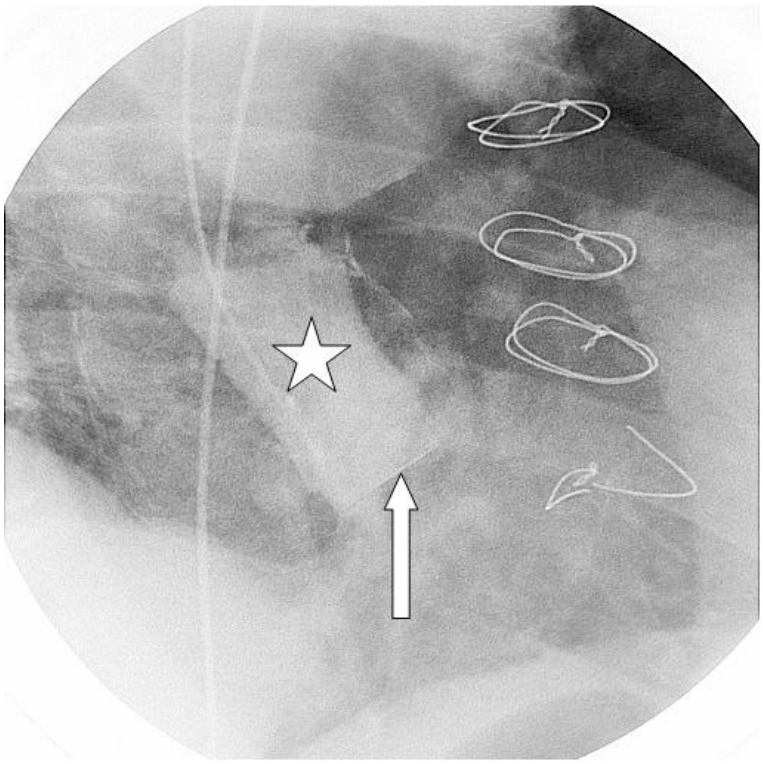

3c: The tube graft and the valve prosthesis (indicated by an arrow) were opacified, whereas the false aneurysm was not opacified (left anterior oblique angiogram).

Figure 3d:

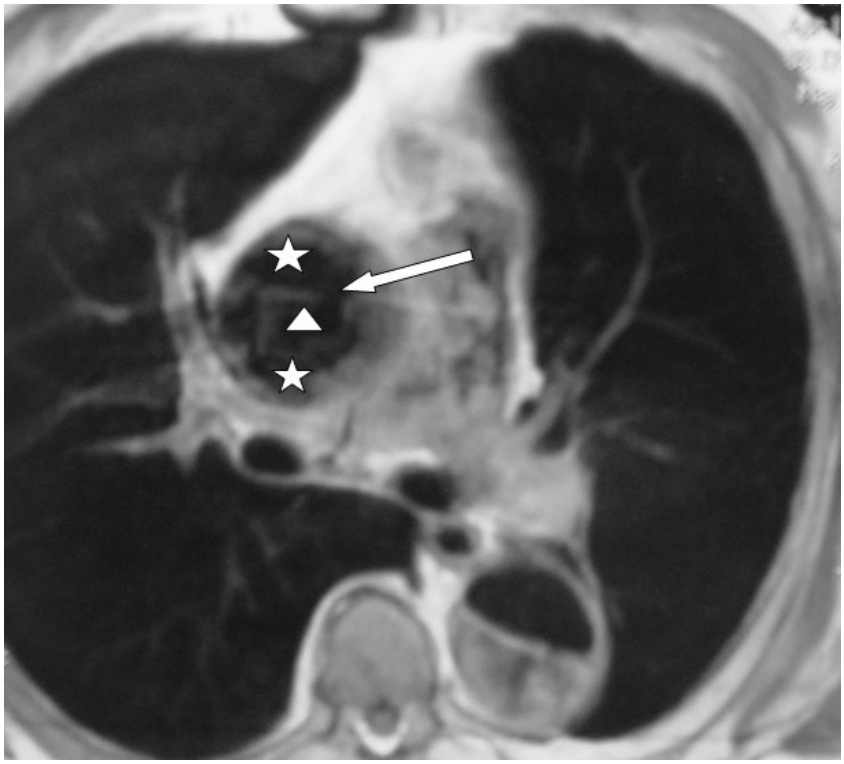

3d: A transversal MRI image. The false aneurysm was represented by two stars and the real lumen was represented by a triangle. The arrow indicated the suture line dehiscence site.

Summary for IVUS and AD

1, Acute aortic dissection includes five subtypes: classic aortic dissection (CAD), intramural hematoma (IMH), penetrating atherosclerotic ulcer (PAU), subtle aortic dissection (SAD) and traumatic aortic dissection (TAD) according to 2001 ESC experts' group. CAD, IMH, and together with PAU are called as acute aortic syndrome (AAS).

2, AD has high mordality and mortality and needs urgent diagnosis. Currently, CT (sprial CT with multi-dector), MRI, TEE and aortography are four frequently used imaging modalities. Although they have high sensitivity and specificity, all of them have their limitations.

3, Our study performed IVUS imaging with a mechanic 9-MHZ probe in 15 consecutive patients with established or suspected AD from September 2002 to July 2005. We demonstrated that IVUS imaging is very helpful in most of such patients (80%), because it can supply us additional data beyond four currently used imaging techniques, which is useful in diagnosis and management of patients with AD, we also demonstrated that a 9-MHZ probe is superior to a 20-MHZ probe in a big aorta.

4, TEE doesn't permit us inspect abdominal aorta, and also it has blind zones at ascending aorta and aortic arch. While IVUS imaging can supply us an interior view of whole aorta (from ascending aorta to iliac branches) and has no blind zones.

5, Our study used spiral CT with 4 detectors. We found it was not sensitive to detect subtle AD and small PAUs, also it is difficulty to differentiate IMH and partly thrombosed false lumen. Although, nowadays, many centers use spiral CT with 64 detectors, theoretically, it has lower solution than IVUS. But till now, there is no study performed to compare this kind of machine with IVUS in patients with AD.

6, Although MRI is more sensitive than CT in distinguishing IMH and partly thrombosed false lumen, it also has lower resolution than IVUS imaging.

7, As to aortography, it is a good tool in detecting CAD and PAU, but it can't directly detect IMH.

8, In summary, from our study, we demonstrated that IVUS imaging has a very high sensitivity and specificity in diagnosis of different subtypes of AD. When compared with currently frequent used four imaging techniques, its main superiorities are IVUS has an unique interior view and without blind zones for whole aorta, it doesn't need contrast that will be harmful for kidney function, it has a very high resolution which

can ensure IVUS detects small changes of aorta, finally, it can be simultaneously performed with endovascular procedures like fenestration and stenting.

Part II

The current imaging techniques in detecting a vulnerable plaque.

II-1:Introduction:

Coronary atherosclerosis is by far the most frequent causes of ischemic heart disease, and plaque disruption or erosion with superimposed thrombosis is the main cause of the acute coronary syndromes (ACSs) of unstable angina, myocardial infarction, and sudden death. The composition and vulnerability of plaque rather than its volume or the consequent severity of stenosis produced have emerged as being the most important determinants for the development of the thrombus-mediated ACSs.[1, 2] Three characteristics of a rupture-prone plaque were reported: the amount of lipid in the core of the plaque, the thinness of the fibrous cap, and the degree of inflammatory cell infiltrate. Virmani R et al have shown that the mean necrotic core size is greatest in pathological specimens of ruptured plaques.[3] Davies MJ et alhave estimated that the atheroma is at risk of rupture when at least 40% of the total plaque area is composed of lipid.[4] Thin fibrous caps (usually measuring 65-150 μm) have been found from autopsy specimens to be associated with plaque rupture.[5] The thinnest portion of the cap is at the shoulder region and appears to be most prone to rupture. The third characteristic of high-risk plaque is inflammation. A high degree of macrophage infiltration into and around the fibrous cap has been found in specimens of acute plaque rupture.[3]These macrophages release matrix-digesting enzymes such as macrophage myeloperoxidase responsible for the degradation of the fibrillar collagen that forms the structure of the fibrous cap.Several studies have challenged the notion that ACS result only from pathology at a focal site in the coronary bed. An intravascular ultrasound (IVUS) study performed by Rioufol G et al has shown that 79% of the patients with ACS have evidence of two or more plaque ruptures.[6] Goldstein JA et al looked at angiograms of 253 patients presenting with an acute MI and found that 39.5% of them had evidence of multiple complex plaques at presentation. [7] Buffon A et al found an elevated level of neutrophil myeloperoxidase in the great cardiac vein of patients having unstable angina thought to be due to lesions in the left anterior descending (LAD) or in the right coronary artery, despite the fact that the right coronary artery territory is not drained by the great cardiac vein. The neutrophil activation throughout the coronary bed led them to conclude that unstable angina is a generalized endothelial inflammatory process.[8] Moreover, Plaque disrupture itself is a asymtomatic, and the associated rapid plaque growth is usually clinically silent. Autopsy data indicated that 9% of “normal” healthy persons.

have asymtomatic disrupted plaques in their coronary arteries, increasing to 22% in persons to 22% in persons with diabetes or hypertension.[9] Futhermore, In 33% of ACS, there is only a superficial erosion of a markedly stenotic and fibrotic plaque with overlying thrombosis, without frank rupture or significant inflammatory cell infiltrate.[3] Goldschmidt-Clermont PJ et al described plaque rupture as a result of an imbalance between plaque cell injury (a local process) and plaque repair (a systemic process driven by marrow-derived cellular elements).[10] Three major factors appear to determine the thrombotic response to plaque disruption/erosion: (1) character and extent of exposed plaque components (local thrombogenic substrates); (2) degree of stenosis and surface irregulartities that activate platelets (local folw disturbances); and (3) thrombotic-thrombolytic equilibrium at the time of plaque disruption (systemic thrombotic tendency).In this review, we will discuss currently used invasive and non-invasive imaging modalities that aim at detecting rupture-prone or high risk or vulnerable plaques. However, we should keep in mind the systemic forces that play into plaque destabilization. Only incorporating both anatomical and functional information, can we understand the mechanisms of acute coronary events in 'at-risk' patients.

II-2:Invasive imaging modalities:

II-2-1:Coronary artery angiography:

The development of coronary artery angiography in the 1950s provided the first in vivo imaging of the coronary arteries. It has become our standard invasive method for diagnosing coronary artery disease (CAD). Histopathological correlations of angiographic lesion morphologies have shown that lesions with irregular borders and intraluminal lucencies correspond to complex plaque with associated hemorrhage and thrombosis. Concentric stenoses with smooth borders and no intraluminal lucencies correspond to more stable plaques.[11]The main limitation of angiography is that it only provides information about the vessel lumen without characterizing the vessel wall. The reliability of the degree of angiographic stenosis is affected by three followed factors: visual assessment of the degree of stenosis has significant intra-operator variability; it can only be diagnosed by comparing an area to an adjacent reference segment that is assumed to be disease free, whereas there is often no normal referent segment because atherosclerosis is usually diffuse; positive remodeling firstly described by Glagov S et al make a diseased vessel undetectable angiographically. Only at a very advanced (plaque occupies 40% vessel area) stage of the plaque is evident by angiography.[12] Moreover, most importantly, we know that the degree of lumenal stenosis does not correlate with the risk of a lesion leading to an ACS and that these events often occur from rupture of a modestly stenotic plaque not detectable by angiography. For these reasons, angiography is not an optimal modality for identifying vulnerable plaques.

II-2-2: Intracoronary angioscopy:

Intracoronary angioscopy allows direct visualization of the plaque surface, color of the luminal surface (red, white, or yellow), presence of thrombus, and macroscopic feasures (tears, ulcerations, and fissures). Plaques seen as yellow on angioscopy are lipid rich on histopathology, often have an irregular intimal surface, and are commonly found in patients with ACS. White plaques contain more fibrous tissue, are less prone to rupture, and are more commonly observed in patients with stable angina. One study attempted to predict coronary events on the basis of the angioscopic appearance of plaque in 157 patients. Thirty-nine patients had yellow plaques, and 118 had white plaques. At 12-month follow-up, acute coronary events,

confirmed by angioscopy to be the result of thrombus arising from the site of the ruptured culprit plaque, were more common in association with yellow than white plaques (28 vs. 3%).[13] Although currently Angioscopy is the only imaging technique that can detect plaque erosion, which results in 35% of the whole ACS, it remains primarily a research tool because of its multiple limitations. It is an invasive method that is unable to cross severely stenotic lesions, visualize the proximal 2 cm of the main coronary arteries, enter small-caliber vessels, or provide information about the layers of the vessel wall.[14]

II-2-3:Intracoronary thermography:

Inflammation is a hallmark feature of vulnerable plaques. Vulnerable atherosclerotic plaques are hot and their surface temperature correlates with an increased number of macrophages and decreased fibrous-cap thickness. Intracoronary thermography is a technique to directly measure temperature heterogeneity between plaque surface and normal vessel wall by using different designed catheters with thermistor(s) and wires with thermal sensors at the distal tip. In an ex vivo study, Madjid M et al measured thermal heterogeneity of atherosclerotic plaques by using a needle thermistor. In the absence of blood flow,they found significant temperature variations ranging from 0.2°C to 2.2°C. Measured temperature had a positive correlation with macrophage density ($r = 0.66$; $p = 0.0001$) and an inverse correlation with smooth-muscle-cell density ($r = -0.41$; $p = 0.0001$).[15]Naghavi M et al developed a contact-based “thermo-basket” catheter for measuring the in vivo temperature over the arterial wall. This is a thermocouple-based basket catheter equipped with four small, flexible wires with built-in thermocouples and a thermal sensor in its central wire for simultaneous monitoring of the blood temperature. The device has a thermal resolution of 0.02°C with a sampling rate of 20 temperature readings per second.[16] This catheter has been demonstrated to be able to detect temperature heterogeneity over the atherosclerotic plaques in the femoral arteries of inbred atherosclerotic dogs and the aortas of Watanabe rabbits.[16, 17] Verheye S et al developed an over-the-wire thermography catheter with four thermistors. They used it in 20 New Zealand rabbits randomized to either a normal diet or a cholesterol-rich diet for six months. They found marked temperature heterogeneity (up to 1°C) in the hypercholesterolemic rabbits at sites of thick plaques where histology showed a high macrophage density.[18] Coronary flow may exert a “cooling effect” on measured coronary

temperature. However, there are some discrepancies in the effect of blood flow on coronary temperature measurement. Stefanadis K et al have found that complete obstruction of blood flow may increase the degree of detected temperature heterogeneity by 60% to 76%. [19] Whereas, Verheye S et al have shown that normal physiological flow conditions reduce temperature heterogeneity only by 8% to 13% compared to surface temperature measured in the absence of flow.[20] Stefanadis L et al conducted the first human intracoronary thermographic study in 1999 by using a single-channel, thermistor-based catheter. In this study, temperature differences (ΔT) between atherosclerotic plaque and healthy vascular wall was 0.10 ± 0.11°C in patients with stable angina pectoris (SAP), 0.68 ± 0.34°C in those with unstable angina (UA), and 1.47 ± 0.69°C in patients with acute myocardial infarction (AMI).[21] However, in more recent studies, lower degrees of temperature difference have been reported by Webster M et al, Verheye S et al, and Schmermund A et al.[22-24] These differences may be caused in part by the discrepancies in the use of various medications (e.g, statins, aspirin) which may stabilize hot plaques, and more importantly, the effects of thermography catheters on blood flow. The larger thermistor used by Stefanadis et al almostly obstructed blood flow, whereas more recent studies have used catheters which did not obstruct blood flow. The study of Webster M et al has clearly shown that the cutoff temperature significantly affects the number of hot plaques. They studied 6 patients with UA and 14 patients with SA. A cutoff temperature of ≥0.1°C yielded 10 patients with no temperature heterogeneity, 4 patients with a single hot spot, 3 patients with 2 hot spots, and 3 patients with 3 hot spots. However, an alternative cutoff of ≥0.2°C results in only 2 of 17 patients with a hot spot, and 1 patient with 2 such lesions. [22]Based on published data, there are some discrepancies in intracoronary temperature heterogeneity and serum inflammatory markers. The study of Stefanadis C et al showed a strong correlation between C-reactive protein (CRP) and serum amyloid A levels with detected differences in temperature ($r = 0.796$, $p = 0.01$ and $r = 0.848$, $p = 0.01$, respectively).[25] Wainstein MV et al found an apparently higher mean CRP level in patients with higher temperature heterogeneity compared to those without elevated temperature .[26] In contrast, Webster M et al showed that the number of hot plaques did not correlate with the CRP level.[22] Toutouzas K et al have shown a strong and positive correlation between the coronary remodeling index and the ΔT between the atherosclerotic plaque and healthy vascular wall. They have also reported a

correlation between the serum matrix metalloproteinase (MMP)-9 concentration and ΔTs.[27]

Stefanadis C et al investigated the midterm prognostic effect of human coronary atherosclerotic plaque temperature. They found that the temperature difference (ΔT) between the atherosclerotic plaque and the healthy vessel wall was a strong predictor of adverse cardiac events (odds ratio 2.14, p = 0.043). [28]

Currently, several thermography catheters are being studied in clinical trials. These clinical trials need to determine the safety, reproducibility, and benefits of this imaging technique. Major questions remain to be answered: What is the best cutoff value to define a hot plaque? What would be the sensitivity and specificity of such cutoff values in different clinical settings? Is it best to find focal increases in temperature or to define the general temperature burden in coronary segments? Is proximal occlusion necessary for thermography studies? Once a hot plaque or artery is identified, what would be the best clinical approach to manage it?

Figure 1: an example of thermography system (Volcano Thermography System).

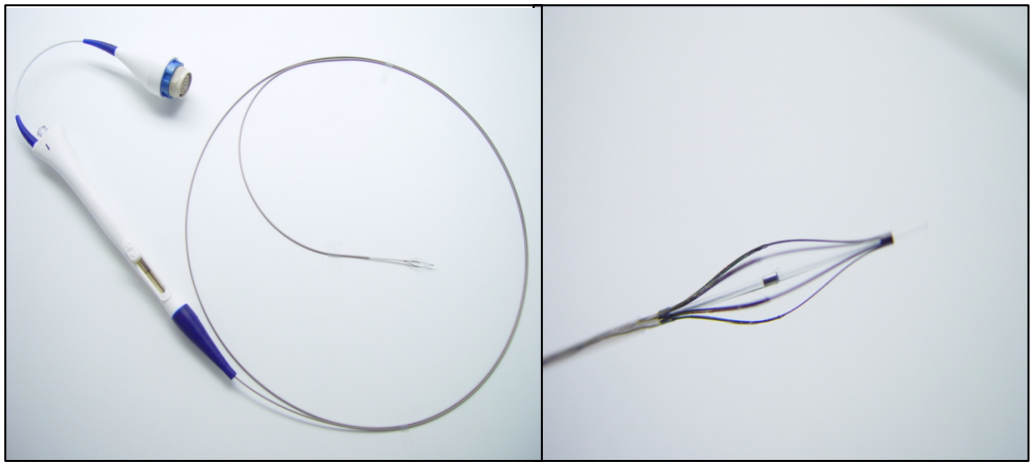

II-2-4: Optical coherence tomography:

Optical coherence tomography (OCT) is a recently developed method of catheter-based, high-resolution intravascular imaging that has demonstrated considerable potential as a method for assessing unstable plaque. It is analogous to ultrasound, measuring the backreflection of infrared light rather than sound. OCT has several advantages: firstly, it has higher resolution(an axial resolution of 2-30 μm and a lateral resolution of 5-30 μm) than any currently available imaging technology; secondly, its acquisition rates are near video speed, faster than many other technologies for assessing plaque; thirdly, the typical OCT catheters contain no transducers within their frame, which makes them both small and inexpensive; finally, because OCT uses light, a variety of spectroscopic techniques are available, including polarization spectroscopy, absorption spectroscopy, elastography, OCT Doppler, and dispersion analysis.

In the mid-1990s, Tearney GJ et al postulated that the high resolution of OCT made it a potentially useful technology for imaging atherosclerotic plaque. [29]Also these same authours successfully performed micron scale imaging of both in vitro human aorta and coronary arteries. The morphology of atherosclerotic plaque was accurately determined by OCT when compared with the corresponding histopathology.[30, 31] In vivo OCT imaging was initially performed of aortas in New Zealand White rabbits before human studies.[32] Because light-scattering occurs from red blood cells, saline flushes were required during imaging at a rate of 2 to 3 cc/s. Data was obtained at 4 frames/s and saved on super VHS format (state-of-the-art systems now preserve the data digitally). Data was also performed in vivo comparing the ability of IVUS (40 MHz) and OCT to assess stent approximation in the rabbit, where OCT was determined to be superior. [33]In vivo human studies are currently underway by Lightlab Imaging in addition to several other groups. These studies have confirmed the ability of OCT to characterize plaque by using a 0.017-inch imaging guidewire in the presence of a saline flush. Neointimal hyperplasia is noted in the OCT image but is poorly defined on the IVUS image. Additional studies have included the assessment of stent placement and estimation of macrophage concentration. [34, 35].Major limitations of OCT are its attenuation by blood and its limited penetration in tissue. Blood significantly attenuates the ability of OCT to image through blood.

Approaches to overcome this limitation are saline flushes, balloon occlusion, and index matching. A second potential limitation of OCT is that its penetration through the arterial wall is in the range of 2 to 3 mm. Although this is generally sufficient for imaging of most arteries, with some large necrotic cores, the entire length of the core can not be imaged. Several approaches to overcome this are proposed, which include increase of the dynamic range, improved choices in median wavelength, use of a parallel ultrasound beam, and image processing techniques.

Figure 2: A thin-capped fibroatheroma detected by OCT (the white arrow indicated the thin fibrous cap and the white star represented the lipid core, image adapted from Schmitt JM, Petersen CL. Imaging and characterization of coronary lesions with optical coherence tomography. 2002 IEEE International Symposium on Biomedical Imaging, Washington, DC, July 7-10, 2002, 106-9).

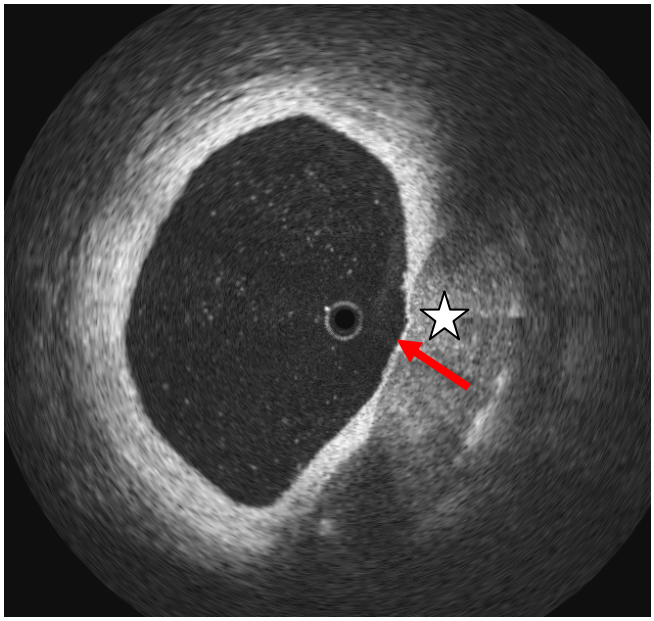

II-2-5: Raman spectroscopy:

Spectroscopy directs light of specific wavelengths onto tissue and collects light scattered from the tissue into a spectrometer. Each tissue has a unique pattern of light absorbance at different wavelengths. This allows for the creation of a spectroscopic 'fingerprint' for each tissue type. Spectroscopy can be performed in the coronary bed. Spectral modeling is used to discriminate coronary arterial tissue into three categories: nonatherosclerotic plaque, noncalcified plaque, and calcified plaque.

Raman spectroscopy is an optical technique that characterizes the chemical composition of biological tissue. Raman spectra can be obtained by procession the collected light that is scattered by a tissue as it is illuminated with a laser. Raman spectroscopy can be combined with other catheter-based imaging techniques, such as IVUS, to localize and quantify cholesterol and calcium salts in atherosclerotic plaque. Current limitations of Raman spectroscopy are the strong background fluorescence, the absorbance by blood of the laser light, and the relatively long acquisition time. Because this is a 1-dimentional technique (no depth information), it may be more powerful when combined with other imaging technique.

II-2-6: Near-Infrared (NIR) Spectroscopy:

Near-Infrared (NIR) spectroscopy also yields information on the chemical composition of tissue. NIR spectroscopy (750 to 2500nm) has the advantage of deep penetration.[36] Recently, the use of NIR spectroscopy has been explored for the characterization of the composition of atherosclerotic lesions. Moreno PR et al have studied the use of NIR spectroscopy to identify high-risk plaque. Their in vitro studies showed that spectroscopy could identify lipid pools, thin fibrous caps, and inflammatory cell infiltrates in autopsy specimens of human aortas.[37] In vivo studies using a NIR catheter system are now ongoing in humans in an attempt to identify high-risk plaque in patients with known coronary disease undergoing elective intervention. Similar to Raman sepctroscopy, NIR Spectroscopy could potentially be used as a complement to an imaging modality such as IVUS or OCT to combine visual inspection of anatomy with the tissue characterization afforded by spectroscopy.

II-2-7:Intravascular ultrasound (IVUS):

IVUS imaging is based on transmitting and receiving high frequency sound waves. The time between transmission and reception of the wave is directly related to the distance between the source and reflector. IVUS is performed as part of cardiac catheterization using catheters equipped with ultrasound probes at their tip. The IVUS probe utilizes high ultrasound frequencies (20-50 MHz) to generate a gray-scale image with an axial resolution of 150 μm and a lateral resolution of 250 μm. The catheter tip is placed just distal to the lesion and withdrawn during continuous imaging. This invasive modality permits direct and real-time imaging of ahteroma and provides a cross-sectional, tomographic perspective of the vessel and atherosclerotic disease. IVUS is able to assess areas that are difficult to visualize by angiography such as diffusely diseased segments, eccentric lesions, ostial or bifurcation lesions, left main lesions, and foreshortened vessels.On the basis of plaque echogenicity, IVUS is able to distinguish some of the components of atherosclerotic plaque. Highly echoreflective regions with acoustic shadows correspond to calcified tissue. Hypoechoic regions correspond to lipid-rich tissue. Hyperechoic regions represent fibrous tissue. This allows for a general assessment of a plaque as 'soft' or 'hard' based on the relative amount of lipid versus fibrous tissue in the core. The resolution of IVUS does not allow it to quantify the thickness of the fibrous cap or the degree of inflammatory cell infiltrate.By distinguishing the blood-intimal border and the external elastic membrane (EEM), IVUS is able to provide precise measurements of lumen area, intima-media area, and EEM. Using these measurements, IVUS has confirmed the in vitro findings of Glagov that vessels may appear normal by angiography at the site of significant lesions due to positive remodeling.[38]It has also been shown that the process of negative remodeling, leading to lumenal narrowing, occurs in more advanced lesions and in response to stent placement (restenosis). IVUS studies have looked at the relationship of types of remodeling and clinical presentation of patients with CAD. One study looked at 85 patients with unstable and at 46 patients with stable coronary syndromes using IVUS. Positive remodeling was significantly more common in unstable versus stable lesions (51.8 vs. 19.6%), whereas negative remodeling was more common in stable versus unstable lesions (56.5 vs. 31.8%).[39]Yamagishi M et al have used IVUS to relate morphology of plaque to instability of plaque. They identified 114 sites of plaque by IVUS in patients with

coronary disease that did not correlate with lesions >50% by angiography. They prospectively followed these patients. Twelve patients had coronary events at one of the previously identified sites. In comparison to sites that did not become unstable, the culprit sites were characterized by a large plaque burden with an echolucent zone representing a lipid-rich core. [40]Kotani J et al used IVUS to evaluate 78 coronary arteries in 38 consecutive patients with acute MI. They found that culprit plaques had three distinctive features by IVUS: positive remodeling, thrombus, and a large plaque mass, again confirming the hypothesis that there are lesion-specific morphologies that determine plaque instability.[41]IVUS has a number of limitations. The interpretation is based on visual inspection. Echogenicity and texture of different tissue may appear very similar. It is generally excellent at determining the thickness and the echogenicity of the vessel wall, but it does not consistently provide actual histology. It is difficult to distinguish between thrombus and lipid-rich plaque on IVUS. There is often significant artifact. Oblique-plane imaging when the probe is not perpendicular to the vessel wall can lead to distortion of the image. The 1-mm catheter is too large to pass through severe stenoses.

Figure 3: The middle image is angiogram. The left and the right images are sonograms, the left one revealed an eccentric plaque on the site indicated by a red arrow and the right one documented a ruptured plaque on the site indicated by a yellow arrow.

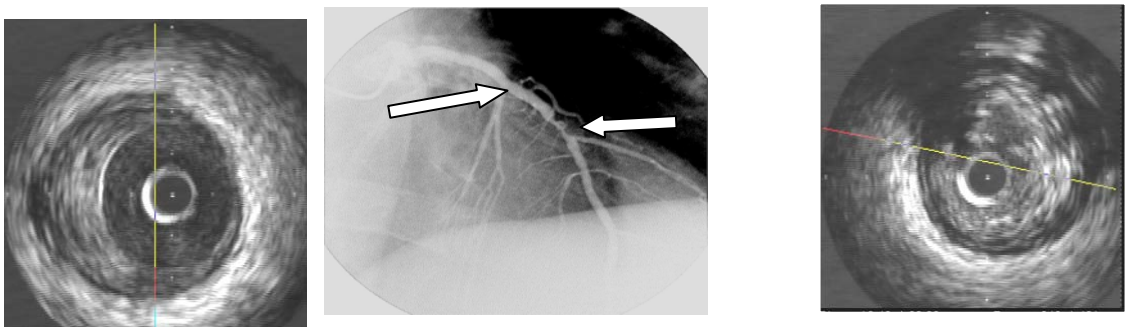

II-2-8: IVUS elastography/palpography:

Elastography is a technique that assesses the local elasticity (strain and modulus) of tissue. It is based on the principle that the deformation of the tissue by a mechanical determined using ultrasound. For intravascular purposes, the intraluminal pressure is used as the exciation force. The radial strain in the tissue is obtained by cross-correlation techniques on radio frequency signals. The strain is color-coded and plotted as a complimentary image to the IVUS echogram. IVUS elastrography and IVUS palpography (which uses the same principle but is faster and more robust) have been extensively validated using simulations and by performing experiments in vitro and in vivo with diseased arteries from animals and humans.

In vitro the technique was validated using diseased human coronary and femormal arteried. Especially between fibrous and fatty tissue, a high significant difference in strain ($p=0.0012$) was found. Additionally, a high-strain at the human-vessel wall boundary has an 88% sensitivity and 89% specificity for identifying such plaques.[42]

In vivo the technique was validated in an atherosclerotic Yucatan minipig animal model. In this study, plaques were classified as absent, early fibrous lesion, or advanced fibrous plaque. The average strains in the plaque-free arterial wall (0.21%) and the early (0.24%) and advanced lesions (0.22%) were similar. Higher average strain values were observed in fatty lesions than in fibrous plaques ($p=0.007$). Receiver operating characteristic analysis revealed a sensitivity and specificity at 100% and 80%, respectively, to identify fatty plaques. The presence of a high-strain spot (strain>1%) has 92% sensitivity and 92% specificity to identify macrophages. [43]

In a patient study, de korte et al revealed high-strain value (1-2%) in thin –cap fibrous atheroma and found that calcified material has low-strain value (0-0.2%). [44]IVUS elastrography and IVUS palpography have several limitations: firstly, due to the unknown arterial stress distribution elastograms can not be directly interpreted as a morphology and material composition image; secondly, radial strain depends upon the materail properties of an artery including geometry and used catheter position; thirdly, a three-dimensional (3D) elastrograms technique is needed to be constructed to rapidly identify high-strain spots over the full length of a coronary artery; lastly, a certain cut-off strain value with high sensitivity and specificity needs to be established, and also its predictive value for future cardiac events is needed to be demonstrated by large prospective patient's cohort studies.

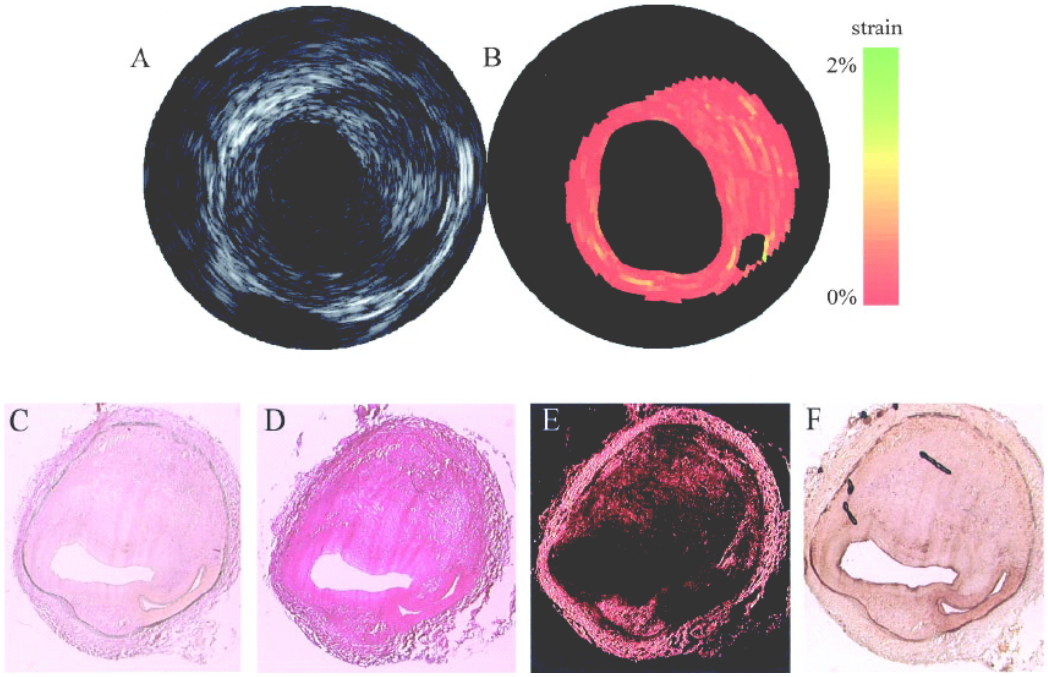

Figure 4: IVUS (upper left image) and IVUS elastography (upper right image) and histology (lower images). (Adapted from de Korte CL et al. Circulation. 2002; 105: p 1627-30).

II-2-9: Integrated backscatter IVUS (IB-IVUS):

Integrated scatter intravascular ultrasound (IB-IVUS) is an improved conventional IVUS (C-IVUS) technique that focuses on evaluating and mathematically transforming the radiofrequency signal from ultrasound waves into a color-coded representation of plaque characteristics such as lipid, fibrous tissue, calcification, and necrotic core. In studies of the myocardium, calibrated myocardial IB was significantly correlated with the volume fraction of interstitial fibrous. In preliminary in vitro studies of atherosclerotic arterial wall, IB values reflected the structural and biochemical composition of atherosclerotic lesions and could differentiate fibrofatty lesions, fatty lesions and calcification.[45] Kawasaki M et al validated IB-IVUS technique in the right common carotid and femoral arteries. In their study, IB values were determined using a 5–12 MHz multifrequency transducer, setting the region of interests (ROIs) (11 × 11 pixels) on the echo tomography of the entire arterial wall and comparing it with histologic features. IB values of ROIs were divided into five categories: category 1 (thrombus) $4 < IB \leq 6$; category 2 (media and intimal hyperplasia or lipid pool in the intima) $7 < IB \leq 13$; category 3 (fibrous) $13 < IB \leq 18$, category 4 (mixed lesion) $18 < IB \leq 27$ and category 5 (calcification) $28 < IB \leq 33$. They demonstrated that color-coded maps constructed with IVUS-IB precisely reflected the histologic features of media and intima.[46]

Also these same authors validated IB-IVUS technique in coronary arteries by use of a 40 MHz catheter, and radiofrequency signals were digitized at 2 GHz in 8-bit resolution. IB values were divided into five categories: category 1 (thrombus) $-88 < IB \leq -80$; category 2 (media and intimal hyperplasia or lipid core in the intima) $-73 < IB \leq -63$; category 3 (fibrous) $-63 < IB \leq -55$, category 4 (mixed lesion) $-55 < IB \leq -23$ and category 5 (calcification) $-30 < IB \leq -23$. The differences among thrombus, fibrous tissue, mixed lesion, calcification and lipid core were significant. However, lipid core, intimal hyperplasia and media had similar IB values. There was a good correlation between IB values and histology. Comparison between coronary angioscopy and IB-IVUS revealed that the surface color of plaques in angioscopy reflected the thickness of the fibrous cap rather than the size of the lipid core.[47] Yokoyama M et al observed the effects of lipid-lowering drugs on plaques by using IVUS-IB techniques. Fifty consecutive patients undergoing percutaneous coronary intervention (PCI) were enrolled. IVUS-IB were acquired from non-PCI-targeted echolucent plaques. The patients were randomly assigned into 2 group: group S (n=25) taking atorvatatin

10mg/d and group C (n=25) as control. After 6-month follow up, IVUS-IB values were substantially increased and plaque volume was significantly reduced. [48]Sano K et al used IB-IVUS technique to study the relationship between angiographically normal coronary lesions and risk factors. In their study, angiographically normal coronary lesions were analyzed by IB-IVUS in 30 patients with SAP. They found that the diabetes mellitus (DM) group had significantly bigger lipid cores and thinner intimal hyperplasia compared with the non-DM group, and the hypertension (HT) group had significantly more intimal hyperplasia compared with non-HT group.[49] Amano T et al conducted a study by use of IB-IVUS to evaluate the impact of metabolic syndrome (MetS) on tissue characteristics of angiographically mild to moderate coronary lesions and they found that MetS indepedently correlated with the percentage of lipid volume.[50]Kawasaki M et al compared the diagnostic accuracy of OCT, IB-IVUS and conventional IVUS for tissue characterization of human coronary plaques. They found that by using histological images as a gold standard, the sensitivity of OCT for characterizing calcification, fibrous and lipid pool was 100%, 98% and 95%, respectively, the specificity of OCT was 100%, 94% and 98%, respectively. The sensitivity of IB-IVUS was 100%, 94% and 84%, respectively, and the specificity of IB-IVUS was 99%, 84% and 97%, respectively. The sensitivity of C-IVUS as 100%, 93%, and 67%, respectively. The specificity of C-IVUS was 99%, 61%, and 95%, respectively.[51]

Sano K et al performed a study to assess vulnerable plaques causing ACS using IB-IVUS. The subjects were 140 patients with AP, and 160 coronary lesions without significant stenosis were selected for evaluation. At the follow-up (30 +/- 7 months), 12 plaques caused ACS after the initial IVUS examination. Ten of the 12 plaques had IB-IVUS parameters recorded at baseline. These 10 plaques were classified as vulnerable plaques (VP), and the other plaques were classified as stable plaques (SP; n = 143). Plaque burden, eccentricity, remodeling index and percentage lipid area were greater in VP than in SP. Percentage fibrous area was smaller in VP than in SP. The sensitivities, specificities, and positive predictive values of percentage fibrous area (90%, 96%, and 69%, respectively) and percentage lipid area (80%, 90%, and 42%, respectively) for classifying VP were evaluated.[52]

IB-IVUS has several limitations: 1) Ultrasonic backscatter is angle-dependent, and this may limit quantitative ultrasonic diagnosis; 2) the position of IVUS tranducer will affect IB values; 3) the reverberation phenomena has an effect on the evaluation of IB values of the posterior arterial wall; 4) there are lack of large randomized trails that demonstrated the preditive accuracy of future cardiac events by use of IB-IVUS values.

Figure 5: (A) Three-dimensional (3D) color-coded maps of the coronary arterial plaques constructed by 3D intravascular ultrasound with integrated back scatter; (B) 3D color-coded maps of each characteristic. The number of voxels of each tissue characteristic was automatically calculated. (Adapted from M. Kawasaki M et al. J Am Coll Cardiol. 2005; 45: p1946–53).

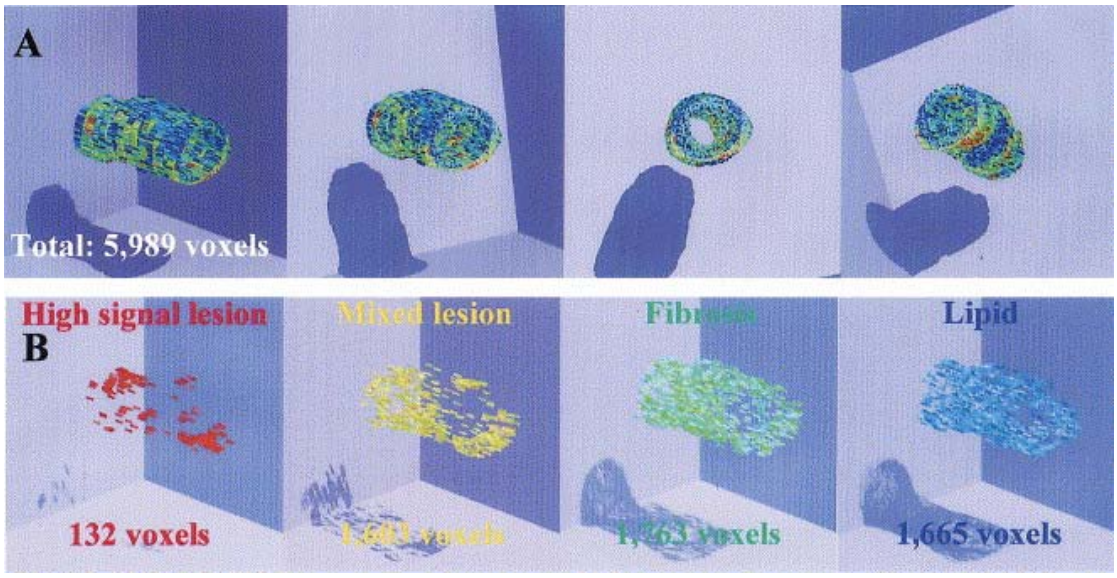

II-2-10: Wavelet-IVUS:

The theoretical basis of wavelet analysis was first developed by Grossmann and Morlet in 1983.[53] Wavelet analysis of RF IVUS signals is a novel mathematical model for assessing focal differences within arterial walls. Color coding of the wavelet correlation coefficient derived from the radiofrequency (RF) signal allows detection of changes in the geometrical profile of time-series signals to derive an image of plaque components. With wavelet analysis, Murashige A et al showed that lipid-rich plaques, derived from necropsy specimens and subsequently confirmed as such by histology, could be detected with a sensitivity of 83% and specificity of 83% in an in vitro system. Furthermore, IVUS imaging of the coronary arteries performed in 13 patients showed similar results with confirmation of the presence of lipid-rich components by histology after obtaining tissue by directional atherectomy.[54]

Figure 6: Representative examples of in vivo Wavelet analysis of radiofrequency (RF) intravascular ultrasound (IVUS) signals from a lipid-laden plaque **(A)** and from a fibrous plaque without a lipid core **(B)**. The **left panel** shows conventional IVUS images, the **middle panel**, the results of Wavelet analysis, the **right panel**, histologic cross section of the corresponding directional coronary atherectomy specimen with Hematoxylin-Eosin and Azan stains. A similar pattern of color mapping was observed from the RF signal vector of a lipid-laden plaque as seen in the in vitro study. (from Murashige A et al. J Am Coll Cardiol. 2005; 45 : p1954–60).

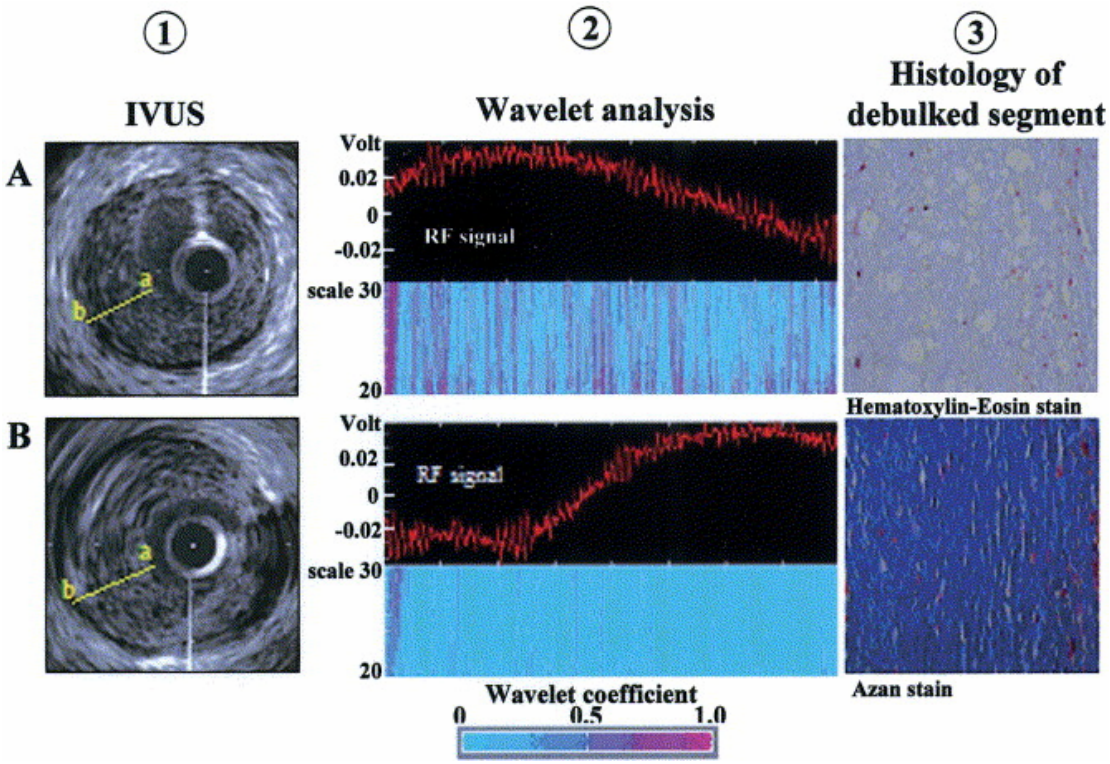

II-2-10:Virtual histologic IVUS (IVUS-VH):

“Virtual histology” applies spectral analysis of the IVUS backscatter RF signal to characterize plaque components on the basis of tissue characteristics such as density, compressibility, concentration of various components, and size. With quantitative spectral parameters and advanced mathematical techniques to classify plaque composition, this approach has been validated with histological techniques on ex vivo coronary specimens in classifying lesions as dense calicium, fibrofatty, necrotic core, and lipid-rich areas. [55]This methodology allows real-time, 3D plaque cross-sectional and longitudinal views of the entire vessel and allows one to visualize the complete length of the artery and assess individual plaque components.

Rodriguez Granillo GA et al found that the volumetric output of the IVUS-VH sofeware underestimated measurement when acquired with a 30 MHz catheter, however, after applying a mathematical adjustment method for ultraound propogation delay caused by the outer sheath of the 30 MHz catheter, relative differences of direct measurement were negligible.[56]

Also, these same authors demonstrated that the geometrical and compositional output of IVUS-VH was acceptably reproducible.[57]

Rodriguez-Granillo GA et al have done a number of works in applying IVUS-VH. They compared IVUS-VH with IVUS palpography by using 123 matched cross-sections (CSs) of 27 vessels, and found that the mean strain was higher in CSs with necrotic core than in CSs with no necrotic core. The sensitivity, specificity, positive predictive value and negative predictive value of IVUS-VH to detect high strain were 75%, 44.4%, 56.3% and 65.1%, respectively. A significant inverse relationship was present between calcium and strain levels. After adjusting for univariate predictors, the necrotic core was identified as the only independent predictor of high strain.[58] They performed three-vessel IVUS-VH interrogation in 40 patients. Twenty eight plaque ruptures was detected in 26 vessels. Plaque rupture sites showed a higher content of necrotic and a trend towards higher calcified component.[59] Also these same authors investigated non-culprit, non-obstrutive (<50%) lesions in 55 patients. They classified IVUS-derived thin-cap fibroatheroma (IDTCFA) lesions as focal necrotic core-rich (≥10% of the cross-sectional area) being contact with the lumen.

ACS presented a significantly higher prevalence of IDTCFA than SAP. A clear clustering pattern was seen along the coronaries with 35(35.4%), 31(31.3%), 19(19.2%) and 14(14.1%) IDTCFAs in the first 10mm, 11 to 20mm, 21 to 30mm and ≥ 31mm segment, respectively.[60]

By using preintervention IVUS-VH images, Hong MK et al compared coronary plaque composition between ACS and SAP in 318 patients. VH-IVUS-derived thin-cap fibroatheroma (VH-TCFA) was defined as necrotic core ≥ 10% of plaque area without overlying fibrous tissue in a plaque burden ≥ 40%. Lesions were classified into 3 groups: ruptured, VH-TCFA, and non-VH-TCFA plaque. Unstable lesions were defined as either VH-TCFA or ruptured plaque. They found that culprit lesions in patients with ACS were more unstable and had greater amounts of necrotic core and smaller amounts of fibrofatty plaque compared with target lesions in patients with SAP.[61]

Nasu K et al used IVUS-VH technique to observe coronary plaque characteristics in patients with type II DM and they found that the percent of necrotic core and dense calcium were significantly large in patients with DM than in patient with no DM. Compared with the non-DM group, the DM group presented with a significantly higher presence of at least one VH-IVUS-derived thin-cap fibroatheroma.[62]

There are some discrepancies in validating IVUS-VH in vivo studies. In a porcine model of complex coronary lesions, Granada JF et al showed that when compared with histology, IVUS-VH correctly identified the presence of fibrous, fibro-fatty and necrotic tissue in 58.33%, 38.33% and 38.33%, respectively. The sensitivity of IVUS-VH for detection of fibrous, fibro-fatty and necrotic core tissue was 76.1%, 46% and 41.1%, respectively. They revealed that there was no strong correlation between IVUS-VH and histology, so they concluded that IVUS-VH wouldn't allow significant prediction of individual values.[63]Nasu K et al performed IVUS-VH before and after a single debulking cut using directional atherectomy in 30 patients (15 with SAP; 15 with ACS). Debulking region of in vivo histology image was predicted by comparing pre- and post- debulking VH images. They showed that the results of IVUS-VH data correlated well with histopathologic examination. Predictive accuracy from all patients data was 87.1% for fibrous, 87.1% for fibro-fatty, 88.3% for necrotic core and 96.5% for dense calcium regions, respectively. In addition, the frequency of necrotic core

was significantly higher in the ACS group than in the SAP group.[64] Therefore, oen needs not only in vivo studies to verify the reliability of IVUS-VH for differentiating plaque components, but also large prospective randomized trials to assess the predictive value of IVUS-VH for future cardiac events.

Figure 7: IVUS-VH images from our study.

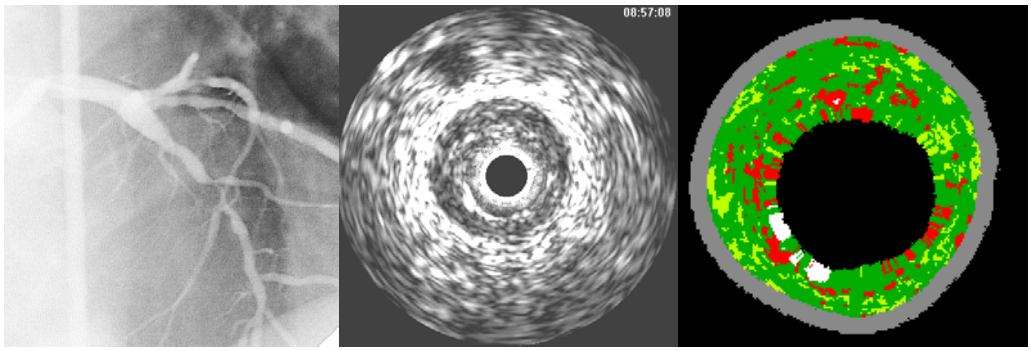

PreDCA CAG PreDCA IVUS PreDCA IVUS-VH

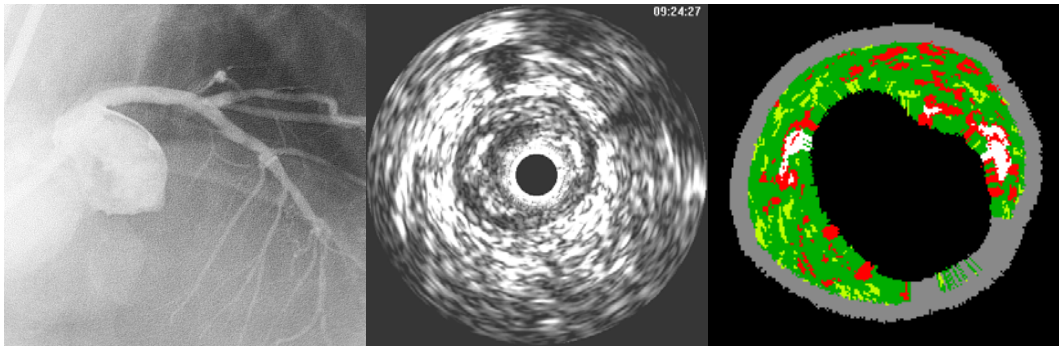

PostDCA CAG Post DCA IVUS PostDCA IVUS-VH

II-3: Non-invasive imaging techniques:

II-3-1: Ultrafast Computed Tomography (UFCT):

Ultrafast Computed Tomography (UFCT) allows image acquisition at a faster rate than conventional computed tomography (CT). Fast imaging is essential elimination of cardiac and respiratory motion artifacts. Atherscleroticcalcification is found more frequently in advanced lessions, and may occur in small early lesions.

Magnetic resonance imaging (MRI), X-ray angiography, and IVUS can identify calcified deposits in blood vessels; however, only electro-beam CT (EBCT) and fast-gated helical or sprial CT can measure the amount or volume of calcium. In EBCT, x-ray radiation passs through the patient and is detected by two 240^{o} detector rings. To measure coronary calcium, 30 to 40 contiguous, 3-mm-thick slices are obtained from the aortic root to the apex of the heart. The scans are usually acquired during one or two separate breath holds. Non-EBCT systems use a continuous rotating x-ray source. Recently, non-EBCT system have been introduced, using multidetector arrays for short rotation times that improving imaging speed. For example, a 4-slice detector array system provides 8-fold improved performance over single-slice CT system. Comparision of coronary calcium assessment by EBCT and non-EBCT systems demonstrated good correlation.

Histological and UFCT studies support the association of tissue densities ≥130 Hounsfield units with calcified plaques. [65] However, high-risk plaques often lack calcium. There is an association between coronary calcium and obstructive cardiovascular disease (CVD), and it has been suggested that the amount of coronary events.[66] However, the predictive value of coronary calcification, at least in high-risk subjects, may be not superior to that of standard coronary risk factors. In addition, a high calcium score is sensitive but not a specific marker for coronary stenosis. The greatest potential for coronary calcium scores appears to be in the detection of advanced coronary atherscleroses in patients who are apparently at intermediate risk. The new volumetric method for calcium detected the effect of lipid-lowering on coronary calcification. Nevertheless, there is no evidence to support that changes in coronary calcification may correspond to changes in cardiovascular events.

UFCT angiography with intravenous injection of a contrast medium is widely used for detection of stenosis in peripheral vessels. With the advent of faster and high-

resolution imaging and soft-tissue delineation with UFCT, assessment of coronary stenosis and the detection of noncalcified coronary plaques are being explored.

Intravenous contrast EBCT can now be used to create three-dimensional images of the major epicardial coronary arteries with tomographic imaging during a single breath-hold. When compared with coronary angiography in 200 patients, EBCT demonstrated a sensitivity and specificity of approximately 80 and 90%, respectively, for a luminal stenosis of >50%.[67]The major limitations of noninvasive angiography by CT remains the image quality. In a study of 125 patients, 25% of 500 coronary segments were not adequately visualized. Since imaging occurs during end-diastole, the right coronary artery and the left circumflex artery, which run in the coronary groove, may not be well visualized as a result of motion during diastolic atrial contraction.[68] Another problem is artifact from respiratory motion and from heavy calcification. The newer 64-slice detector systems are showing an improved image quality over the older scanners. There is still significant variability in technique from center to center, making it difficult to give general recommendations about its use. Finally, as with coronary angiography, CT angiography is unable to characterize specific lesions in enough detail to identify the features of high-risk plaque. There is likely to be a role for CT angiography, and we await the determination of the most appropriate patient population for its application. Some proposed uses are in patients with atypical chest pain and in patients with previously equivocal stress tests.

Figure 8: Electron-beam CT angiograms (Adapted from Achenbach S et al. N Engl J Med. 1998;339: p 1964-71).

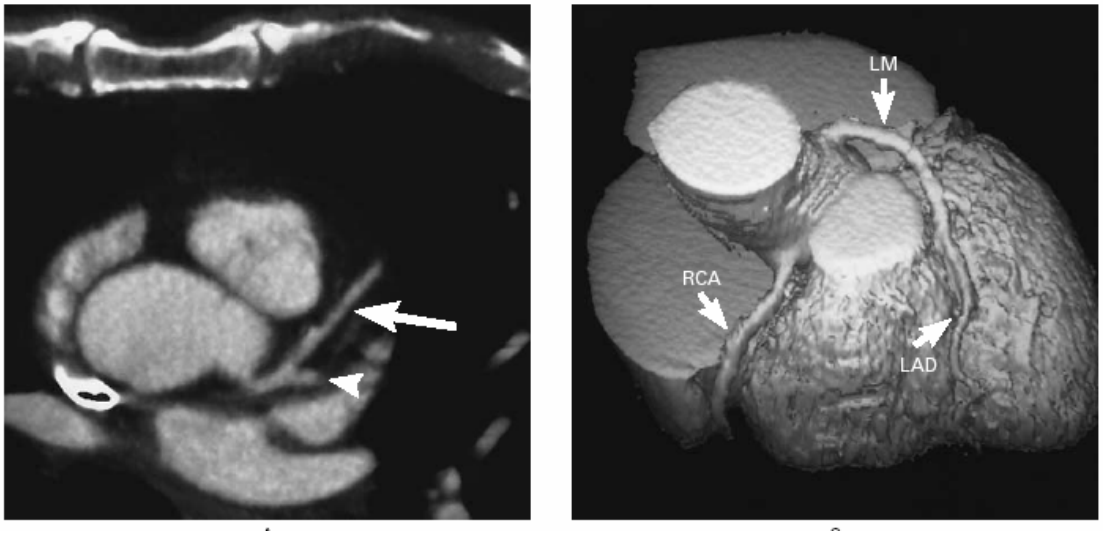

II-3-2: Magnetic Resonance Imaging (MRI):

Magnetic resonance imaging (MRI) represents the best noninvasive technology for imaging the three traditional components of vulnerable plaques: necrotic core, fibrous cap, and inflammatory infiltrate. MR has a high spatial resolution and is able to differentiate components of plaque based on features such as chemical composition, water content, molecular motion, or diffusion. A patient is subjected to a high local magnetic field which aligns the protons in the body. The protons are excited by a radiofrequency pulse and the signals detected by receiver coils. The timing of the excitation pulses and the magnetic field gradients determine the image contrast. The quality of the final image is determined by the signal, the contrast, and the level of background noise.

MRI has been used to image and characterize plaques in the carotids. T2-weighted images have been quantified in vivo before surgery and correlated with in vitro values after endarterectomy. Hatsukami TS et al introduced the use of bright-blood MRI to assess thickness and integrity of the fibrous cap in carotid artery plaques. These authors showed that the observation of fibrous cap rupture correlated with a recent history of transient ischemic attack or stroke. [69]In the coronary bed, MRI has been used to assess overall plaque size, necrotic core size, fibrous cap, composition, and intraplaque hemorrhage. Bright areas on T2-weighted images correspond to fibrous tissue, whereas dark areas correspond to lipid-rich regions. MRI is also unique in its ability to visualize thrombus and assess its size and anatomic location on T2-weighted images at least 48 h after thrombus formation. MRI of the coronary vessel wall can be performed with high-resolution, black-blood sequences that minimize the signal from the blood. Fayad ZA et al have used this technique to image epicardial coronary vessels and showed a statistically significant difference in wall thickness between normal subjects and patients with angiogram-proven stenoses of >40%.[70]MRI has been used in an experimental setting to monitor progression and regression of plaque. There are preliminary data showing a role for MRI in documenting arterial remodeling at the site of native atherosclerosis. Corti R et al showed that lipid-lowering therapy in asymptomatic hyperlipidemic patients led to regression of atherosclerotic lesions in the carotids and aorta at 12 months. However, a 10-year follow-up on a carotid MRI study showing reduced plaque lipid content

though unchanged overall size in patients receiving lipid-lowering therapy.[71]MRI contrast agents have been used to enhance components of the vessel wall and to identify inflammation and thrombus. Currently, the only clinically approved agents are gadolinium based. On T1-weighted images of carotid arteries a gadolinium-based agent has been shown to enhance areas of plaque rich in microvascularization, a marker of local inflammation. Fibrin-targeted, paramagnetic, lipid-encapsulated perfluorocarbon nanoparticles, formulated with gadolinium, bind densely to fibrin clots and potentially could allow MRI to detect microthrombi that form on the intimal surface of unstable plaque. Ruehm SG et al have shown that ultrasmall superparamagnetic iron oxides are phagocytosed by macrophages in atherosclerotic plaque of hyperlipidemic rabbits in a quantity sufficient to be detected by MRI. [72] Kooi ME et al have extended the use of ultrasmall superparamagnetic iron oxides to in vivo imaging of macrophages in human carotid plaques. There is also the potential to develop contrast agents that target matrix metalloproteinases and enhance areas rich in proteolytic activity.[73]The main limitations to the use of MRI for evaluating coronary plaque are cardiac and respiratory motion artifact, nonlinear course of vessels, and small size and location of vessels. Patient breath-holding has been the main technique used to minimize motion artifact. Newer techniques use navigator gating to assess cardiac and diaphragmatic positions, compensate for motion, and thus eliminate the need for breath-holding. Further advances in external coils and imaging acquisition should allow for thinner slices and better quality images. Acquisition of isotropic voxels, facilitating reconstruction of the coronary arteries in exhaustive views, can compensate for vessel tortuosity. Semiautomatic image-processing techniques have been developed to better quantify vessel wall area, volume, and overall plaque burden. Other experimental approaches to evaluating plaque are intravascular and transesophageal MRI.

Figure 9: MR images of plaques (Adapted from Thomas S et al. Circulation. 2002; 102: p 959-64).

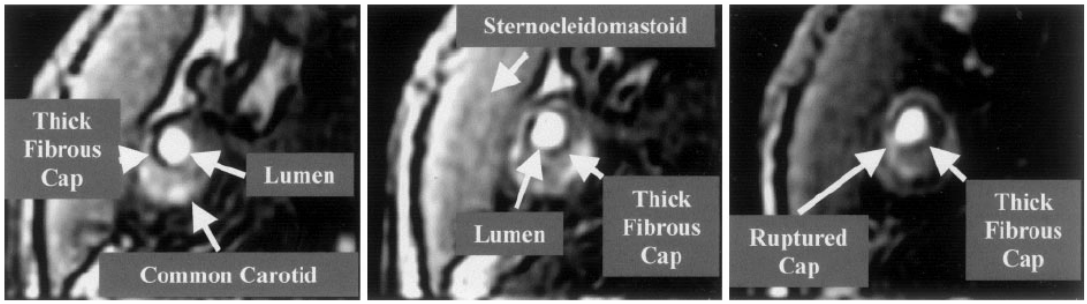

II-4: Conclusions:

One should keep in mind that not all ACSs are caused by plaque rupture (35% ACSs result from plaque erosion) and not all ruptured plaques result in ACSs (some of them are clinically silent). The definitions of three characteristics of a vulnerabe plaque mainly came from post mortem studies. Using these definitions to detect so called vulnerable plaque will sometime misleading. Moreover, till now, although using this definition of the vulnerability, no one single image technique can accomplish the task. Therefore, in order to detect the vulnerable plaques, there is still a long way for one to invest new techniques or to improve current modalities. Combinating two or more imaging techniques and biomakers may aid us to succed.

References:

1. Ambrose JA ,Tannenbaum MA, Alexopoulos D, Hjemdahl-Monsen CE, Leavy J, et al. Angiographic progression of coronary artery disease and the development of myocardial infarction. J Am Coll Cardiol. 1988;12: P56-62.
2. Little WC, Constantinescu M, Applegate RJ, Kutcher MA, Burrows MT, et al. Can coronary angiography predict the site of a subsequent myocardial infarction in patients with mild-to-moderate coronary artery disease? Circulation. 1988;78:P 1157-1166.
3. Virmani R, Kolodgie FD, Burke AP, Farb A, Schwartz SM. Lessons from sudden coronary death: A comprehensive morphological classification scheme for atherosclerotic lesions. . Arterioscler Thromb Vasc Biol. 2000;20:P1262-1275.
4. Davies MJ, Richardson PD, Woolf N, Katz DR, Mann J. Risk of thrombosis in human atherosclerotic plaques: Role of extracellular lipid, macrophage, and smooth muscle cell content. . Br Heart J. 1993;69:P377-381.
5. Burke AP, Farb A, Malcom GT, Liang YH, Smialek J, et al. Coronary risk factors and plaque morphology in men with coronary disease who died suddenly. N Engl J Med. 1997;336:P1276-1282.
6. Rioufol G, Finet G, Ginon I, André-Fouet X, Rossi R, et al. Multiple atherosclerotic plaque rupture in acute coronary syndrome: A three-vessel intravascular ultrasound study. Circulation. 2002;106:P804-808.
7. Goldstein JA, Demetriou D, Grines CL, Pica M, Shoukfeh M, et al. Multiple complex coronary plaques in patients with acute myocardial infarction. N Engl J Med. 2000;343:P915-922.
8. Buffon A ,Biasucci LM, Liuzzo G, D'Onofrio G, Crea F, et al. Widespread coronary inflammation in unstable angina. N Engl J Med. 2002;347:P5-12.
9. Davies MJ. Stability and instability: Two faces of coronary atherosclerosis. Circulation 1996;94(8):P 2013-2020.
10. Goldschmidt-Clermont PJ, Kandzari DE, Sketch MH Jr, Phillips HR. Inflammation, platelets, and glycoprotein IIb/IIIa inhibitors. J Invasive Cardiol. 2002;14(suppl E):P18E-26E.
11. Levin DC, Fallon JT. Significance of the angiographic morphology of localized coronary stenoses: Histopathologic correlations.Circulation. 1982;66:P316-320.

12. Glagov S, Weisenberg E, Zarins CK, Stankunavicius R, Kolettis GJ. Compensatory enlargement of human atherosclerotic coronary arteries. N Engl J Med. 1987;316:P1371-1375.
13. Uchida Y, Nakamura F, Tomaru T, Morita T, Oshima T, et al. Prediction of acute coronary syndromes by percutaneous coronary angioscopy in patients with stable angina. Am Heart J. 1995;130: P195-203.
14. Fayad ZA, Fuster V. Clinical imaging of the high-risk or vulnerable atherosclerotic plaque. Circ Res. 2001;89:P305-316.
15. Madjid M, Naghavi M, Malik BA, Litovsky S, Willerson JT et al. Thermal detection of vulnerable plaque. Am J Cardiol. 2002;90:P36L–39L.
16. Naghavi M, Madjid M, Gul K, Siadaty MS, Litovsky S, et al. Thermography basket catheter in vivo measurement of the temperature of atherosclerotic plaques for detection of vulnerable plaques.Catheter Cardiovasc Interv. 2003;59(1):P52–59.
17. Madjid M, Naghavi N, Willerson JT and Casscells W. Thermography a novel approach for identification of plaques at risk of rupture and/or thrombosis. In: V. Fuster, Editor, Assessing and Modifying the Vulnerable Atherosclerotic Plaque, Futura Publishing Company, Inc, Armonk, NY. 2002:P107–127.
18. Verheye S, De Meyer GR, Van Langenhove G, Knaapen MWM, Kockx MM. In vivo temperature heterogeneity of atherosclerotic plaques is determined by plaque composition. Circulation. 2002;105:P1596–1601.
19. Stefanadis C, Toutouzas K, Tsiamis E, Mitropoulos I, Tsioufis C, et al. Thermal heterogeneity in stable human coronary atherosclerotic plaques is underestimated in vivo the “cooling effect” of blood flow. J Am Coll Cardiol. 2003;41(3):P 403–408.
20. Verheye S, De Meyer GR, Krams R, Kockx MM, Van Damme LC, et al. Intravascular thermography immediate functional and morphological vascular findings. Eur Heart J. 2004;25(2):P158–165.
21. Stefanadis C, Diamantopoulos L, Vlachopoulos C, Tsiamis E, Dernellis J, et al. Thermal heterogeneity within human atherosclerotic coronary arteries detected in vivo a new method of detection by application of a special thermography catheter. Circulation. 1999;99(15):P1965–1971.
22. Webster M, Stewart J, Ruygrok P. Intracoronary thermography with a multiple thermocouple catheter initial human experience (abstr). Am J Cardiol. 2002;90:P 24H.
23. Verheye S, Van Langenhove G, Diamantopoulos L, Serruys PW, Vermeersch P. Temperature heterogeneity is nearly absent in angiographically normal or mild

atherosclerotic coronary segments interim results from a safety study (abstr). Am J Cardiol. 2002;90:P24H.

24. Schmermund A, Rodermann J, Erbel R. Intracoronary thermography. Herz. 2003;28:P505–512.

25. Stefanadis C, Diamantopoulos L, Dernellis J, Stratos C, Vavuranakis M, et al. Increased local temperature in human coronary atherosclerotic plaques an independent predictor of clinical outcome in patients undergoing a percutaneous coronary intervention. J Mol Cell Cardiol. 2000;32(5):P43–52.

26. Wainstein MV, Ribierro JP, Zago J. Coronary plaque theromography heterogeneity detected by Imetrx thermocoil guidewire. Am J Cardiol. 2003;92:P5L.

27. Toutouzas K ,Stefanadis C, Tsiamis E. The temperature of atherosclerotic plaques is correlated with matrix metalloproteinases concentration in patients with acute coronary syndromes. J Am Coll Cardiol. 2001;37:P356A.

28. Stefanadis C, Toutouzas K, Tsiamis E, Stratos C, Vavuranakis M, et al. Increased local temperature in human coronary atherosclerotic plaques an independent predictor of clinical outcome in patients undergoing a percutaneous coronary intervention. J Am Coll Cardiol. 2001;37(5):P1277–1283.

29. Tearney GJ, Brezinski ME, Bouma BE, Boppart SA, Pitris C, et al. In vivo endoscopic optical biopsy with optical coherence tomography. Science. 1997;276(5321):P2037–2039.

30. Brezinski ME, Tearney GJ, Bouma BE, Boppart SA, Hee MR, et al. Imaging of coronary artery microstructure with optical coherence tomography. Am J Cardiol. 1996;77(1):P92–93.

31. Brezinski ME, Tearney GJ, Bouma BE, Izatt JA, Hee MR, et al. Optical coherence tomography for optical biopsy properties and demonstration of vascular pathology. Circulation. 1996;93(6):P1206–1213.

32. Fujimoto JG, Boppart SA, Tearney GJ, Bouma BE, Pitris C, et al. High resolution in vivo intra-arterial imaging with optical coherence tomography. Heart. 1999;82(2):P128–133.

33. Häusler G, Lindner MW. Coherence radar and spectral radar—new tools for dermatological diagnosis. J Biomed Opt. 1998;3:P21–31.

34. Bouma BE, Tearney GJ, Yabushita H, Shishkov M, Kauffman CR, et al. Evaluating of intracoronary stenting by intravascular optical coherence tomography. Heart. 2003;89(3):P317–320.

35. Macneil BD, Jang IK, Bouma BE, Iftimia N, Takano M, et al. Focal and multi-focal plaque macrophage distributions in patients with acute and stable presentations of coronary artery disease. J Am Coll Cardiol. 2004;44(5):P972–979.
36. Zhu Q, Conant E, Chance B. Optical imaging as an adjunct to sonography in differentiating benign from malignant breast lesions. J Biomed Opt. 2000;5:P 229-236.
37. Moreno PR, Lodder RA, Purushothaman KR, Charash WE, O'Connor WN, et al. Detection of lipid pool, thin fibrous cap, and inflammatory cells in human aortic atherosclerotic plaques by near-infrared spectroscopy. Circulation. 2002;105(8):P:923-927.
38. Losordo DW, Rosenfield K, Kaufman J, Pieczek A, Isner JM.Focal compensatory enlargement of human arteries in response to progressive atherosclerosis: In vivo documentationusing intravascular ultrasound. Circulation. 1994;89(6):P2570-2577.
39. Schoenhagen P, Ziada KM, Kapadia SR, Crowe TD, Nissen SE, et al. Extent and direction of arterial remodeling in stable versus unstable coronary syndromes: An intravascular ultrasound study. Circulation. 2000;101(6):P598-603.
40. Yamagishi M, Terashima M, Awano K, Kijima M, Nakatani S, et al. Morphology of vulnerable coronary plaque: Insights from follow-up of patients examined by intravascular ultrasound before an acute coronary syndrome. J Am Coll Cardiol 2000;35(1):P106-111.
41. Kotani J, Mintz GS, Castagna MT, Pinnow E, Berzinqi CO, et al. Intravascular ultrasound analysis of infarct-related and non-infarct-related arteries in patients who presented with an acute myocardial infarction. Circulation. 2003;107(23):P2889-2893.
42. de korte CL, Pasterkamp G, Van der Steen AF, Woutman HA, Bom N et al. Characterization of plaque compositions with intravascular ultrasound elastrography in human femoral and coronary arteries in vitro.Circulation. 2000;102(6):P 617-623.
43. de Korte CL, Sierevogel MJ, Mastik F, Strijder C, Schaar JA, et al. Identification of atherosclerotic plaque components with intravascular ultrasound elastography in vivo: a Yucatan pig study. Circulation. 2002 Apr 9;105(14):P1627-1630.
44. de Korte CL, Carlier SG, Mastik F, Doyley mm, van der Steen AF, et al. Morphological and mechanical information of coronary arteries obtained with intravascular elastography; feasibility study in vivo. Eur Heart J. 2002 Mar;23(5):P405-413.

45. Komiyama N, Berry GJ, Kolz ML, Oshima A, Metz JA, et al. Tissue characterization of atherosclerotic plaques by intravascular ultrasound radiofrequency signal analysis: an in vitro study of human coronary arteries. Am Heart J. 2000;140(4):P565-574.

46. Kawasaki M, Takatsu H, Noda T, Ito Y, Kunishima A, et al. Non-invasive quantitative tissue characterization and two-dimensional color-coded map of human atherosclerotic lesions using ultrasound integrated backscatter: comparison between histology and integrated backscatter images. J Am Coll Cardiol. 2001;38(2):P486-492.

47. Kawasaki M, Takatsu H, Noda T, Sano K, Ito Y,et al. In vivo quantitative tissue characterization of human coronary arterial plaques by use of integrated backscatter intravascular ultrasound and comparison with angioscopic findings. Circulation. 2002;105(21):P 2487-2492.

48. Yokoyama M, Komiyama N, Courtney BK, Nakayama T, Namikawa S,et al. Plasma low-density lipoprotein reduction and structural effects on coronary atherosclerotic plaques by atorvastatin as clinically assessed with intravascular ultrasound radio-frequency signal analysis: a randomized prospective study. Am Heart J. 2005 Aug;150(2):P287.

49. Sano K, Kawasaki M, Okubo M, Yokoyama H, Ito Y, et al. In vivo quantitative tissue characterization of angiographically normal coronary lesions with risk factors-a study using integrated backscatter intravascular ultrasound. Circ J. 2005;69(5):P 543-549.

50. Amano T, Matsubara T, Uetani T, Nanki M, Marui N, et al. Impact of metabolic syndrome on tissue characteristics of angiographically mild to moderate coronary lesions: integrated backscatter intravascular ultrasound study. J Am Coll Cardiol. 2007;49(11):P1149-1156.

51. Kawasaki M, Bouma BE, Bressner J, Houser SL, Nadkarni SK, et al. Diagnostic accuracy of optical coherence tomography and integrated backscatter intravascular ultrasound images for tissue characterization of human coronary plaques. J Am Coll Cardiol. 2006;48(1):P81-88.

52. Sano K, Kawasaki M, Ishihara Y, Okubo M, Tsuchira k, et al. Assessment of vulnerable plaques causing acute coronary sysndrome using integrated backscatter intravascular ultrasound. J Am Coll Cardiol. 2006;47(4):P 734-741.

53. Daubechies I, Grossmann A. An integral transform related to quantization. J Mat Phys. 1980;21:P2080–2090.
54. Murashige A, Hiro T, Fujii T, Imoto K,Murata T, et al. Detection of Lipid-Laden atherosclerotic plaque by wavelet analysis of radiofrequency intravascular ultrasound signals:in vitro validation and preliminary in vivo application. J Am Coll Cardiol. 2005;45(12):P 1954-1960.
55. Nair A, Kuban BD, Tuzcu EM, Schoenhagen P, Nissen SE, et al. Coronary plaque classification with intravascular ultrasound radiofrequency data analysis. Circulation. 2002;106(17):P2200-2206.
56. Rodriguez-Granillo GA, Bruining N, Mc Fadden E, Ligthart JM, Aoki J, et al. Geometrical validation of intravascular ultrasound radiofrequency data analysis (Virtual Histology) acquired with a 30 MHz boston scientific corporation imaging catheter. Catheter Cardiovasc Interv. 2005 Dec;66(4):P 514-518.
57. Rodriguez-Granillo GA, Vaina S, García-García HM, Valgimigli M, Duckers E, et al. Reproducibility of intravascular ultrasound radiofrequency data analysis: implications for the design of longitudinal studies. Int J Cardiovasc Imaging. 2006 Oct;22(5):P 621-631.
58. Rodriguez-Granillo GA ,Garcia-Garcia H, Valgimigli M, Schaar JA, Pawar R, et al. In vivo relationship between compositional and mechanical imaging of coronary arteries. Insights from intravascular ultrasound radiofrequency data analysis. Am Heart J. 2006;151(5):P 1025.e1021-1026.
59. Rodriguez-Granillo GA ,Garcia-Garcia H, Valgimigli M, Vaina S, van Mieghem C, et al. Global characterization of coronary plaque rupture phenotype using three-vessel intravascular ultrasound radiofrequency data analysis. Eur Heart J. 2006;27(16):P 1921-1927.
60. Rodriguez-Granillo GA, Garcia-Garcia H, Mc Fadden EP, Valgimigli M, Aoki J, et al. In vivo intravascular ultrasound-derived thin-cap fibroatheroma detection using ultrasound radiofrequency data analysis. J Am Coll Cardiol. 2005;46(11):P2038-2042.
61. Hong MK, Mintz GS, Lee CW, Suh J, Kim JH, et al. Comparison of virtual histology to intravascular ultrasound of culprit coronary lesions in acute coronary syndrome and target coronary lesions in stable angina pectoris. Am J Cardiol. 2007;100(6):P 953-959.

62. Nasu K, Tsuchikane E, Katoh O, Fujita H, Surmely JF, et al. Plaque Characterization by Virtual Histology Intravascular Ultrasound Analysis in Type II Diabetic Patients. Heart. 2007 Jul;23.

63. Granada JF, Wallace-Bradley D, Win HK, Alviar CL, Builes A,et al. In vivo plaque characterization using intravascular ultrasound-virtual histology in a porcine model of complex coronary lesions. Arterioscler Thromb Vasc Biol. 2007;27(2):P 387-393.

64. Nasu K ,Tsuchikane E, Katoh O, Vince DG, Virmani R, et al. Accuracy of in vivo coronary plaque morphology assessment: a validation study of in vivo virtual histology compared with in vitro histopathology. J Am Coll Cardiol. 2006;47(12):P2405-2412.

65. Rumberger JA, Simons DB, Fitzpatrick LA, Sheedy PF, Schwartz RS. Coronary artery calcium area by electron-beam computed tomography and coronary atherosclerotic plaque area: a histopathologic correlative study. Circulation. 1995; 92: P 2157-2162.

66. Raggi P, Callister TQ, Cooil B, He ZX, Lippolis NJ, et al. Identification of patients at increased risk of first unheralded acute myocarial infarction by electron-beam computed tomography. Circulation. 2000;101:P850-855.

67. Budoff MJ, Oudiz RJ, Zalace CP, Bakhsheshi H, Goldberg SL,et al. Intravenous three-dimensional coronary angiography using contrast-enhanced electron-beam computed tomography. Am J Cardiol. 1999;83:P840-845.

68. Achenbach S, Moshage W, Ropers D, Nossen J, Daniel WG. Value of electron-beam computed tomography for the noninvasive detection of high-grade coronary artery stenoses and occlusions.N Engl J Med 1998;339(27):1964-1971.

69. Hatsukami TS, Ross R, Polissar NL, Yuan C. Visualization of fibrous cap thickness and rupture in human atherosclerotic carotid plaque in vivo with high-resolution magnetic resonance imaging.Circulation. 2000;102:P 959-964.

70. Fayad ZA, Nahar T, Fallon JT, Goldman M, Aguinaldo JG, et al. In vivo magnetic resonance evaluation of atherosclerotic plaques in the human thoracic aorta: A comparison with transesophageal echocardiography. Circulation. 2000;101:P 2503-2509.

71. Corti R, Fayad ZA, Fuster V, Worthley SG, Helft G, et al. Effects of lipid-lowering by simvastatin on human atherosclerotic lesions: A longitudinal study by

high-resolution, noninvasive magnetic resonance imaging. Circulation. 2001;104:P249-252.

72. Ruehm SG, Corot C, Vogt P, Kolb S, Debatin JF. Magnetic resonance imaging of atherosclerotic plaque with ultrasmall superparamagnetic particles of iron oxide in hyperlipidemic rabbits. Circulation. 2001;103:P 415-422.

73. Kooi ME, Cappendijk VC, Cleutjens KB, Kessels AG, Kitslaar PJ, et al. Accumulation of ultrasmall superparamagnetic particles of iron oxide in human atherosclerotic plaques can be detected by in vivo magnetic resonance imaging. Circulation. 2003;107::P2453-2438.

Changes in Unstable Coronary Atherosclerotic Plaque Composition After Balloon Angioplasty. In vivo spectral analysis of intravascular ultrasound radiofrequency data.

This article has been accepted by Am J Cardiol and will be published in early 2008.

Hu Wei, MD, Francois Schiele, MD, PhD, Vincent Descotes-Genon, MD, Pierre Legalery, MD,Nicolas Meneveau, MD, Marie-France Seronde, MD, Fiona Ecarnot, MSc, Jérome Varini, MS, Jean-Pierre Bassand, MD.

Abstract:

Backgrounds: Angioplasty in the setting of acute coronary syndrome sometimes leads to unexpected complications like distal embolization or no reflow phenomenon, even when effective antithrombotic drugs are used. This suggest that the mechanism of angioplasty of unstable atherosclerotic stenoses remains uncompletly documented.

Objectives: To assess the mechanism of balloon angioplasty (BA) of unstable atherosclerotic stenosis using intravascular ultrasound (IVUS) gray scale (GS) and spectral radio frequency analysis (Virtual Histology, Volcano Corp. Rancho Cordova, CA, USA).

Methods: In 20 patients, IVUS GS and Virtual histology (VH) analysis were performed before and after BA. The region of interest was 40 mm long, 10 mm in proximal and distal reference segments and the 20 mm long segment covered by the balloon. At each mm, lumen and plaque cross sectional areas (CSA) were assessed by IVUS GS and plaque composition (fibrous, fibro-fatty, dense calcium and necrotic core) by VH. Quantitative and qualitative changes were determined by comparison between pre- and post-BA images.

Results: At baseline, the composition of the plaque at the region of interest was 61% fibrotic tissue, 15% fibro-fatty tissue, 15% necrotic tissue and 7% dense calcium tissue. BA was uncomplicated in all patients and resulted: at lesion site, in a 80% increase of Lumen CSA. At balloon segment, 35% of the lumen enlargement was due to an increase in total vessel CSA and 65% to a significant decrease in Plaque CSA. This reduction in plaque CSA resulted from a longitudinal redistribution of the tissue towards the reference segments. IVUS-RF analysis showed that the fibrous and fibro fatty tissue were able to move longitudinally, whereas the calcium remained at the same level. Last, 1/3 of the necrotic tissue (volume 15mm3) was lost after BA, suggesting that embolisation has occured.

Conclusions: Unstable atherosclerotic coronary plaques were composed of 61% fibrosis, 15% fibro fatty and 15% necrotic tissue. 35% of lumen enlargement was explained by vessel stretching, and 65% by plaque volume decrease. The decrease

in plaque volume was the result of longitudinal redistribution of fibrotic and fibro fatty tissue and of the disappearance of one third of the necrotic tissue present at baseline.

Key words: coronary atherosclerotic plaque; balloon angioplasty; intravascular ultrasound; virtual histology.

Introduction

In the era of drug eluting stents (DES), a study of the mechanism of the balloon angioplasty (BA) seems backward-looking and of little interest. Nevertheless, angioplasty with or without stent in a recently complicated or thrombotic lesion may lead to acute complications like distal embolization, no reflow phenomenon or suboptimal tissue reperfusion, all of which can impact outcome 1,2. These complications are often unexpected and not completely resolved by the use of combination of antithrombotic drugs or distal protection devices. This suggest an incomplete knowledge of the effects of angioplasty in recently complicated coronary lesions3.

In stable lesions, the pioneers of angioplasty explained the mechanism of lumen enlargement after balloon angioplasty (BA) as a plaque compression, comparable to “footprints in the snow”. These early explanations, based on angiography, were not confirmed when Intravascular Ultrasound (IVUS) became available : indeed, IVUS provided gray scale (GS) images from the coronary artery walls, making it possible to assess lumen and plaque areas and volumes4. Furthermore, thanks to motorized pullback, longitudinal analyses and volumetric measurements were also possible. So, in stable lesions, IVUS studies concluded that acute lumen gain after BA was the result of vessel stretching and plaque remodeling (axial or longitudinal redistribution, compression or embolization) 5.

Plaque composition seems to be an important determinant in the mechanism of BA: the degree of vessel stretching and of plaque remodelling depends on the amount of atherosclerotic material6 but also on the clinical presentation7, stable angina or acute coronary syndrome. The availability of a new IVUS modality based on spectral analysis of IVUS radiofrequency ultrasound backscatter signals8-10 (Virtual Histology (Volcano Corp. Rancho Cordova, CA, USA) (VH)) has the potential to provide further information about plaque composition, validated by comparison with histology in explanted10 and in vivo11 human coronary arteries.

The aim of the study was to determine, by means of VH , the effects of BA in recently complicated lesions, and to assess the changes in plaque volume and composition at lesion and reference sites after BA.

Methods

Study Design:This was a single-centre, prospective, observational study, conducted from October 2005 to February 2006.

Population: Patients with recent (<3 days) ACS, submitted to coronary angiography and requiring angioplasty were eligible if the lesion was suitable for angioplasty and located in a non-occluded native coronary artery. Angiographic exclusion criteria were: presence of thrombus at angiography, ostial or left main location, bifurcation lesion, or long lesion (>20mm), excessive tortuousity, small vessels (<2.5mm) or with abnormal blood flow
(Thrombolysis In Myocardial Infarction <3). A written consent form was obtained from all participants before the procedure.

Balloon angioplasty procedure: BA was used as for “predilatation”, i.e. before stent implantation and not with the aim of achieving an optimal result. A 20 mm long compliant balloon (Maveric, Boston Scientific, USA) was used in all patients, the size was selected according to visual estimation (balloon to artery ratio=1:1) and inflated only once at 8-12 atmospheres for at least one minute, in order to achieve significant lumen enlargement.
Procedures were performed under effective anticoagulation and triple antiplatelet therapy: aspirin 250 mg, clopidogrel 75mg/day (600 mg loading dose given at least 24 hours before) and glycoprotein IIb/IIIa receptor inhibitors.

IVUS acquisition: After an intracoronary bolus injection of 0.5 mg isosorbide dinitrate, IVUS-GS and VH images were acquired simultaneously using a commercially available 20MHz phased-array catheter (2.9F Eagle Eye, Volcano Corp, Rancho Cordova, California, USA). During image acquisition, the catheter was withdrawn using an automatic pullback device at the speed of 0.5mm/sec and RF data capture was gated on the ECG. GS images were recorded on CD Rom and RF

data on DVD for off line analysis, using the Volcano dedicated console. (Volcano Corp. Rancho Cordova, California, USA).

IVUS analysis:

Determination of the regions of interest: The segment of interest was 40 mm long, centred by the minimal lumen CSA. The location of this region of interest was determined using natural landmarks (ostium, side branch or characteristic calcification) from GS images. The corresponding RF image was that recorded at the same time (since IVUS-RF acquisition is gated on the ECG, the number of images/second depends on the heart rate). The analysis was performed at 40 levels (each mm). Three segments were determined: the “balloon segment” corresponding to the 20 mm segment around the minimal lumen CSA, and the proximal and distal segments measuring 10 mm each (figure 1).

Quantitative and qualitative analysis: The minimal vessel (V-CSA) and lumen (L-CSA) cross sectional areas were assessed from IVUS-GS images by manual delimitation of the external elastic membrane and the blood/intima interface. Plaque CSA was calculated as (V-CSA)-(L-CSA). IVUS-RF analysis needed vessel and lumen border detection using automatic (but manually corrected) contour tracing. Measurements were performed according to standard recommendations12,13. The absolute values and percentages of fibrotic, fibro-fatty, necrotic core and dense calcium tissues were averaged for the three regions of interest. Volumetric measurements were calculated using Simpson’s rule, over the whole region of interest (40 mm), as well as for the three segments (balloon segment, distal and proximal reference segments).

Reproducibility of GS and VH measurements: the reproducibility of measurements was assessed in 30 randomly selected slices from the first six patients (5 slices per patient). IVUS GS and RF were acquired twice (two separate pullbacks) and images were analysed by the same operator in two different sessions. The intra-class correlation coefficient, calculated from analysis of variance for repeated measurements, was 0.94 for V-CSA and 0.96 for L-CSA and ranged from 0.93 to 0.96 for tissue characterisation by VH (table 1).

Statistics: All statistical analyses were performed using SAS software (Version 8, SAS Institute, USA). Continuous data were presented as mean± 1 standard deviation (SD) and categorical data were presented as frequencies. The paired continuous data were compared using 2-tailed paired Student's *t* test and non-paired continuous data were compared using 2-tailed Group *t* test. A P value <0.05 was considered as significant.

Results:

Baseline and BA procedure:

Twenty patients, 16 male, mean age 61±12 years, admitted for recent acute coronary syndrome, were included in the study: 10 presented with non ST segment elevation MI, 6 with ST segment elevation MI and 4 with unstable angina. Patient characteristics are displayed in table 2. BA was performed in all patients with a 20 mm long balloon. The average balloon/artery ratio was 1.03±0.2, the mean inflation pressure was 10±2 atmospheres. By angiography, no dissection was visible. Quantitative coronary angiography showed a significant increase in minimal lumen diameter (1.11±0.39 mm versus 1.68±0.45 mm; p<0.0001) and in percent of diameter stenosis (63±11 versus 40±12%, p<0.01). There was no significant change in lumen diameter at reference levels.

IVUS results:

The V-CSA was comparable at lesion site and at reference levels. At baseline, plaque burden represented on average two thirds of V-CSA at lesion site, but only 45% of V-CSA at the reference segments (figure 2). According to the VH results, the proportion of the four types of tissue of the plaque was homogeneous, without any difference between the lesion and the reference levels. The longitudinal distribution of the plaque components is presented in the figure 3. Plaque content was mainly fibrotic (61% of the CSA), dense calcium was the least important component (7%), and fibro-fatty and necrotic tissue represented respectively 16% and 15%.

After BA, the lumen volume of the region of interest increased significantly (from 193 to 380 mm3, p<0.001), the vessel volume increased from 493 to 638 mm3 (p<0.001) and there was a non significant trend for a decrease in plaque volume (from 300 to 275 mm3, p=0.08). These changes were not homogeneously distributed along the region of interest (figure 3). At balloon segment, there was a significant increase in lumen CSA, (+1.92 mm², p=0.01), an increase in Vessel CSA (+ 0.70mm², p=0.04)

and a decrease in plaque CSA (- 1.27mm², p=0.03). Conversely, at reference levels, the opposite was observed, with an increase in plaque CSA and a decrease in lumen CSA. These changes were significant at the proximal reference segment. Thus, the increase in lumen at balloon segment (+2.1mm²) resulted from vessel enlargement for one third (+0.7 mm²) and decrease in plaque (2.1 mm²), mainly due to a longitudinal shifting of the tissue towards the reference segments (figure 2, table 4).

After BA, along the region of interest, the proportion of fibrotic, fibro-fatty and dense calcium tissue remained unchanged, when expressed in absolute values or percentages (figure 3, table 3). Conversely, the amount of necrotic tissue decreased significantly from 45±10 to 30±11mm3 (p=0.002). This 15mm3 decrease was consistent with the changes in plaque volume found by IVUS-GS analysis. Longitudinal analysis of the changes showed a longitudinal shifting of fibrotic and fibro-fatty tissue towards the proximal reference segment (table 3). Conversely, the decrease in necrotic tissue at balloon segment was not compensated by an increase at reference segment.

Discussion :

This study was the first to assess, using IVUS-GS and VH analysis, the results of a BA in recently complicated lesions and according to the plaque composition. We observed that lumen enlargement after BA was not only a combination of vessel stretching and longitudinal plaque redistribution, but also the result of a decrease in necrotic tissue, which could support the hypothesis of tissue embolization.

***Methodology*:**

Patient selection and BA: The study population was composed of patients with recent (24-72 hours) ACS. Occluded vessels, or presence of thrombus at angiography or IVUS were excluded. We selected only patients with single vessel disease, with a lesion coherent with the ECG changes. To avoid artefacts due to stent implantation, we limited our study to the effects of BA, and to avoid deep dissections after BA, the use of oversized or IVUS-sized balloon was discouraged. As a result, after BA, the lumen enlargement was significant, but lower than that observed at angiography and

by IVUS-GS in previous studies14, and IVUS analysis was not hindered by deep dissections.

***IVUS acquisition and analysis*:** In order to achieve optimal longitudinal reconstruction, we used a motorised pullback set at 0.5 mm/sec and the presence of natural landmarks (like calcifications or side branches) to determine the longitudinal position of the IVUS-GS catheter, as recommended by expert consensus documents12,13. The time of the recording was visible on all IVUS-GS images. Since IVUS-RF was recorded gated on the ECG, we used the time indicated on the recording to identify the corresponding VH and GS images. Since heart rate was >55/min in all patients, at least 70 VH images were suitable during the exploration of the 20 mm segment of interest (balloon segment and references segments). A similar methodology for longitudinal analysis was used in a previous study with VH imaging11. Our reproducibility analysis showed satisfactory results, making it possible to assess changes in necrotic tissue CSA as low as 0.01±0.04 mm^2. Translated into a volumetric assessment over a 40 mm long segment, the measurement error in volume should therefore not exceed 2.0 mm3.

***Mechanism of lumen enlargement**:* The mechanism of lumen enlargement, namely vessel stretching and plaque remodelling, was consistent with previous reports after BA15 or stent implantation16. However, compared with previous IVUS studies5, where only “stable” lesions were analyzed, our data do not support the hypothesis that plaque volume is conserved after
BA. Indeed, in our IVUS-GS results, changes in plaque volume along the 40 mm region of interest were non significant. Using multiple measurements along the entire region of interest, 1 mm apart, we observed longitudinal tissue redistribution towards the reference levels, mainly to the distal reference segment, also consistent with previous studies5,16. As a result of this longitudinal tissue redistribution, a significant reduction in L-CSA after BA at the proximal reference segment was observed, and this has never been observed in previous studies.

Effect of BA according to plaque composition: Differences in the mechanism of BA according to the nature of the plaque (stable or unstable) have previously been observed in IVUS-GS analyses7, namely greater plaque remodelling in unstable

lesions. The additional information obtained from VH was the observation that , in recently unstable lesions, plaque remodelling depended on tissue type. After BA, no change in the amount or longitudinal location was observed for “deep calcium” . Conversely, fibrotic, fibro-fatty and necrotic tissue were able to move longitudinally. This lack of changes in calcific tissue after BA has previously been observed in IVUS-GS studies17.

Decrease in necrotic tissue: A non-significant decrease in plaque volume after BA was observed by volumetric analysis with both IVUS-GS and VH. However, VH analysis made it possible to assess volume changes of the different tissues present in the plaque. A significant decrease in necrotic tissue was observed (45±10 vs 27±11, p=0.002 respectively before and after BA). The amount of “lost” necrotic tissue represented 18 mm3, i.e. one third of the total necrotic tissue present at baseline. Errors in the measurement can be ruled out, since a change of 18 mm3 is far greater than the maximal measurement error (2mm3) estimated from our reproducibility analysis. Except for necrotic tissue, the decrease in necrotic tissue volume at the lesion segment after BA was not compensated by an equivalent increase at reference segments. Thus, some necrotic tissue was “lost”, supporting the hypothesis of embolization. It is possible that some of the necrotic tissue may have been diluted into the plaque during BA, making it undetectable by VH. Distal tissue embolization from unstable plaque is another possible explanation for this phenomenon. Even if distal embolization may result from thrombus and not from atherosclerotic tissue, we cannot rule out that the “lost” necrotic tissue corresponded to distal embolization. The results of studies with distal protection devices suggest that embolization of debris is more likely to occur in patients with ruptured plaque18. Moreover, previous studies have demonstrated that, even in stable patients and therefore in lesions not supposed to be thrombotic, enzyme rise after angioplasty may occur in 5-30% This is more likely in lesions with large plaque burden19, supporting the hypothesis that not only thrombus, but also atherosclerotic tissue may embolize after BA. Despite the multiple comparisons between VH and histology9-11,20,21, the accurate composition of the tissue labelled as “necrotic core” by VH remains unclear. In fact, this tissue can be composed of various types such as cholesterol clefts, foam cells, microcalcifications and necrotic regions. Whatever the actual composition of the tissue, the capacity of the tissue labelled as “necrotic” by

VH to embolize during BA suggest that angioplasty of lesions containing this type of tissue may incur a higher risk of complication.

Study limitations : This study suffers from several limitations. (1) The sample size of the population is relatively small. (2) This study was limited to pre-dilatation angioplasty, with intentionally undersized balloons, and without stent implantation This made it possible to analyse the mechanisms of BA in this specific context, but gave no insight into the mechanisms of lumen enlargement and stenting. (3) The usual limitations associated with IVUS-GS studies also apply, namely image quality, and the precision of the automatic pullback. (4) Specific limitations are related to the IVUS-RF recording, analysis and interpretation., such as the role of heart rate when images are gated on the ECG, longitudinal localisation, the accuracy of the types of tissue as labelled by the VH software.

Conclusions and clinical implications : This study used, for the first time, VH to assess the mechanism of BA. All types of tissue, except calcium, may move longitudinally from lesion to reference segments. The most interesting result was to show that one third of the necrotic tissue detected at lesion site at baseline was “lost”, supporting the hypothesis of embolization. If further studies confirmed that the amount of necrotic tissue before angioplasty correlates with angioplasty complications (such as enzyme release), VH could be used to identify high risk lesions.

Table 1: The intra- and inter-observer reproducibility of IVUS-GS and VH measurements.

	1st time	2nd time	difference	95% CI of the difference	ICC
Lumen (mm^2)	6.92±1.89	6.91±1.97	0.20	-0.006; +0.41	0.959
Plaque (mm^2)	3.28±0.68	3.34±0.66	0.16	-0.06; 0.38	0.941
Fibrous (mm^2)	4.49±3.33	4.55±3.41	-0.003	-0.15; 0.14	0.935
Fibro-fatty (mm^2)	0.99±0.86	0.99±0.80	0.01	-0.02; 003	0.954
Necrotic (mm^2)	0.82±0.90	0.81±0.91	0.01	-0.03; 0.05	0.943
Calcium (mm^2)	0.73±0.82	0.73±0.81	-0.007	-0.03; 0.02	0.965

1st time and 2nd time referred to two different times by the same observer;

CI: confidence interval;

ICC : intraclass corefficient correlation

Necrotic : necrotic core

Calcium : dense calcium tissue

Table 2: Clinical and angiographic characteristics.

Clinical characteristics	
Age (years)	61±12
Males	15 (83%)
Hypertension	9 (50%)
Hypercholesterolemia	13 (72%)
Smokers	9 (50%)
Diabetes mellitus	5 (28%)
Family history	5 (28%)
Type of Acute Coronary Syndrome	
Non ST elevation MI	10 (50%)
ST elevation MI	6 (30%)
Unstable angina	4 (20%)
Target lesion	
Left anterior descending	8 (40%)
Left circumflex	2 (10%)
Right coronary artery	10 (50%)

Table 3: Geometrical and compositional changes after predilatation by BA at lesion site, proximal and distal reference sites.

	Distal reference site		p	Lesion site		p value	Proximal reference site		p value
	Before BA	After BA	value	Before BA	After BA		Before BA	After BA	
Lumen CSA (mm^2)	8.97±3.31	8.38±3.10	0 .11	3.58±0.59	5.54±2.56	0.003	9.22±2.79	8.45±2.56	0.019
Vessel CSA (mm^2)	16.89±6.24	16.83±6.77	0.898	16.39±5.31	17.09±5.39	0.031	16.75±4.94	17.05±4.96	0.138
Plaque CSA (mm^2)	7.92±4.15	8.35±4.87	0.449	12.82±5.03	11.55±5.03	0.031	7.53±3.65	8.61±3.74	<0.0001
Plaque (%)	44.9±13.3%	47.1±11.9%	0.204	76.2±7.4%	66.3±11.9%	0.001	43.7±12.3%	59.7±8.7%	<0.0001
Fibrous (mm^2)	2.88±2.54	3.14±3.21	0.506	5.74±2.72	5.28±2.88	0.151	2.34±1.89	3.18±2.10	<0.0001
Fibrous (%)	61.8±15.3%	62.8±10.9%	0.666	60.9±13.7%	65.5±11.4%	0.034	63±16.9%	61.5±16.7%	0.808
Fibro-Fatty (mm^2)	0.71±0.64	0.84±0.76	0.325	1.80±1.78	1.40±1.03	0.246	0.63±0.57	0.99±0.78	0.001
Fibro-Fatty (%)	15.4±9.5%	18.9±11.1%	0.101	16.9±12.2%	17.8±8.9%	0.654	14.6±11.4%	19.4±11.5%	0.009
Necrotic (mm^2)	0.71±0.68	0.55±0.65	0.084	1.54±1.33	0.96±0.84	0.032	0.72±0.86	0.57±0.60	0.118
Necrotic%	16.8±13.4%	11.2±9.2%	0.028	16.9±12.5%	11±8.7%	0.019	15.9±12.2%	14.8±21.3%	0.843
Calcium (mm^2)	0.28±0.39	0.33±0.46	0.116	0.48±0.56	0.52±0.63	0.422	0.29±0.53	0.32±0.49	0.704
Calcium (%)	6±7.7%	7.1±8.6%	0.214	5.4±6.3%	5.7±6.5%	0.653	6.4±8.7%	4.3±6.1%	0.197

CSA : cross sectional area; Necrotic=necrotic core; Calcium=dense calcium; BA=balloon angioplasty

Table 4: Geometrical and compositional volume changes after BA for the entire lesion segment:

	Before BA	After BA	P value
Lumen (mm^3)	193±25	380±28	0.001
Vessel (mm^3)	493±71	658±76	0.001
Plaque (mm^3)	300±44	275±45	0.40
Fibrous (mm^3)	184±26	185±29	0.91
Fibro-fatty (mm^3)	50±12	46±10	0.31
Necrotic (mm^3)	45±10	27±11	0.002
Dense Calcium (mm^3)	21±9	17±7	0.12

BA=balloon angioplasty

Figure 1: Selection of the zone and segments of interest.

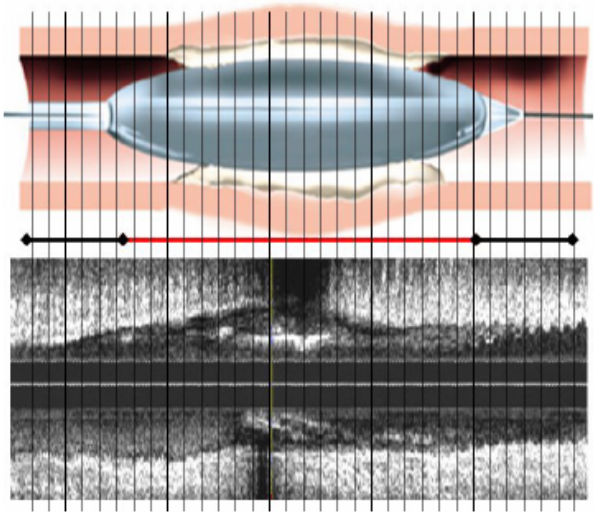

The region of interest was 40 mm long, centred on the minimal lumen cross sectional area, as assessed by intravascular ultrasound Gray Scale.

Quantitative and qualitative intravascular ultrasound analyses were performed every mm.

Three segments were determined: the proximal reference segment (10 mm long), the balloon segment (20 mm long) and the distal reference segment (10 mm long).

The corresponding Intravascular Ultrasound Radiofrequency images were selected by the time of acquisition.

Figure 2 : Longitudinal distribution in lumen cross sectional area (left panel) and in plaque cross sectional area (right panel) along the 40 mm of the region of interest.

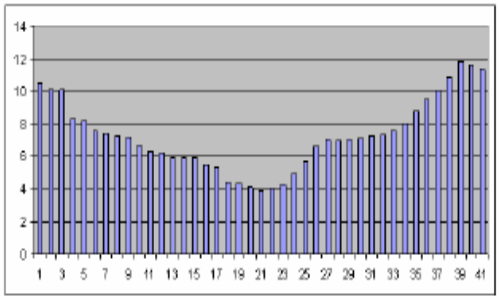

Longitudinal distribution in Lumen Area

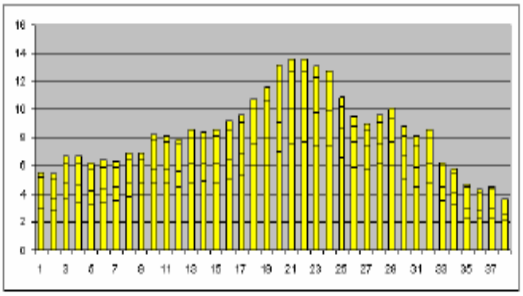

Longitudinal distribution in Plaque Area

Figure 3: Longitudinal distribution of the plaque content along the region of interest. Before balloon angioplasty (left panel) and after balloon angioplasty (right panel).

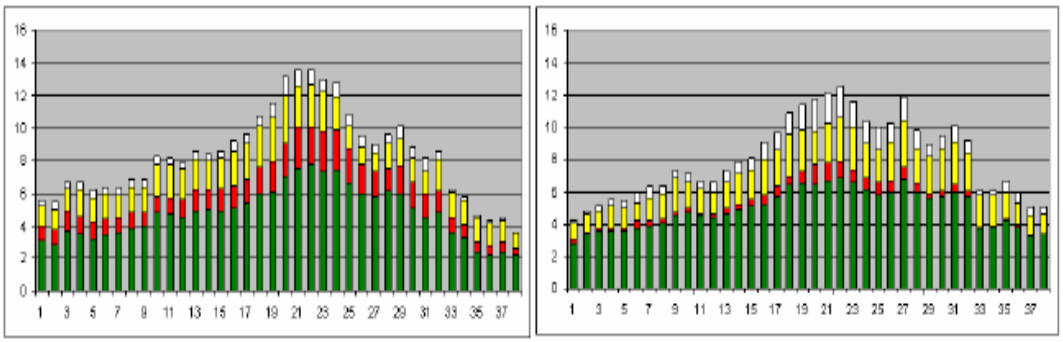

Grenn : fibrotic tissue

Red: necrotic core tissue

Yellow: fibro-fatty tissue

White : dense calcium tissue

Figure 4 : Longitudinal changes in lumen cross sectional area (left panel) and in plaque area (right panel) after balloon angioplasty.

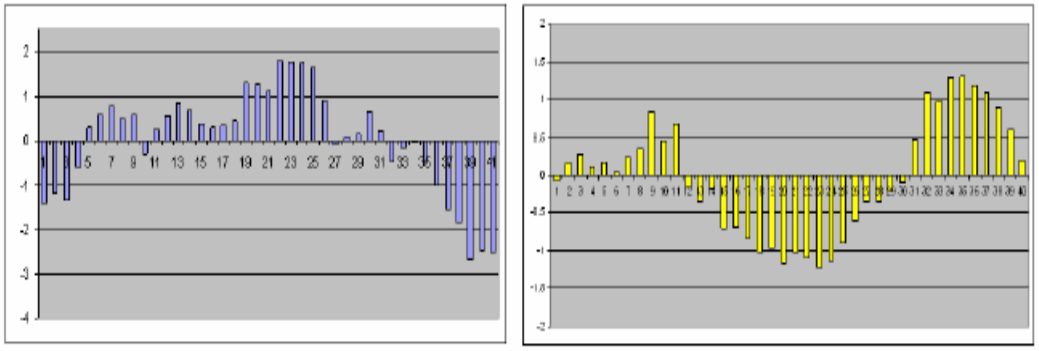

Longitudinal changes in Lumen Area Longitudinal changes in Plaque Area

References:

1. Van't Hof AW, Liem A, Suryapranata H, Hoorntje JC, De Boer MJ, Zijlstra F. Angiographic Assessment of Myocardial Reperfusion in Patients Treated with Primary Angioplasty for Acute Myocardial Infarction. Myocardial Blush Grade. *Circulation*.1998;97:2302-06.

2. Kastrati A, Mehilli J, Neumann FJ, Dotzer F, ten Berg J, Bollwein H, Graf I, Ibrahim M, Pache J, Seyfarth M, Schuhlen H, Dirschinger J, Berger PB, Schomig A. Abciximab in patients with acute coronary syndromes undergoing percutaneous coronary intervention after clopidogrel pretreatment: the ISAR-REACT 2 randomized trial. *Jama*. 2006;295:1531-8.

3. Mehta S, Cannon AD, Fox KA, Wallentin LC, Boden W, Spacek R, Widimsky P, Mc Cullough P, Hunt D, Braunwald E, Yusuf S. Routine vs Selective Invasive Strategies in Patients With Acute Coronary Syndromes. 2005;JAMA:2908-2917.

4. Nissen SE, Yock P. Intravascular ultrasound: novel pathophysiological insights and current clinical applications. *Circulation*. 2001;103:604-16.

5. Mintz GS, Pichard AD, Kent KM, Satler LF, Popma JJ, Leon MB. Axial plaque redistribution as a mechanism of percutaneous transluminal coronary angioplasty. *Am J Cardiol*. 1996;77:427-30.

6. Timmis SB, Burns WJ, Hermiller JB, Parker MA, Meyers SN, Davidson CJ. Influence of coronary atherosclerotic remodeling on the mechanism of balloon angioplasty. *Am Heart J*. 1997;134:1099-106.

7. Kearney P, Erbel R, Rupprecht HJ, Ge J, Koch L, Voigtlander T, Stahr P, Gorge G, Meyer J. Differences in the morphology of unstable and stable coronary lesions and their impact on the mechanisms of angioplasty. An in vivo study with intravascular ultrasound. *Eur Heart J*. 1996;17:721-30.

8. Moore MP, Spencer T, Salter DM, Kearney PP, Shaw TR, Starkey IR, Fitzgerald PJ, Erbel R, Lange A, McDicken NW, Sutherland GR, Fox KA. Characterisation of coronary atherosclerotic morphology by spectral analysis of radiofrequency signal: in vitro intravascular ultrasound study with histological and radiological validation. *Heart*. 1998;79:459-67.

9. Komiyama N, Berry GJ, Kolz ML, Oshima A, Metz JA, Preuss P, Brisken AF, Pauliina Moore M, Yock PG, Fitzgerald PJ. Tissue characterization of atherosclerotic plaques by intravascular ultrasound radiofrequency signal analysis: an in vitro study of human coronary arteries. *Am Heart J*. 2000;140:565-74.

10. Nair A, Kuban BD, Obuchowski N, Vince DG. Assessing spectral algorithms to predict atherosclerotic plaque composition with normalized and raw intravascular ultrasound data. *Ultrasound Med Biol*. 2001;27:1319-31.
11. Nasu K, Tsuchikane E, Katoh O, Vince DG, Virmani R, Surmely JF, Murata A, Takeda Y, Ito T, Ehara M, Matsubara T, Terashima M, Suzuki T. Accuracy of in vivo coronary plaque morphology assessment: a validation study of in vivo virtual histology compared with in vitro histopathology. *J Am Coll Cardiol*. 2006;47:2405-12.
12. Di Mario C, Gorge G, Peters R, Kearney P, Pinto F, Hausmann D, von Birgelen C, Colombo A, Mudra H, Roelandt J, Erbel R. Clinical application and image interpretation in intracoronary ultrasound. Study Group on Intracoronary Imaging of the Working Group of Coronary Circulation and of the Subgroup on Intravascular Ultrasound of the Working Group of Echocardiography of the European Society of Cardiology. *Eur Heart J*. 1998;19:207-29.
13. Mintz GS, Nissen SE, Anderson WD, Bailey SR, Erbel R, Fitzgerald PJ, Pinto FJ, Rosenfield K, Siegel RJ, Tuzcu EM, Yock PG. American College of Cardiology Clinical Expert Consensus Document on Standards for Acquisition, Measurement and Reporting of Intravascular Ultrasound Studies (IVUS). A report of the American College of Cardiology Task Force on Clinical Expert Consensus Documents. *J Am Coll Cardiol*. 2001;37:1478-92.
14. Schiele F, Meneveau N, Gilard M, Boschat J, Commeau P, Ming LP, Sewoke P, Seronde MF, Mercier M, Gupta S, Bassand JP. Intravascular ultrasound-guided balloon angioplasty compared with stent: immediate and 6-month results of the multicenter, randomized Balloon Equivalent to Stent Study (BEST). *Circulation*. 2003;107:545-51.
15. Honye J, Mahon DJ, Jain A, White CJ, Ramee SR, Wallis JB, al-Zarka A, Tobis JM.
Morphological effects of coronary balloon angioplasty in vivo assessed by intravascular ultrasound imaging. *Circulation*. 1992;85:1012-25.
16. Maehara A, Takagi A, Okura H, Hassan AH, Bonneau HN, Honda Y, Yock PG, Fitzgerald PJ. Longitudinal plaque redistribution during stent expansion. *Am J Cardiol*. 2000;86:1069-72.
17. von Birgelen C, Mintz GS, Bose D, Baumgart D, Haude M, Wieneke H, Neumann T, Brinkhoff J, Jasper M, Erbel R. Impact of moderate lesion calcium on mechanisms

of coronary stenting as assessed with three-dimensional intravascular ultrasound in vivo. *Am J Cardiol*. 2003;92:5-10.
18. Mizote I, Ueda Y, Ohtani T, Shimizu M, Takeda Y, Oka T, Tsujimoto M, Hirayama A, Hori M, Kodama K. Distal protection improved reperfusion and reduced left ventricular dysfunction in patients with acute myocardial infarction who had angioscopically defined ruptured plaque. *Circulation*. 2005;112:1001-7.
19. Mehran R, Dangas G, Mintz GS, Lansky AJ, Pichard AD, Satler LF, Kent KM, Stone GW, Leon MB. Atherosclerotic plaque burden and CK-MB enzyme elevation after coronary interventions : intravascular ultrasound study of 2256 patients. *Circulation*. 2000;101:604-10.
20. Nair A, Kuban BD, Tuzcu EM, Schoenhagen P, Nissen SE, Vince DG. Coronary plaque classification with intravascular ultrasound radiofrequency data analysis. *Circulation*. 2002;106:2200-6.
21. Murashige A, Hiro T, Fujii T, Imoto K, Murata T, Fukumoto Y, Matsuzaki M. Detection of Lipid-Laden Atherosclerotic Plaque by Wavelet Analysis of Radiofrequency Intravascular Ultrasound Signals. In Vitro Validation and Preliminary in Vivo Application. *J Am Coll Cardiol*. 2005;45:1954-1960.

Summary for IVUS-VH

1, IVUS-VH is an improved IVUS imaging technique which uses the spectral analysis of backscatter data and codes plaque compositions (fibrous, fibro-fatty, dense calcium and necrotic core) into four different colors. It supplies us a real-time 2D cross-sectional image which includes not only morphologic but also compositional information of a plaque.

2, IVUS-VH has been validated in an in vitro study, however, there are some discrepancies between two in vivo studies. We also performed an in vivo study to testify the accuracy of IVUS-VH by comparing IVUS-VH and histology, and we found good correlation between IVUS-VH and histology (unpublished data). Thus, we believe that IVUS-VH has a high accuracy in differentiating four different plaque compositions.

3, When combining the published data and ours, we find that IVUS-VH has a good reproducibility, The area or volume data supplied by IVUS-VH has a good correlation with those were supplied by conventional IVUS.

4, From October 2005 to February 2006, we conducted a single-centre, prospective, observational study by using IVUS-VH to observe plaque compositions' changes after PTCA. In our study, we enrolled 20 patients with ACSs. Our study showed that: 1), unstable atherosclerotic coronary plaques were composed of 61% fibrosis, 15% fibro fatty and 15% necrotic tissue; 2), 35% of lumen enlargement was explained by vessel stretching, and 65% by plaque volume decrease; 3), The decrease in plaque volume was the result of longitudinal redistribution of fibrotic and fibro-fatty tissue and of the disappearance of one third of the necrotic tissue present at baseline.

5, We are expecting the results of an undergoing large prospective trial named as PROSPECT, of which at least two arteries are investigated by IVUS-VH. The characteristics of an unstable plaque will be concluded by future ACSs, and the predictive value of IVUS-VH will be defined.

6, Combining IVUS-VH with other imaging techniques or biomarkers may be a good choice for detecting a vulnerable plaque.

Publications

1. Wei H, Guoping Lu, Weifeng Shen, et al. The dose-effect relationship of Pravastatin to vascular endothelial function of patients with coronary artery disease. Section of Cardiovascular Disease. 2002; Vol 29(1): p 50-52.

2. Wei H, Schiele F, Meneveau N, et al. The value of intravascular ultrasound imaging in diagnosis of aortic penetrating atherosclerotic ulcer. Euro Intervention. 2006; Vol 1: P 432-437.

3. Wei H, Schiele F, Meneveau N, et al. Potential interest of intra-aorta ultrasound imaging for the diagnosis of aortic penetrating atherosclerotic ulcer. Int J Cardiovasc Imaging . 2006; Vol 22: P 653-656.

4. Wei H, Schiele F, Descotes-Genon V, et al. Changes in Unstable Coronary Atherosclerotic Plaque Composition After Balloon Angioplasty. In vivo spectral analysis of intravascular ultrasound radiofrequency data. This article has been accepted by the Journal of Am J Cardiol and will be published in early 2008.

5. Wei H, Schiele F, Meneveau N, et al. The value of intravascular ultrasound imaging in following up patients with replacement of the ascending aorta for acute type A aortic dissection. This article had been submitted to the Journal of Chinese Med J and revised to be considered.

6. An abstract titled as “The value of IVUS imaging in acute aortic syndrome” was orally presented at ESC meeting in 2005 in Sweden.

7. An abstract titled as “The compositional changes of coronary atherosclerotic plaque after predilatation by balloon angioplasty: an in vivo spectral analysis of intravascular ultrasound radiofrequency data” was orally presented at ESC meeting in 2006 in Spain.

8. Legalery P, Schiele F, Seronde MF, Meneveau N, Wei Hu, et al. One year outcome of patients submitted to routine fractional flow reserve assessment to determine the need for angioplasty. Eur Heart J. 2005; Vol 26(24): p 2623-2629.